for, and consequences of, such events as pion condensation in dense nuclear matter, the occurrence and features of nuclear shock waves, and simple pion production. Different formulations and assumptions lead to qualitatively different predictions. Hence, experimental data about almost any aspect of these new situations will force qualitative advances in our understanding of the larger reality of the "nuclear" state of matter. The ability of the CSC system to accelerate light- and medium-mass nuclei up to 200 MeV/amu and all nuclei up to the sonic boundary will make it the preeminent, if not unique, facility for exploring this realm. Correspondingly, such studies should occupy the central role in the research program. The fact that the required beam energies will occur with high intensities and good quality ensures that the facility can be utilized to probe these phenomena through several generations of increasingly more detailed and sophisticated experiments.

In a different realm, collisions of massive nuclei produce environments for electron orbits which should lead to fundamentally new effects in atomic physics, thus allowing tests of basic aspects of quantum electrodynamics. Greiner[3] and his school have emphasized the importance of experiments utilizing heavy-ion collisions to answer such questions. Some problems, such as extrapolations of current nuclear-molecular x-ray work, are immediately open to further study with heavier masses and higher energies. Other topics require the solution of very difficult experimental problems, and some depend on

problematical consequences of heavy-ion collisions. The extreme difficulty of the most important experiments makes it likely that the substantive questions will demand an attack in depth by many groups with many different approaches. Hence, while the upper energy ranges of the CSC system are not necessary for these studies, the superior beam qualities may make the CSC the instrument of choice for what are ultimately the crucial experiments.

References

1. G.F. Bertsch, private communication.
2. T.D. Lee, Berkeley, 1974
3. W. Greiner, Berkeley, 1974.

.1 Quantum electrodynamics and atomic physics in strong fields.

The magnitude of positive electric charge which can be localized when two heavy nuclei collide presents unique opportunities to test and expand our knowledge of atomic physics processes and of the fundamental ideas of quantum electrodynamics. The theoretical work which has called attention to many of these opportunities has been strongly led by Greiner and his associates. Peiper and Greiner in 1969[1] refocused attention on a problem which, despite sporadic efforts,[2-6] had remained unsolved since the invention of the relativistic quantum mechanics for electrons by Dirac. This problem concerns the dramatic consequences which follow upon the lowering of the energy of the 1s electron orbit into the negative energy continuum at some high ($Z \gtrsim 170$) value of the nuclear charge.

The effect is illustrated in Figure 1, where the nucleus is taken to be a single uniformly charged sphere. Peiper and Greiner gave the correct theoretical interpretation of what happens when the 1s state joins the lower continuum, namely that a vacancy can be filled by emission of a positron. After the positrons are produced in the "high Z catastrophe", the space surrounding the nucleus must become charged in order to satisfy charge conservation. This produces the so-called "charged vacuum" plus a number of positrons and it was seen that this process could be viewed as the "decay of the neutral vacuum". After this conceptual breakthrough there was a search for mechanisms which might stabilize the vacuum.[7-9]

None were found, and the ideas of Ref. 1 were developed in detail.[10-14] There now seems to be full agreement on this interpretation of the theory. Nonetheless, the uniqueness of the phenomenon and its fundamental origins demand that the theoretical predictions be experimentally verified.

The present consensus is that the best prospect of creating a neutral vacuum in an over-critical field will occur during the collision of two very heavy ions. Unfortunately, even beyond the complications introduced by two charge centers, the time dependence of the nuclear Coulomb fields during a heavy-ion collision will complicate the spectrum of positrons produced. It appears that a thorough quantitative understanding of atomic collisions will be necessary in order to understand both the primary and background phenomena associated with this effect.

An important theoretical advance in the theoretical study of heavy-ion collisions was achieved when Muller, et al.[15] solved the problem of relativistic electrons bound to two separated stationary nuclear charges, the so-called "two center" problem. It was soon realized however that the purely adiabatic approach, which had been useful in explaining the earliest experiments[16-20] in which x-rays apparently associated with the composite nuclear charge were observed in heavy-ion collisions, has limited validity. The effects of rotational coupling in the collision should lead to induced as well as spontaneous x-ray transitions.[22-23] However, this complication actually yields a needed new feature in that these induced transitions should display a distinctive feature by which noncharacteristic x-rays can be identified; namely, the high-

energy continuum x-rays should exhibit a directional anisotropy with respect to the beam axis. The observation[24-26] of this anisotropy constituted vital experimental evidence to support the occurrence of "molecular-orbital" phenomena in heavy-ion collisions. Still, not all aspects of the calculations for this sort of phenomena have been verified experimentally. Tseyrruya, et al.[27], did not observe the impact-parameter dependence of the noncharacteristic x-rays predicted for 35 MeV C-C collisions and Thoe, et al.,[26] observed an apparent breakdown of the molecular orbital picture as the collision energy was increased. Further, other mechanisms, such as collective radiations,[28] may be important.

Experiments which clearly test present predictions and those of succeeding theoretical formulations are hence essential. The behavior of theory and nature as the adiabaticity parameter ($v_{collision}/v_{K\ orbit}$) is varied through the range ~1/20 to ~1 for the light to the heaviest ions must become known and understood. The results of Thoe, et al.[26] which show (see Fig. 2) no asymmetry in the C-C quasimolecular x-ray spectrum at $v_c/v_k \sim 1$, immediately suggest that heavier systems be investigated as a function of collision velocity up to this same limit. Their existing data in the Si-Al region show strong asymmetries at the 1 MeV/amu level of velocity, as do the Ni-Ni data of Greenberg, et al.[24]

It is not clear at present what the optimum technique for identifying the decay of the neutral vacuum will be; that is, what will constitute the most definitive signature that the phenomenon has in fact occurred. Initial ideas centered upon

the detection of the positrons, but it is clear that this will be quite difficult. Corrections to the adiabatic approximation have, of course, implications for the shape of the positron spectrum produced during the close collisions of very heavy ions as well as for the x-rays. Indeed, the time dependence of the nuclear electric fields leads to the production of extra positrons both before and during the creation of the critical potential since the motion can transfer energy to the electron-positron field. The combined spectrum of "induced" and "spontaneous" positrons was calculated in the recent work of Smith, et al.[29] and further calculations[30] have attacked the additional complications which are inherent in positron observation because of such effects as the pair formation following nuclear Coulomb excitation.

For reasons such as those just mentioned it is clear that a most precise understanding of the various phenomena will be necessary, requiring complex coincidence and correlation experiments. The effects of the strong magnetic fields generated in the collisions[31] may produce asymmetries which will help identify the sources of the various positron radiations. Alternatively, it may develop that detailed studies of the x-ray production and anomalies associated with the dip into the negative energy continuum offer the best avenue towards identifying the effect.[32] Such an approach will require detailed theoretical understanding of the energy dependence and nucleus-photon angular correlations of the sort illustrated in Fig. 3 (see Ref. 33). What seems certain, in any case, is that along the way to the study of the decay of the neutral vacuum,

many new features will be learned about time-dependent relativistic quantum mechanics and atomic physics.

References

1. W. Pieper and W. Greiner, Zeit, f. Physik 218(1969)327.
2. L.I. Schiff, H. Snyder and J. Weinberg, Phys. Rev. 57 (1940)315.
3. I. Pomeranchuk and J. Smorodinsky, J. Phys. USSR 9(1945)97.
4. K. N. Case, Phys. Rev. 80(1950)797.
5. F.G. Werner and J.A. Wheeler, Phys. Rev. 109(1958)126.
6. D. Rein, Diplomarbeit, University of Frankfurt, 1964.
7. P.G. Reinhard, W. Greiner and H. Arenhovel, Nucl. Phys. A166(1971)173.
8. L.P. Fulcher and W. Greiner, Lettre Nuovo Cimento 2(1971) 279.
9. J. Rafelski, L.P. Fulcher and W. Greiner, Phys. Rev. Letters 27(1971)958.
10. B. Muller, H. Peitz, J. Rafelski and W. Greiner, Phys. Rev. Letters 28(1972)1235.
11. J. Rafelski, B. Muller and W. Greiner, Nucl. Phys. B38 (1974)585.
12. L. Fulcher and A. Klein, Phys. Rev. D8)1973)2455.
13. L. Fulcher and A. Klein, Ann. Phys. 84(1974)335.
14. L. Fulcher, J. Rafelski and A. Klein, to be submitted to Physics Reports.
15. B. Muller, J. Rafelski and W. Greiner, Phys. Letters 47B (1973)5.
16. F.W. Saris, et al., Phys. Rev. Letters 28(1972)717.

17. P.H. Mokler, H.J. Stein and P. Armbruster, Phys. Rev. Letters 29(1972)827.

18. J.M. MacDonald, M.D. Brown, and T. Chiao, Phys. Rev. Lett. 30(1973)471.

19. W.E. Meyerhof, et al., Phys. Rev. Lett. 30(1973)1279.

20. C.K. Davis and J.S. Greenberg, Phys. Rev. Lett. 32 (1974)1215.

21. F.G. Jundt, et al., Phys. Rev. 10(1974)1053.

22. B. Muller, R. K. Smith and W. Greiner, Physics Letters 49B(1974)219.

23. B. Muller and W. Greiner, Phys. Rev. Letters 33(1974) 469.

24. J. S. Greenberg, C.K. Davis and P. Vincent, Phys. Rev. Letters 33(1974)473.

25. G. Kraft, P.K. Mokler and H.J. Stein, Phys. Rev. Letters 33(1974)476.

26. R.S. Thoe, et al., Phys. Rev. Letters 34(1974)64.

27. I. Tserruya, et al., Phys. Rev. Letters 36(1976)1451.

28. J.C.Y. Chen, T. Ishihara and K.M. Watson, Phys. Rev. Letters 35(1975)1574.

29. R.K. Smith, et al., Phys. Rev. Letters 32(1974)554.

30. V. Oberacker, G. Soff, and W. Greiner, Phys. Rev. Lett. 36(1976)1024.

31. J. Rafelski and B. Muller, Phys. Rev. Lett. 36(1976)517.

32. W. Greiner, Berkeley, 1974.

33. B. Muller, R.K. Smith and W. Greiner, Phys. Lett. 53B (1975)401.

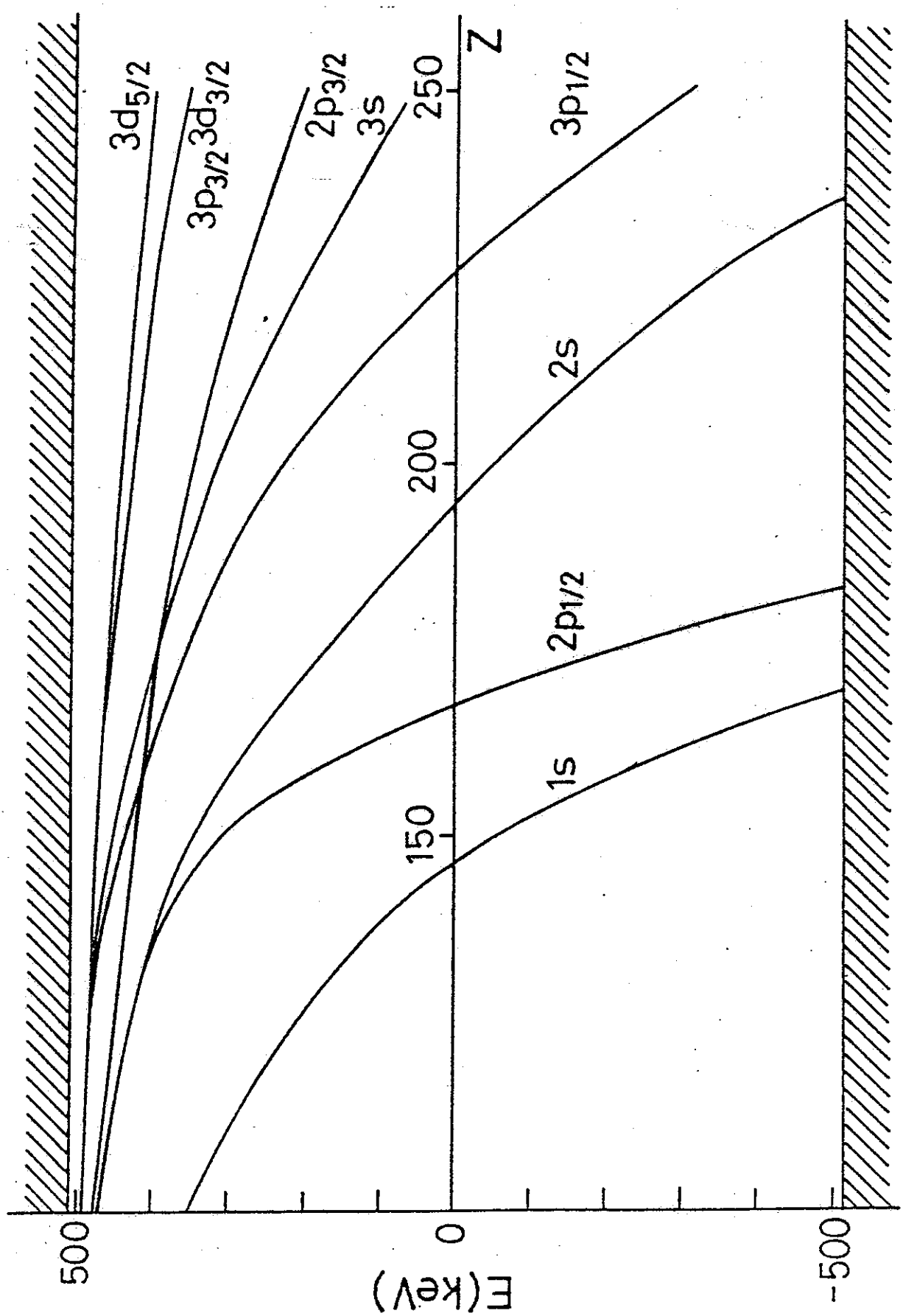
3d5/2
3p3/2
3d3/2
2p3/2
3s
250
Z
3p1/2
2s
200
2p1/2
1s
150
500
0
-500
E(keV)

Fig. 1(III.4.1)

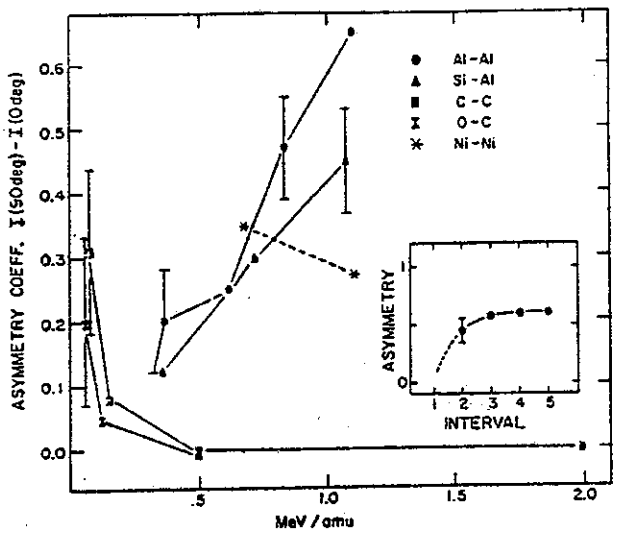

Fig.2.(III.4.1).--(See Ref. 26). Plots of the asymmetry coefficient $\beta \equiv I(90\text{ deg}) - I(0\text{ deg})$, for photon energy intervals indicated in the text, obtained from averaged fits to angular distribution data for C-C, O-C, Al-Al, and Si-Al collisions at the indicated beam energies. The fits with the form $\alpha+\beta \sin\theta$ gave range errors equal to roughly half of the indicated error bars. The inset shows β as a function of photon energy interval for 30 MeV Al-Al collisions, where intervals 1-5 refer to photon energy intervals of 1-3, 3-4, 4-5, 5-6, and 6-8 keV, respectively. No point is plotted for interval 1 because of gross uncertainties in deconvoluting the Mylar-absorber-window absorption characteristic in this interval. The Ni-Ni data are taken from Fig. 2 of Ref. 24 for the photon energy interval displaying maximum asymmetry, and have full error bars $\lesssim$10% in β.

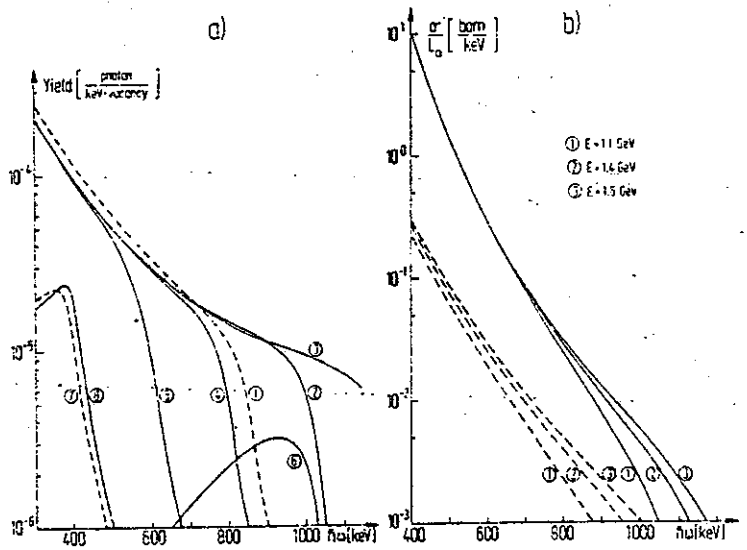

Fig. 3.(III.4.1).--(See Ref. 33). (a) Coincidence spectra in U-U collisions. (1) for E=1.1 GeV and θ_{ion}=45°, (2) to (5) for E=1.6 GeV and θ_{ion}=45°, 90°, 22.5°, 11.2° respectively; (6) gives the contribution of induced radiation to curve (2); (7) and (8) show the negligible contribution to (1) and (2) respectively from the $2p_{1/2}\sigma \rightarrow 1s\sigma$ transition. (b) Singles spectra in U-U collisions. The solid lines give the total spectrum and the broken lines show the contribution from rotationally induced emission. (1)E=1.1 GeV; (2)E=1.4 GeV; (3) E=1.6 GeV; all scattering energies are in the lab system.

Addendum to III.4.1

The most exciting new development in the fields covered by III.4.1 is the measurements of the positron production cross sections just completed at GSI in Darmstadt.[1,2,3] There have also been two important theoretical developments. The first of these[4] is the idea that the induced positron production process discussed in III.4.1 is not the only important production process in which energy is transferred to the electron-positron field from the nuclear electric fields. Approximately equal in importance is the process wherein large numbers of virtual photons in the two-vacuum polarization clouds act coherently to produce electron-positron pairs. In this process, which has been aptly called "vacuum polarization shakeoff", some of the virtual positrons surrounding each of the two centers of charge, with the input of energy from the nuclear electric fields, have become physical positrons. The two processes are of comparable importance, but the size of the induced contribution increases more rapidly with Z.

The first quantitative comparison of theory with experiment is encouraging. The slope of the total positron production rate versus beam energy agrees with the theory, but for Pb-Pb and Pb–U collisions the magnitudes seem to disagree by about a factor of 2. This is not too disturbing since the data points may contain a normalization error, and several theoretical effects that are probably important have not yet been included. For example, excitation of the 1s electrons into higher bound states has not yet been included.

The calculations indicate that for both Pb-Pb and Pb-U collisions there is an energy region in which QED positrons are considerably more numerous than those resulting from nuclear background effects. In neither case would we expect over-critical phenomena to occur (i.e. phenomena in which the effective Z is greater than about 173 as shown in Fig. (III.4.1)) since the critical charge is probably not exceeded. In U-U collisions the low-lying nuclear states are more numerous, and thus the nuclear background is relatively more important. Not all of the important QED effects have been included in the theory; hence we do not know to what extent the data supports it, although the initial estimate is very encouraging. Further, we still do not know if over-critical QED effects can be separated from under-critical QED effects.

Data from coincidence experiments show that the trend of the measured angular distribution is reproduced by the theory. Nuclear background effects have not been included, and including these may significantly improve the agreement between theory and experiment. At present, disentangling the over-critical positrons from other effects in elastic collisions does not seem to be an easy task. But these are just the beginning steps in the new subject of atomic physics at very high fields.

References

1. E. Kankeleit, H. Backe, J.S. Greenberg,et al., GSI preprint.
2. P. Kienle, C. Krozhuharov, E. Kankeleit, et al., GSI preprint.

3. B. Müller, V. Oberacker, J. Reinhardt, G. Soff, W. Greiner, and J. Rafelski, Frankfurt preprint.

4. G. Soff, J. Reinhardt, B. Müller, and W. Greiner, Phys. Rev. Letters 38(1977)592.

III.4.2 "Shock waves", fragmentation, etc.

The availability from the CSC system of intense beams in the 20-200 MeV/amu energy range will allow the study of nuclear matter in an environment that is qualitatively different from those now known. The limiting conditions of known environments are at one extreme those attained with $\gtrsim$1 GeV/amu velocities and at the other those produced with sub-sonic and/or few-nucleon probes.

Experiments[1-4] with the Bevalac system in Berkeley have shown that at full relativistic velocities, heavy-ion collisions exhibit many simplicities. In many ways the ions can be thought of as bags of relativistic particles, and their specific nuclear environments are irrelevant. Since the wavelengths of the particles are small and their mean-free-paths in nuclear matter long, some aspects of the collisions follow directly from cascades of nucleon-nucleon interactions.[5-7] Other observations are largely explained simply in terms of the binding energies and temperatures of the various fragments of dissociation.

The more conventional nuclear environment of past and present day few-particle and heavy-ion nuclear science is confined to a narrow band around "normal" mass and energy density. Coulomb repulsion and the Pauli Principle act to preserve this environment even in the current ~10 MeV/amu collisions of very heavy ions. Although higher velocities are available with Ne, O and C ions, these light systems may be too diffuse to produce significant perturbations of the normal densities.

The realm of nuclear conditions which lies intermediate tween the ~GeV/amu "nucleonic" regime and the ~10 MeV/amu 'normal" regime should manifest a multiplicity of new phenomena. As energies increase to and beyond the ~20 MeV/amu range, the Pauli Principle loses control over the "separation" of the target and projectile systems, and projectile velocities become comparable to the propagation velocities of the disturbance in the nuclear medium. It has been widely suggested that the response of the nuclear material under such conditions may be typified by phenomena which are in some ways analogous to shock waves in fluids.[8-12] The actual form in which the shock wave phenomenon manifests itself differs widely in different theoretical constructs, depending on different assumptions about macroscopic nuclear fluid properties, the nucleon-nucleon interaction, and, of course, the model used to calculate the process. The only relevant experimental tests so far attempted have been at the upper and lower ends of the energy range.[4,13] These first results, at least in some qualitative aspects, are consistent with predictions[12] based on a one-fluid hydrodynamic theory.

Initial experimental exploration for shock-wave type phenomena will commence with projectiles up to around nickel as soon as the injector cyclotron is operational. Coupled operation will allow all projectile-target combinations to be studied to at least the supersonic threshold. The simplest qualitative feature to be isolated is whether collisions occur

in which the preponderance of high velocity material is ejected perpendicular to the beam direction. This would be the signature of a head-on collision[10] in which the conditions for shock-wave formation were satisfied, namely that the nuclear matter in the collision region reached thermal equilibrium in a time short compared to the duration of the collision. Conversely, if the fore-aft directions dominate the cross sections this would be an indication that thermalization must be relatively slow. First studies with the CSC system would probably involve surveys as functions of projectile energy and mass. Eventually, the multiplicity, mass, and energy of the fragments should be determined as well as the aggregate angular distributions.

The quasielastic and CHIP reactions which dominate current experimental study are both processes which are apparently dominated by the surface properties of nuclei. With the variable energy capability of the CSC, the evolution of these surface-dominated reactions at ~10 MeV/amu into the shock-wave type effects which are dominated by volume parameters can be smoothly traced with no lacunae. The CHIP reactions might evolve in any of several different ways at higher energy. The projectile and target might maintain their basic identity, in which case the cross section would just exhibit less relative inelasticity. A signature for the compressibility of the nuclear medium would then be determined from whether there is an enhanced flux forward or backward of the grazing angle. An incompressible nucleus would result in "bouncing", and increased

cross section at large angles. Such an effect has been predicted in time-dependent Hartree-Fock calculations. Alternatively, if the energies above ~10 MeV/amu show increasing fragmentation of the nuclei, with featureless angular distributions, the concept of temperature will probably be useful and lead to information about reaction volumes and collision times.

To date, temperature has been useful for organizing data in two different ways. The first deals with the energy spectra of individual nucleons from a reaction. This has been long known from the traditional evaporation spectrum, characterized by a temperature T≃2 MeV. It is now observed at the highest (>1 GeV/amu) energies that the spectra can be characterized by T≃30 MeV. Study of intermediate energies should be illuminating: does T increase uniformly as the energy goes up, or are there several components to the nucleon distribution, the relative importances of which differ as the bombarding energy increases? Studies with the CSC system at several energies between 5 and 200 MeV/amu will be able to answer such questions. The neutron-time-of-flight facility of the present MSU facility can be utilized to obtain for the first time in this regime comparisons between charged particle and neutron evaporation.

Temperature has also been applied to the relative abundance of fragments produced in collisions, the abundance going as $e^{-Q/T}$. At lower energies, the Q-value is associated with the entire reacting system, and values of T≃7 MeV are found. At Bevalac energies, similar values of T are found, but the Q-value is that for the breakup of the projectile or target alone. In fact, the independence of target and projectile allows the cross sections to be expressed in factored form to good approximation.

Specifically, for B+T→F+anything, one has $\sigma^{F}_{BT}=\gamma^{F}_{B}\gamma_{T}$,[14] where the target factor $\gamma_T \simeq A^{1/4}$. Hence the relative modes of fragmentation are independent of the target and are, in fact, for most fragments only weakly dependent on the beam particle. In addition, presumably reflecting the applicability of limiting fragmentation, the cross sections are independent of energy between 1 and 2 GeV. We know that in the ~10 MeV/amu regime all these simplicities vanish. A detailed study of the energy region where reaction cross sections just begin to depend on target properties should yield a more complete understanding of nuclear dynamics than studies centered at either lower or higher energies. Experiments over a range of energies descending from the CSC limit of 200 MeV/amu, bombarding targets of H, C, Cu and Pb with ^{12}C and ^{16}O to permit a direct comparison with the present Bevalac data, seem to be first called for. Fragments would be detected in the spectrograph, with rigidity, time-of-flight and ΔE-E as labels. This survey would then be followed by experiments with heavier projectiles.

In sum, the energy range of the CSC system is ideally suited to bridge the gap between the known regimes of nucleus-nucleus interactions. This accelerator will make it possible not only to delineate fully the phenomena in this unexplored regime but also to anchor it firmly at both extremes to presently known behavior.

References

1. H.H. Heckman, et al., Phys. Rev. Lett. 28(1972)926; Phys. Rev. Lett. 37(1976)56.

2. D.E. Greiner, et al., Phys. Rev. Lett. 35(1975)152.

3. H.H. Heckman, BeV/Nucleon Workshop, Bear Mountain, New York, 1974.

4. A.M. Poskanzer, et al., Phys. Rev. Lett. 35(1975)1701.

5. H.H. Gutbrod, private communication.

6. H. Feshbach and K. Huang, Phys. Lett. 47B(1973)300.

7. A.S. Goldhaber, Phys. Lett. 53B(1974)306.

8. G.F. Chapline, et al., Phys. Rev. D8(1973)4302.

9. C.Y. Wong and T.A. Welton, Phys. Lett. 49B(1974)234.

10. W. Scheid, H. Müller, and W. Greiner, Phys. Rev. Lett. 32 (1974)741.

11. G.F. Bertsch, Nucl. Phys. A249(1975)253.

12. A.A. Amsden, et al., Phys. Rev. Lett. 35(1975)905.

13. H.G. Baumgardt, et al., Z. Phys. A273(1975)239.

14. P.J. Lindstrom, et al., LBL Report No. LBL-3650.

III.4.3 Abnormal nuclear matter, pion condensation, etc.

Recent theoretical studies[1-4] have raised the question of whether nuclear matter might exist in a very different phase from that presently known terrestrially. This "abnormal" or "superdense" phase might in its most dramatic manifestation be characterized by nuclei with small radii, binding energies of 150 MeV/amu and atomic masses of several hundreds to even thousands. The hypothetical stability of nuclear matter in this phase depends upon fundamental properties of the vacuum and of elementary particles. Present calculations indicate that plausible values for the relevant parameters could lead to a stable super-dense phase. However, a first survey[5] of terrestrial sources for the existence of such nuclei indicates a very low upper bound on its possible concentration.

The Lee-Wick "abnormal nuclei" may be taken as a limiting example of a variety of nuclear phenomena associated with a change of phase from ordinary nuclear matter. Quasi-stable "density-isomers" or "pion condensates" arise in many theoretical formulations when nuclear density is raised to about twice its normal value.[5] Thus, laboratory searches for abnormal nuclear matter must utilize heavy-ion collisions which can produce, even if only momentarily, the requisite density doubling.

Collisions of heavy ions with center-of-mass energies of ~160 MeV/amu should in principle permit complete overlapping of the target and projectile nuclei and hence a doubling of the density. The range of energies 20-200 MeV/amu thus should

encompass much of the optimum range for possible production of an "abnormal" phase since the "nuclear-matter" aspects of heavy-ion collisions give way to "particle-physics" aspects in the ~GeV/amu range.

Verification of the production of abnormal nuclear matter will involve difficult experimental questions since calculations do not thus far predict a unique signature for such events. Of course, if strictly stable abnormal nuclei are produced, evidence will be clear-cut. However, in the more probable instance that the new phase is not stable, its identification will necessitate a thorough understanding of the complete variety of reaction processes at the associated bombarding energies. It has been suggested for example that anomalies in shock-wave phenomena[7] may be attributed to such "density isomer" formation. Anomalously delayed and symmetric fission might be another possible signature. Delineation of the appropriate identifying clues remains an open question at this time, however, and in the absence of significant theoretical progress a broad survey of emission spectra from collisions in the strong compression regime seems to be the logical path for initially pursuing this issue. The characteristics of the CSC facility will be strikingly appropriate for such a search, and such investigations will have a very high priority in the research program.

References

1. A.R. Bodmer, Phys. Rev. D4(1971)1601.

2. T.D. Lee and G.C. Wick, Phys. Rev. D9(1974)2291.

3. T.D. Lee, Rev. Mod. Phys. 47(1975)267.

4. T.D. Lee and M. Margulies, Phys. Rev. D11(1975).

5. R.J. Holt, et al., Phys. Rev. Lett. 36(1976)183.

6. A.K. Kerman, Berkeley, 1974

7. J. Hofmann, et al., Phys. Rev. Lett. 36(1976)88.

III.4.4 Pion production

The threshold behavior of pion production will be a most important component of the research program with the CSC accelerator. Establishing the features of this phenomenon will fundamentally advance the understanding of the pion field and the interactions of nucleons with each other in high-density environments.

The pion field in nuclear matter has been a subject of great theoretical interest recently.[1] There is an attractive (p-wave) interaction between pions and nucleons, which, within some models of the pion-nucleon Hamiltonian, leads to phase transitions in neutron stars and high-density nuclear matter, as discussed in Sec. III.4.3. This phase transition, "pion condensation", involves a static but spatially varying pion field. This would not be directly observable as laboratory pions, but the underlying Hamiltonian which permits collective effects in the static field would also give rise to coherences in the emission of real pions. This has been calculated within a particular Hamiltonian model as pion bremsstrahlung.[2]

Actual pion production is also sensitive to the interactions between nucleons at high density. This is easy to see, for the production requires a large amount of phase space to be available in the colliding system so that nucleon kinetic energy can be converted to pion rest energy. If there is a strong repulsive interaction between nucleons at high density, such as some current theories suggest,[3] the nucleons would slow down so much in the overlap region that it would become unfavorable to produce pions.

A straightforward calculation of pion production in the collisions of heavy nuclei is possible with the assumption of complete incoherence. In this limit all that is important is the momentum distributions of the nucleons and the cross sections for scattering and producing pions in nucleon-nucleon collisions. Such calculations have been quite successful in describing the production of pions from proton-nucleus collisions at energies well above threshold.[4] Because of the Fermi momentum of the nucleons in the two nuclei, the heavy-ion threshold energy for pion production is ~50 MeV/amu. Predicted cross sections[5] for the range 100 MeV/amu to 200 MeV/amu are shown in Fig. 1. The pions produced in these processes would have very low energy in the nucleon-nucleon center-of-mass frame, as shown in Fig. 2. Any significant deviations of the observed experimental cross sections from these predictions will constitute signatures of fundamental and exciting new physical processes: for examples, a much higher rate would show that coherent mechanisms come into dominance at high density; a much lower rate for central collisions would indicate that the nuclear medium is quite incompressible at high density.

There has so far been very little experimental work even touching upon this topic. A search for pions with 70 MeV/amu ^{3}He projectiles yielded a cross section in the sub-nanobarn range[5] and indeed the n-n collision model predicts a very small cross section at this low energy. Another experiment[7] has claimed to see ~1 pion per nuclear interaction for 280 MeV/amu neon collisions in nuclear emulsion. This result is completely inconsistent with the rate and energy spectrum calculated in

the n-n collision model. Reported measurements[8] with still higher energy (520 MeV/amu) ^{14}N also indicate cross sections for production of high-momentum pions much larger than the incoherent nucleon-nucleon model predictions.

It should thus be clear that measurements of pion production cross sections in the range 100-200 MeV/amu will be commenced as soon as the coupled cyclotrons are operational. In this area there is one clear experimental signature, namely the pions themselves. The challenge will be to measure possibly small cross sections of low-energy particles in a high flux of debris. Spectrometer systems developed for study of small-cross-section events in lower-energy heavy-ion experiments may prove very advantageous in this new context. Ultimately, the relationships between emitted pions and nuclear fragments must be quantified to answer questions about possible multiple pion production and the nuclear environment during the collisions in which the pions are generated.

These experiments offer the simultaneous opportunities of learning qualitatively new features about the fundamental characteristics of bulk nuclear matter and of further elucidating pion-nucleon relationships. The knowledge to be gained is a compelling justification for the CSC accelerator.

References

1. G. Bertsch and M. Johnson, Phys. Rev. D12(1975)2230.
2. R. Sawyer, private communication.
3. P. Bonche, J. Negele, and S. Koonin, Phys. Rev. C13(1976) 1226.

4. D. Sparrow, et al., Phys. Rev. C10(1974)2215.

5. G. Bertsch, to be published.

6. N.S. Wall, et al., Nucl. Phys., to be published.

7. P. McNulty and R. Filz, Conference on Nuclear Photography, Vol. II, M. Nicolae (ed) (Institute of Atomic Physics, Bucharest, 1972, p. 170.

8. W. Schimmerling, et al., Phys. Rev. Lett. 33(1974)1170.

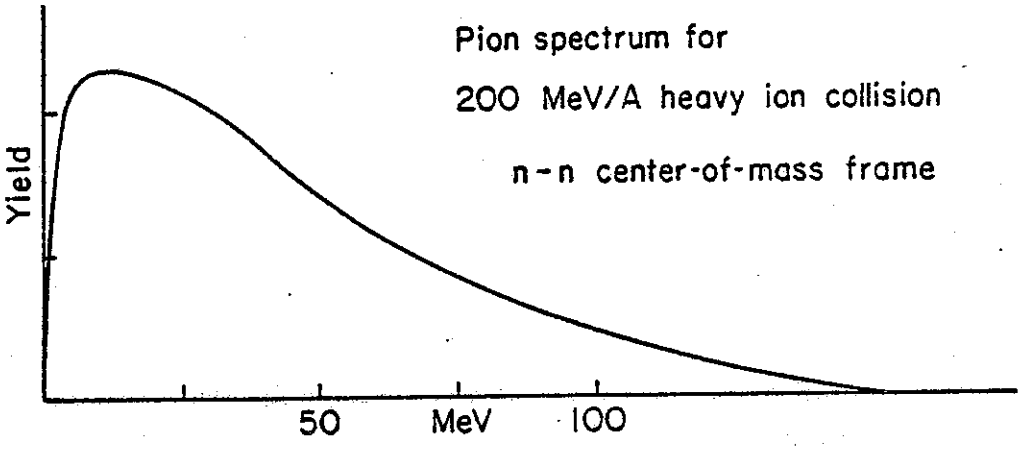

Fig. 2.(III.4.4).--(See Ref. 5). Energy spectrum of pions from heavy-ion collisions at 200 MeV/amu.

Fig. 1.(III.4.4).--(See Ref. 5). Excitation function for incoherent pion production.

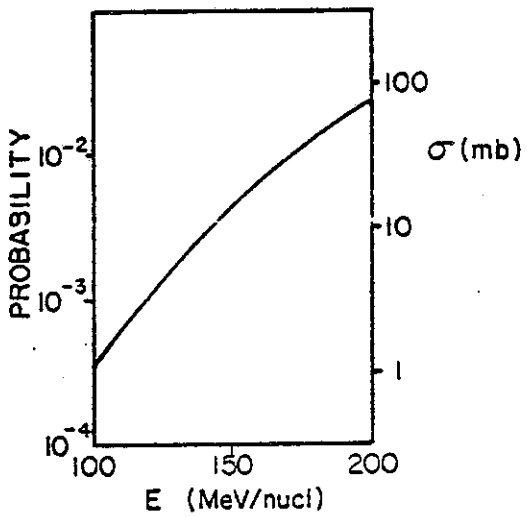

Addendum to III.4

High Density Nuclear Matter

One of the most important motivations for constructing the CSC is to study nuclear matter at high density. There are two natural boundaries defining the range of energy where the effects of compression will be most significant. The lower boundary is set by the velocity of sound in nuclear matter. A reasonable estimate of this velocity, v_s, is:

$$v_s \approx \sqrt{K/9m} \approx \sqrt{250/(9\times938)}\ c$$
$$\approx 0.17c,$$

where K is the compressibility of nuclear matter. Projectiles with higher velocity, i.e. $E > \frac{1}{2}mv_s^2 \approx 14$ MeV/A, will begin to significantly compress the target during the collision. The upper energy boundary is set by the condition that the Pauli principle permits two nuclei to completely overlap in momentum space. The Fermi sphere has a radius of 1.34 fm^{-1}; thus the projectile must carry a momentum of 2 x 1.34 fm^{-1}/A, equivalent to an energy of 150 MeV/A, for this criterion to be satisfied. Of course precise details of the attainable density as a function of energy depend on the equation of state; numerical estimates have been made for potential models neglecting nucleon-nucleon collisions,[1] as well as for a model assuming only collisions and no potential field dynamics.[2]

When the bombarding energy sizeably exceeds the full overlap value, nucleon-nucleon collisions become more important than the overall potential fields in determining the evolution of the system. Experiments at relativistic energies, carried out at the Bevalac, have not shown serious deviations from the predictions of models that assume independent collisions. In experiments

that measure double differential cross sections for protons,[3] the data can be satisfactorily explained by a cascade calculation[4] except for the most forward angles and much of the data can in fact be explained by single collisions alone.[5] Nor does the production of pions by alpha particles at relativistic energies show any deviation from the model of independent production by the projectile nucleons.[6] The multiplicity distribution of pions[7] is also satisfactorily explained by a statistical cascade hypothesis.[8] Deviations from independent collisions will certainly arise at lower energy because the potential field becomes relatively more important, and it is there that most attention should be focused. We now describe the kinds of experimental information which we expect will shed light on high-density dynamics.

Longitudinal Energy

In order to sort out the effects of high density, it is crucial to find an experimental signature separating central collisions (small impact parameter) from peripheral collisions. A characteristic of the collision which ought to be useful in this regard is the energy carried out of the collision along the beam axis. We define this nonrelativistically in the CM system as

$$E_{||} = \sum_i p^2_{||_i}/2m_i$$

Here the sum is over all particles leaving the collision, composite or not. The $p_{||_i}$ is the component of momentum of the ith particle along the beam direction. The longitudinal energy $E_{||}$ will vary from a maximum value close to the incoming CM energy to a minimum

which depends greatly on the physics of the central collision.

Complete thermalization in a central collision gives an $E_{||}$ which is 1/3 of the incoming CM energy. Hydrodynamic models predict $E_{||}$ for central collisions to be even smaller whereas models in which the central field dominates predict a much higher $E_{||}$. At present it seems most likely that the potential models will be closer to reality. The optical potential for 100 MeV nucleons[9] predicts a mean free-path of about 5 fm. For colliding nuclei, the Pauli principle will restrict collisions even further,[10] and we therefore expect a theory in which the potential dominates to have the most validity. If there should turn out to be unusual physics, such as second order phase transitions, the thermalization will be much more complete. A specific model for such a possibility has been made by Ruck et al.[11]

Measurements of the distribution in $E_{||}$ as a function of bombarding energy and projectile-target combination will be very important in testing these models. The use of equal mass targets and projectiles will simplify the theoretical analysis. A simple thermalization model, such as the "fire ball model" that has been applied to relativistic collisions,[3] would yield a distribution in $E_{||}$ that rises smoothly from the minimum $E_{||}$, characteristic of zero impact parameter, to the bombarding energy. In addition, there would be a peak near the bombarding energy due to quasi-elastic collisions. This is sketched in Fig. 1. As the projectile energy is decreased, this curve will alter its character until at some point a second peak appears at small $E_{||}$. This is the deep inelastic scattering phenomenon which is very pronounced at projectile energies of about 10 MeV/A.

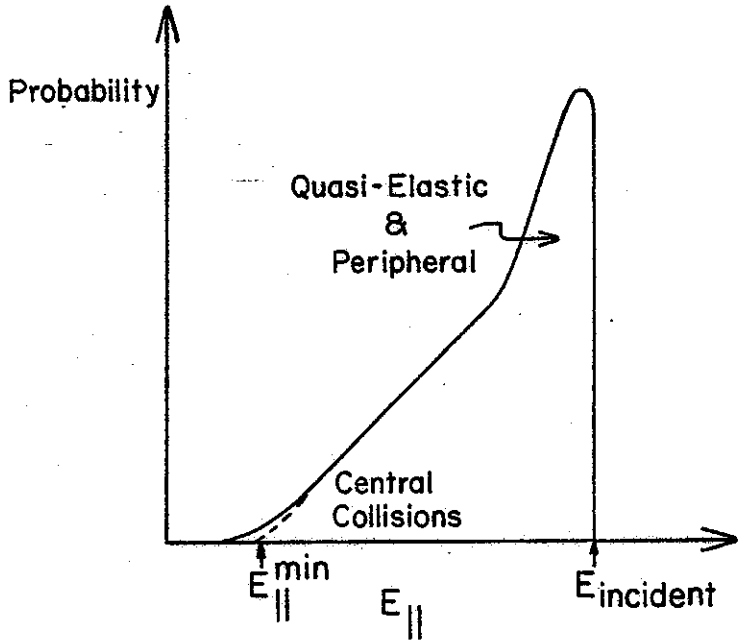

Fig. 1.

We note that the existence of a low energy peak has still not been given a satisfactory explanation; calculations today give large energy losses, but yield a peak only under special assumptions.[12] Thus it is of great interest to extend the energy range of this type of experiment upward to elucidite the deep inelastic phenomenon.

We have already made the point that the value of the minimum $E_{||}$ depends very much on the degree of thermalization in the collision. A phenomenological fit can be made, and then tested by studying the A-dependence of the thermalization. Larger projectiles and targets will have behavior closer to the hydrodynamic limit.

Angular Distributions

When many particles emerge from a collision, as we expect to happen at 100 MeV/A bombarding energy, the angular distribution of particles from a single event becomes measurable. One is always limited by the statistics of the particles emerging from the individual collision, but significant information can be obtained. For example, the angles of about 15 particles can be measured and fitted to a distribution of the form

$$f(\theta,\phi)\alpha\, Y_o+\Sigma_m b_m Y_{2m}(\theta,\phi).$$

The coefficient b_m has an uncertainty of the order of 0.2.[13] Even with this uncertainty, measurements can be useful in elucidating the dynamics of a collision. If the potential field dominates the dynamics, the distribution $f(\theta,\phi)$ will be prolate along the beam axis. In hydrodynamic models, $f(\theta,\phi)$ will be oblate for central collisions. Thus the sign for the b_o is of qualitative significance.

An asymmetry about the beam axis should be present for non-central collisions. The axial asymmetry of $f(\theta,\phi)$, determined by the coefficients b_m for $m\neq 0$, might depend on several different effects. The interaction region in peripheral collisions can be shadowed by the nuclei themselves and this will produce an axial asymmetry in the distribution of higher energy particles. Asymmetry in the distribution of low energy particles (about 5 MeV) might also be present, as a consequence of the decay of rotating nuclei in the plane of rotation. Thus such asymmetry might be sensitive to the angular momentum transfer between the colliding nuclei, as has been found in the lower energy studies.[14]

Pion Production

According to current theoretical ideas on pion-nucleon interactions, nuclear matter is not far from a phase transition involving the pion field. Models for the behavior of the pion in nuclear matter show peculiarities such as a near-zero or negative effective mass for the pion.[15] Under such conditions, pions can be produced in the interactions of nucleons with the potential field,[16] in addition to production in the collisions of nucleons with each other. The rate of pion production is thus increased by the potential field mechanism, and a characteristic angular distribution is predicted for the pions. Production of Cerenkov radiation is an analogous phenomenon involving the electromagnetic field.

On the experimental side, there is not yet any definitive information of the pion production cross section at nonrelativistic energies. Emulsion data published within the last year are in complete disagreement with each other. In one case they show a very high pion multiplicity per collision,[17] but no evidence at all for pions in the other cases.[18,19] A theoretical prediction has been made for this cross section, based on production by nucleon-nucleon collisions alone.[20] An MSU-Berkeley-Tokyo-Osaka group is already attempting a further measurement of pion production below the nucleon-nucleon threshold using a 180° magnetic spectrograph at the Bevalac. In preliminary runs the spectrograph has performed well for both negative and positive pion detection in the sensitive region of pion energy between 20 and 100 MeV. Runs at 200 and 250 MeV/A are planned in the near future, and some of the basic questions will then hopefully be answered. The quantity, quality and availability of Bevalac beams will however sharply limit future exploration either downward in

energy or into global A, Z and θ dependence.

The combination of the CSC and the existing Enge split pole, which will make an excellent pion spectrograph, will permit a very broad attack on the problem of subthreshold pion production. It should be possible, with the intense beam of the CSC to carry out experiments at the nucleon-nucleus threshold (about 150 MeV/A) and even below, where a comparison can be made to the Indiana proton results.[21] The A and Z dependence will be studied. Comparison of π^+ to π^- production for various combinations of T_z for the target and projectile may yield information on the separate neutron and proton contributions.

Even if there is no evidence of coherent production of pions by the potential field, the pions should be a useful probe of the early stages of the collision. Pion elastic scattering data[20] show that low energy pions can have rather long mean-free-paths in nuclei, about 5 fm. Pions will be produced mostly during the earliest part of the collision, if the bombarding energy is not too high. Thus the emerging pions are unique in carrying information from the high density region of the nuclear collision. If the potential field strongly resists the density increase, as is the case for one model,[22] there will be little available nucleon kinetic energy and few pions will be produced. On the other hand, if the potential field is attractive, the nucleons will be accelerated into the high density region and more pions will be produced. Thus the measurement of pion production in this region will provide information on the nuclear equation of state, even if it fails to uncover collectivity in the pion field.

Temperature

The concept of temperature in use today may not be relevant to an ultimate understanding of energetic heavy ion collisions, but it has certainly been useful in organizing the data. There are many situations in which some particle or fragment shows an exponential distribution in kinetic energy; the "temperature" is then the inverse slope of the exponential. Also, relative abundance of the fragment can be described by an exponential distribution in binding energy differences; this yields another temperature. In Table I are summarized the kinds of data so analyzed and the temperatures deduced.

TABLE I.--Temperature in Energetic Heavy Ion Collisions.

Measured Quantities	Projectile Energy	Temperature	Reference
Kinetic Energy Distribution: evaporation neutrons	low	1 MeV	
protons	400 MeV/A	30	a)
low energy He^3	2 GeV/A	25	b)
		60	c)
heavy fragments	2 GeV/A	9	d)
Isotope Abundances	<20 MeV/A	2	e)
	>20 MeV/A	7	e)

a) G.D. Westfall, et al., Phys. Rev. Letters 37,1202(1976).
b) B. Jakobsson, et al., Nuclear Physics A276,523(1977).
c) J. Stevenson, et al., Phys. Rev. Letters 38,1125(1977).
d) D.E. Greiner, et al., Phys. Rev. Letters 35,152(1975). (exper.) and A. Goldhaber, Phys. Letters 52D, 306(1976). (theor.)
e) K. Gelbke, et al., Phys. Letters 65D, 227(1976).

Note that there seems to be a limiting temperature of about 9 MeV for the heavy fragments. Is this because any higher temperature is immediately lost by break-up into more fragments or "boiling"? This intriguing suggestion has been made by David Scott. The Berkeley group have also found an indication that the temperature of the heavy fragment changes rather discontinuously from about 2 MeV to about 8 MeV when the bombarding energy exceeds 20 MeV/A. Could this be caused by another mechanism for the fragment production, such as penetration of the projectile through the nucleus? In the potential field model, nuclei are somewhat transparent at small impact parameters.[1]

The study of fragment energy distributions and isotopic abundances, tracking the behavoir from low energy to high energy, will help to answer these questions.

Peripheral Dynamics

An important issue in the study of heavy ion collisions is the relative importance of the potential field, or mean potential interaction, as compared to the collisions, or fluctuating part of the interaction. This can be studied rather cleanly in the peripheral reaction. Namely, if a projectile and target interact by a two-body collision, both will be excited simultaneously. If the mean field of the interaction dominates, the projectile excitation will be independent of the target excitation. At low energies, the potential field description is excellent. For fragmentation of relativistic nuclei, the potential field description has been applied with some success.[23] However, quantitative tests are needed with projectile and target excitation measured simultaneously, for example using gamma rays to

measure target excitation.

References

1. K. Bonche, et al., Phys. Rev. 313,1226(1976).
2. A.N. Ansden, et al., Phys. Rev. Letters 38,1055(1977).
3. J. Gosset, et al., Phys. Rev. C16,629(1977).
4. Z. Fraenkel and Y. Yariv, unpublished.
5. S. Koonin, Phys. Rev. Letters 39,682(1977).
6. J. Papp, et al., Phys. Rev. Letters 34,292(1978).
7. S. Y. Fung, et al., Phys. Rev. Letters 40,298(1978).
8. M. Gyulassy and F. Kaussmann, Phys. Rev. Letters 40,298(1978).
9. C. Perez and S. Perez, Atomic Data 17,2(1976).
10. G. Bertsch, Phys. Rev. C15,713(1977).
11. B. Ruck, et al., Z. Phys. A277,391(1976).
12. C.M. Ko, et al., to be published.
13. G. Bertsch, Los Alamos preprint LA-UR-78-483.
14. P. Dyer, et al., Phys. Rev. Letters 39,392(1977).
15. G. Bertsch and N. Johnson, Phys. Rev. D12,2230(1975).
16. R. Sawyer, Nucl. Phys. A271,235(1976).
17. P.J. McNulty, et al., Phys. Rev. Letters 38,1519(1977).
18. P. Lindstrom, et al., Phys. Rev. Letters 40,93(1978);
19. R. Kullberg, et al., Phys. Rev. Letters 40,289(1978).
20. D. Malbrough, et al., Los Alamos preprint LA-UR-77-1939.
21. R.E. Pollock, R.D. Bent, P.H. Pile, P.T. Debevec, R.E. Mairs, and M.C. Green, B.A.P.S. 22,1006(1977) and to be published.
22. F. Chin and J.D. Walecka, Phys. Letters 62B,24(1974).
23. H. Feshback and M. Zabak, Annals Physics 107,110(1977).

IV. Technical description of the facility

Detailed planning of a facility to be used in the 1980's and 90's is obviously difficult -- many details of any present plan will with certainty become inappropriate or burdensome as time evolves -- changes will be needed to match the evolution of the scientific discipline. Long-range plans should facilitate change by emphasizing features which enhance flexibility and expandability whenever this is reasonable. Further it is prudent to defer detailed design of elements which will not be needed for a number of years so as to utilize latest developments in instrument technology and experimental technique. Technical planning for the CSC facility has then thus far concentrated on the accelerators since these are the longest lead time item.

The design for the 500 MeV cyclotron proposed here is now largely frozen (and the elements related to the prototype magnet are under construction). The 800 MeV cyclotron is also in an advanced stage of design. Plans for the building and for the beam transport system are less advanced but are laid out in basic details. Plans for experimental apparatus are in a somewhat more qualitative state since ideas as to optimum apparatus will evolve between now and the time when construction of such apparatus would actually start; our apparatus plans are then mainly conceptual ideas at present, and these focus on instrumentation which would be appropriate if we were ready now to proceed with construction. These conceptual plans provide a reasonable basis for estimating costs while avoiding

the wasted effort implicit in going forward with engineering details at this time. (The important element at the proposal stage is to provide an adequate budget allocation for experimental equipment; if our budget, given in Section V, is broken down in categories of building, accelerators, shielding, beam transport system, and experimental equipment, the last category is 30% of the total budget, or $3,960,000; we believe this is a sufficient and appropriate allocation for experimental equipment.) The following subsections review major design features of the facility.

IV.1 The superconducting cyclotrons

Our discussion of the superconducting cyclotrons will primarily review novel design features of such cyclotrons. Conventional components, particularly those which parallel features of our present cyclotron, will generally not be reviewed. If this process leads to omission of points of particular interest to any reader, we will be pleased to supply additional information on any point.

The idea of a superconducting cyclotron was explored at MSU in the early 1960's[1] but was laid aside due to the unreliability of the conductors then available. In 1973 a renewed study of superconducting cyclotrons was undertaken by a group at Chalk River under Fraser.[2] After preliminary exploration, Fraser's group concluded that the evolving superconducting coil technology was such that a cyclotron constructed using such a coil would be a major economic breakthrough leading to much lower construction costs and also to lower operating costs. Superconducting cyclotron studies were then reactivated at MSU in the fall of 1973. Concurrently studies were in progress at the Lawrence Berkeley Laboratory.[3] More recently a study and development program has been initiated at the University of Milan.[4]

The "superconducting cyclotron" is in fact a superconducting main coil combined with a room temperature cyclotron, i.e. trim coils, rf system, vacuum tank and all other components are at room temperature. Such a cyclotron is fundamentally the same as present isochronous cyclotrons but with a magnetic field

which is approximately three times higher, yielding a ninefold increase in energy (nonrelativistically) for the same physical size. Furthermore, the superconducting main coil is similar in size and style to coils used on a number of large bubble chambers and thus involves an established technology. (The oldest of the bubble chamber coils[5] has been in service since 1969 and has proved to be extremely reliable.)

The basic accelerator physics in the new cyclotrons proposed here is a direct take-over of concepts in use in the present MSU Cyclotron. Focusing frequencies, orbit stability limits, orbit resonances, orbit size, number of revolutions, orbit turn separation, resonant extraction system, . . . all closely match the corresponding quantities in the present cyclotron. Qualitatively this implies that beam properties in the new cyclotrons will match corresponding characteristics of the present cyclotron, provided engineering details of the design and construction are of comparable quality. Beyond the qualitative conclusions, extensive quantitative calculations of all orbit features have been made (and with greater accuracy than has previously been possible at the comparable stage of design). We omit detailed review of these calculations. Overall, the calculations indicate excellent behavior in all basic properties. Orbits are stable, well focused and insensitive to reasonable construction errors.[6]

The major areas where the proposed cyclotron system will be different from traditional cyclotrons are: 1) the general mechanical structure (where access is largely from top and bottom versus the traditional median plane access), 2) the super-

conducting main coil, 3) the ion source, 4) the extraction system, and 5) problems related to operating the cyclotrons as a coupled pair. Our discussion of the cyclotron system then focuses on these features.

Before proceeding we note the important role of our expert consultants. These include Mr. J.E. Purcell of General Atomic Corporation (on leave as head of the Superconducting Coil Group at Argonne National Laboratory), Mr. R. Niemann, Acting Head of the Argonne Superconducting Coil Group, Mr. R.J. Burleigh, former head of the Mechanical Engineering Department of Lawrence Berkeley Laboratory, Mr. J. Riedel, former head of the Radio Frequency Group at the Princeton-Pennsylvania Accelerator, Mr. Richard Wolgast, head of the Cryopumping Section of the Lawrence Berkeley Laboratory, and others. These gentlemen are recognized world experts in their specialties; they have played and will continue to play a basic and vital role in the evolution of the superconducting cyclotron concept. With these consultants augmenting our own cyclotron experience, our design group has an expertise in the technical areas relevant to the project which is both broad based and outstanding. We believe that nothing in a technical project contributes more to design efficiency and to ultimate performance than having the best possible design group. We intend to continue throughout the project to use all available channels to maximize the overall expertise of the accelerator group.

IV.1.1 Mechanical structure of the superconducting cyclotrons

The mechanical design of the superconducting cyclotron is heavily influenced by the need for good thermal insulation on the main coil and by the large attractive force (approximately 900 tons) between the upper and lower halves of the coil. These requirements, plus the need for a sharp magnetic field edge to facilitate extraction, favor a design in which the separating structure between the upper and lower main coils is a mostly solid, low-temperature member. Figure 1 shows a schematic drawing of the coil and cryostat with this type of design.

At several points penetrations through the cryostat are necessary to provide for the beam extraction system, the injection system (second cyclotron only), deflector feed-throughs, probes, etc. These penetrations are necessarily small and also complicated since they must be thermally insulated from the coil. The natural main access to the center of the cyclotron is then axially from the top, and the upper part of the yoke will be mounted on a jacking system to precisely raise the upper yoke in pushbutton fashion following the design of a similar system in use on the TRIUMF cyclotron.[7]

Since the cryostat already cuts off most median plane access, it is natural to use a pill-box yoke. Such a yoke has maximum magnetic efficiency and also best contains the stray magnetic field. Figure 2 is a schematic drawing of the cryostat including the pill-box yoke and the pole tips. Figure 3 is a photograph of the actual yoke awaiting inspection in the fabricator's shop.

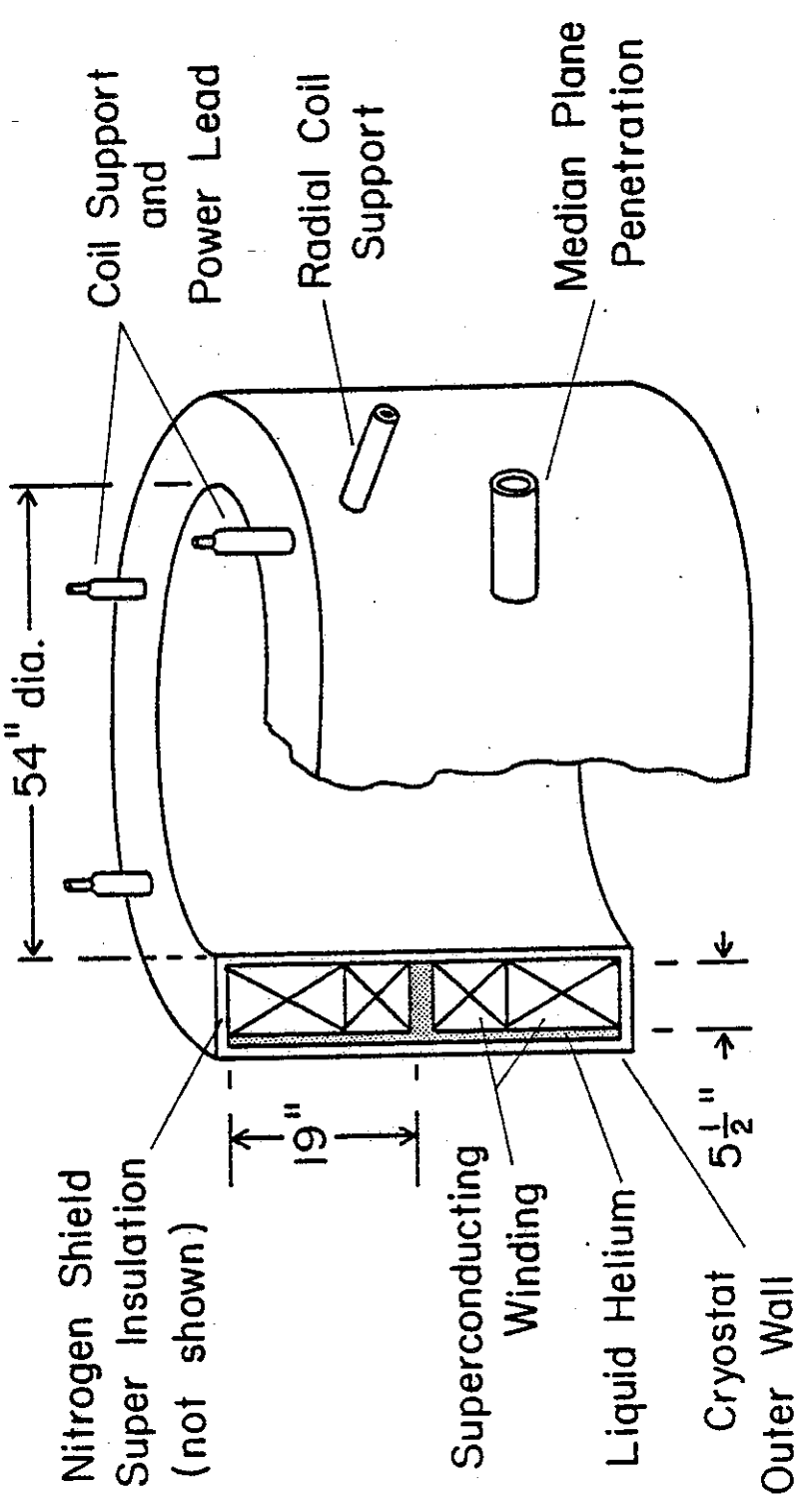

Fig. 1(IV.1).--Schematic diagram of the superconducting coil and cryostat. Winding active area has 60" inner diameter and ±1.5" spacing from median plane. Amp-turns=2x(2,360,000).

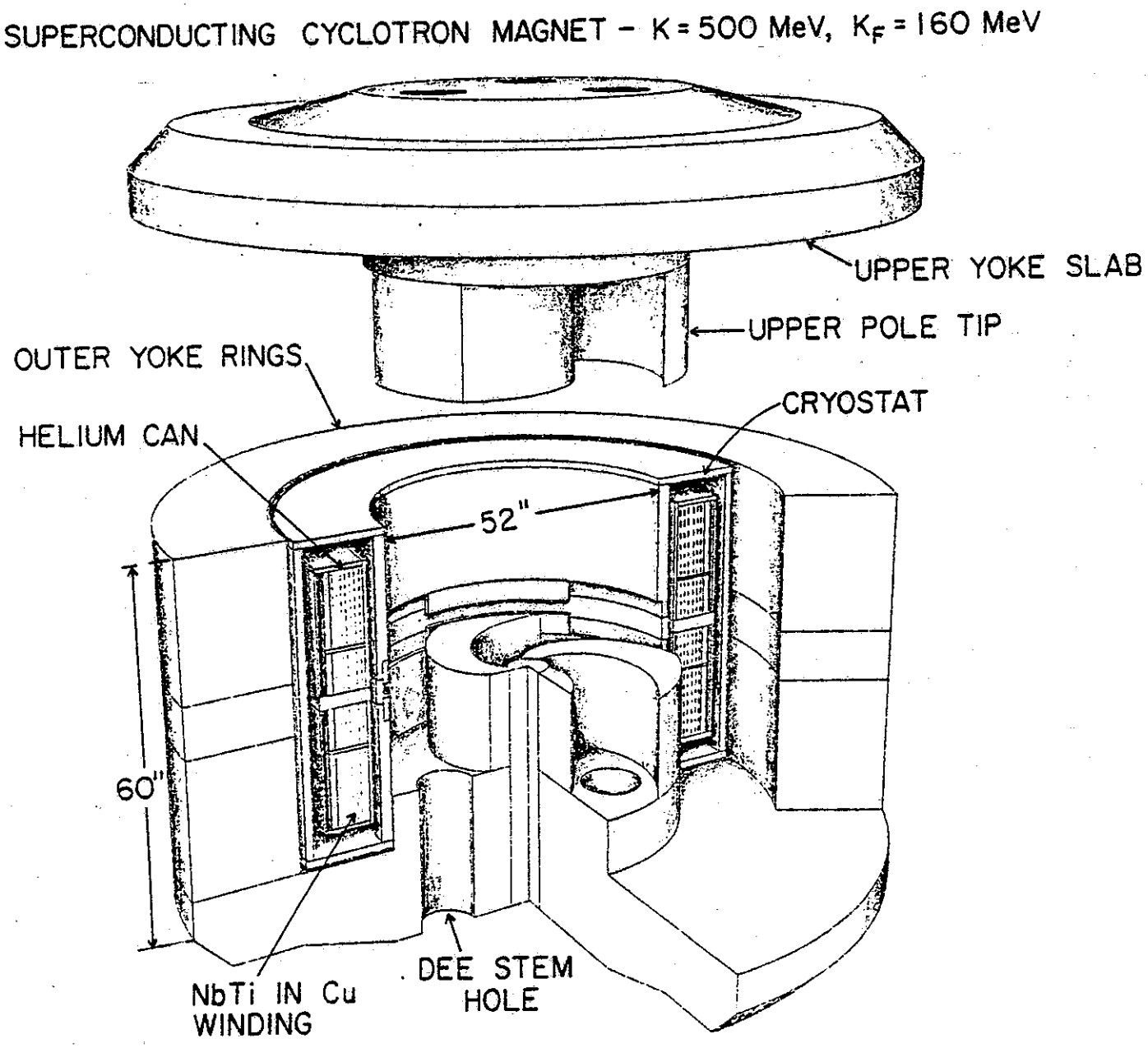

Fig. 2(IV.1).--Perspective view of the complete superconducting magnet with cryostat in position and upper yoke slab raised. Note the cylindrical outer yoke and propeller-like spiral pole tips.

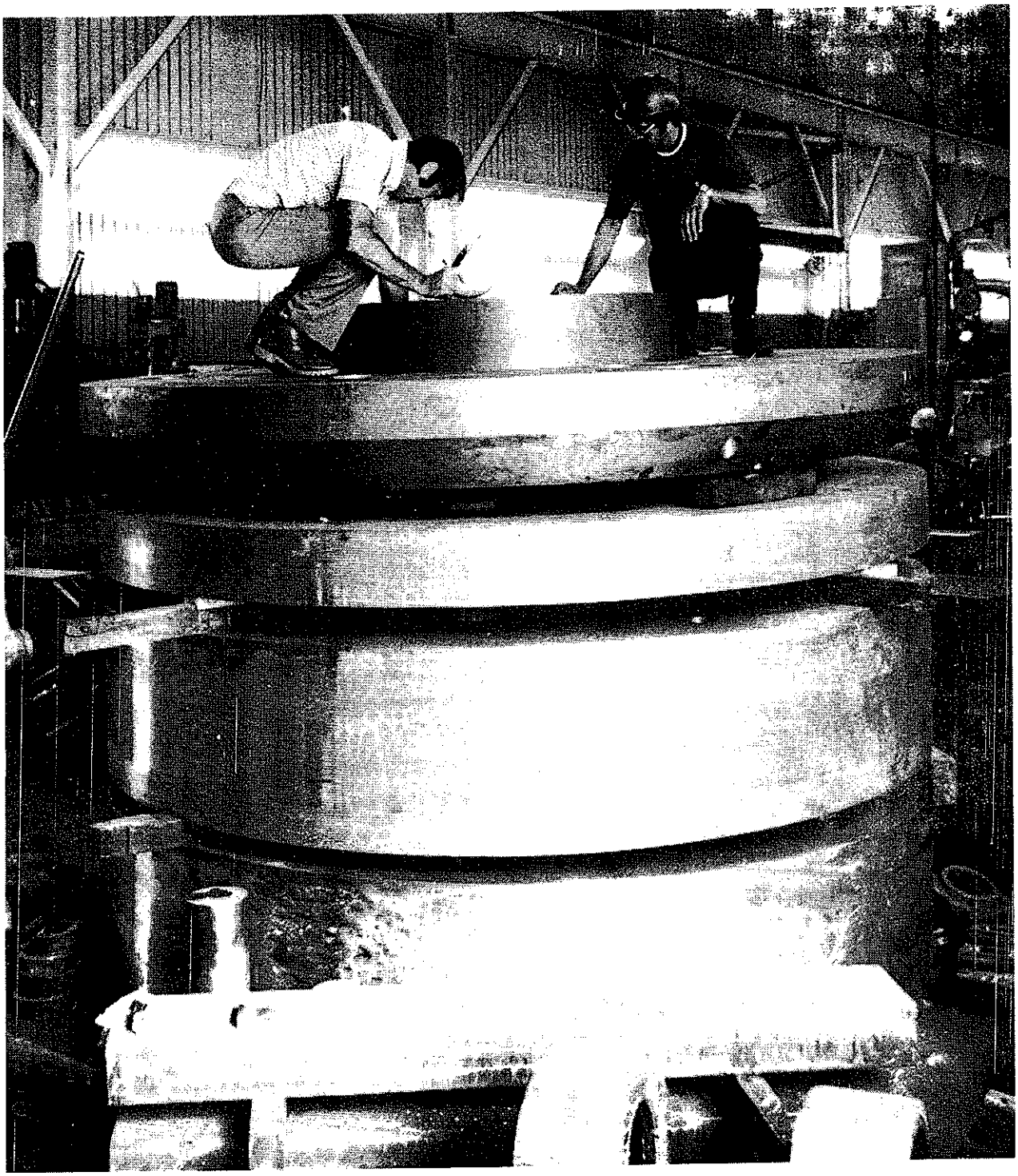

Fig. 3(IV.1).--Photograph of the magnet yoke stacked in the fabricator's shop awaiting final assembly. The yoke is ten feet in overall diameter, weighs approximately 90 tons (total for five pieces) and is fabricated from cast 1020 steel. Magnetic tests of samples taken from the castings indicate excellent magnetic uniformity. Ultrasonic tests indicate that the castings are free from voids.

Further mechanical details of the two cyclotrons are shown in Figures 4, 5, and 6, which give vertical section views of the 500 MeV and 800 MeV cyclotrons, and a horizontal section view of the 500 MeV machine.

In both cyclotrons the acceleration system is a dee-in-valley design with three dees mounted on quarter wave stems which extend up and down. Tuning of the dees is by a hydraulically clamped sliding short on the main stems, with a capacitive electrode for fine tuning. Both cyclotrons operate over the same tuning range, namely 27 to 84 Mhz, and are driven from a single master oscillator. In the first cyclotron, operation is on either the 3rd or 9th harmonic of the orbital frequency, depending on the Q/A of the ion. The three dees therefore operate in phase and can be mechanically joined at the center. At the transition to the 800 MeV cyclotron, the design requires a threefold decrease in the harmonic number (see Sec. IV.1.5) so that operation in this cyclotron is on the first harmonic or the third harmonic. (When the 800 MeV machine is in the first harmonic mode, the dees must be phased by 120°, a feature which has been used only once before in cyclotrons,[8] but which is considered routine by rf experts.)

Resonant frequencies of the proposed dee structure have been verified in a half scale rf model. A full scale model is planned for checking details of the drive system. The small size and low capacitance of the dees (~30 pf/dee) result in low rf power. For the 500 MeV cyclotron, estimates of rf power including corrections for stray ions, imperfect joints,

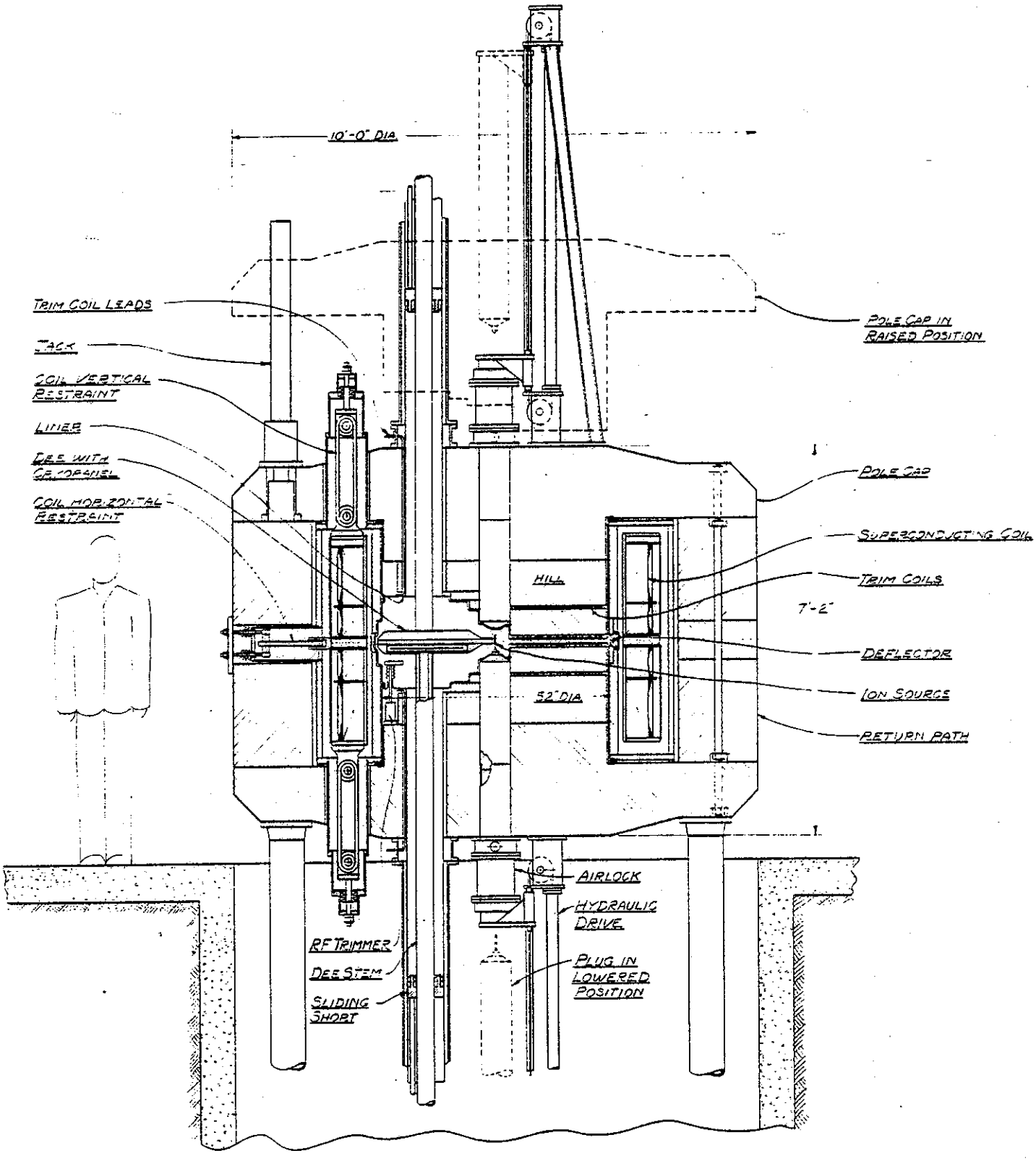

Fig. 4(IV.1).--Vertical section view of the 500 MeV superconducting cyclotron showing major components.

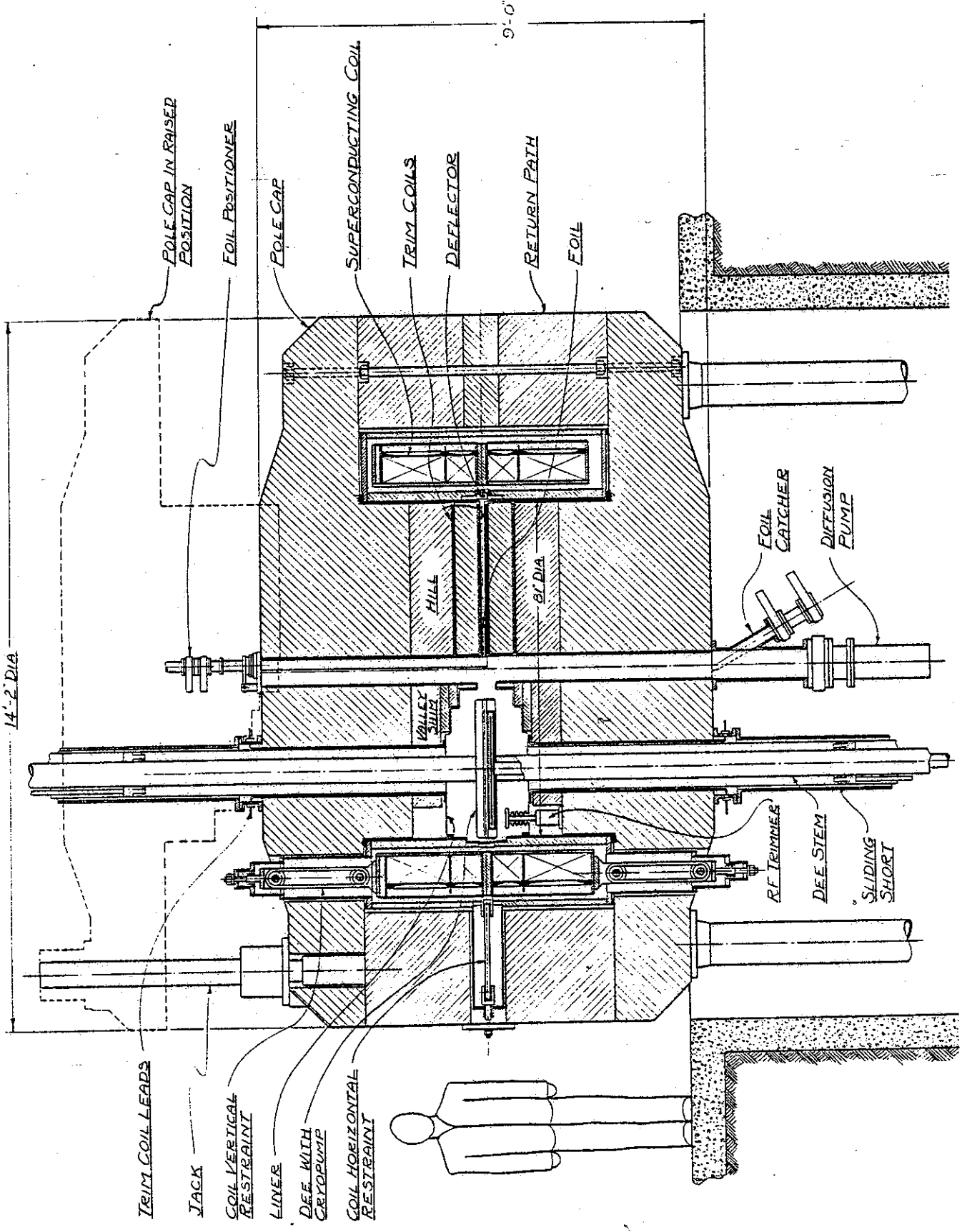

Fig. 5(IV.1).--Vertical section view of the 800 MeV superconducting cyclotron showing major components.

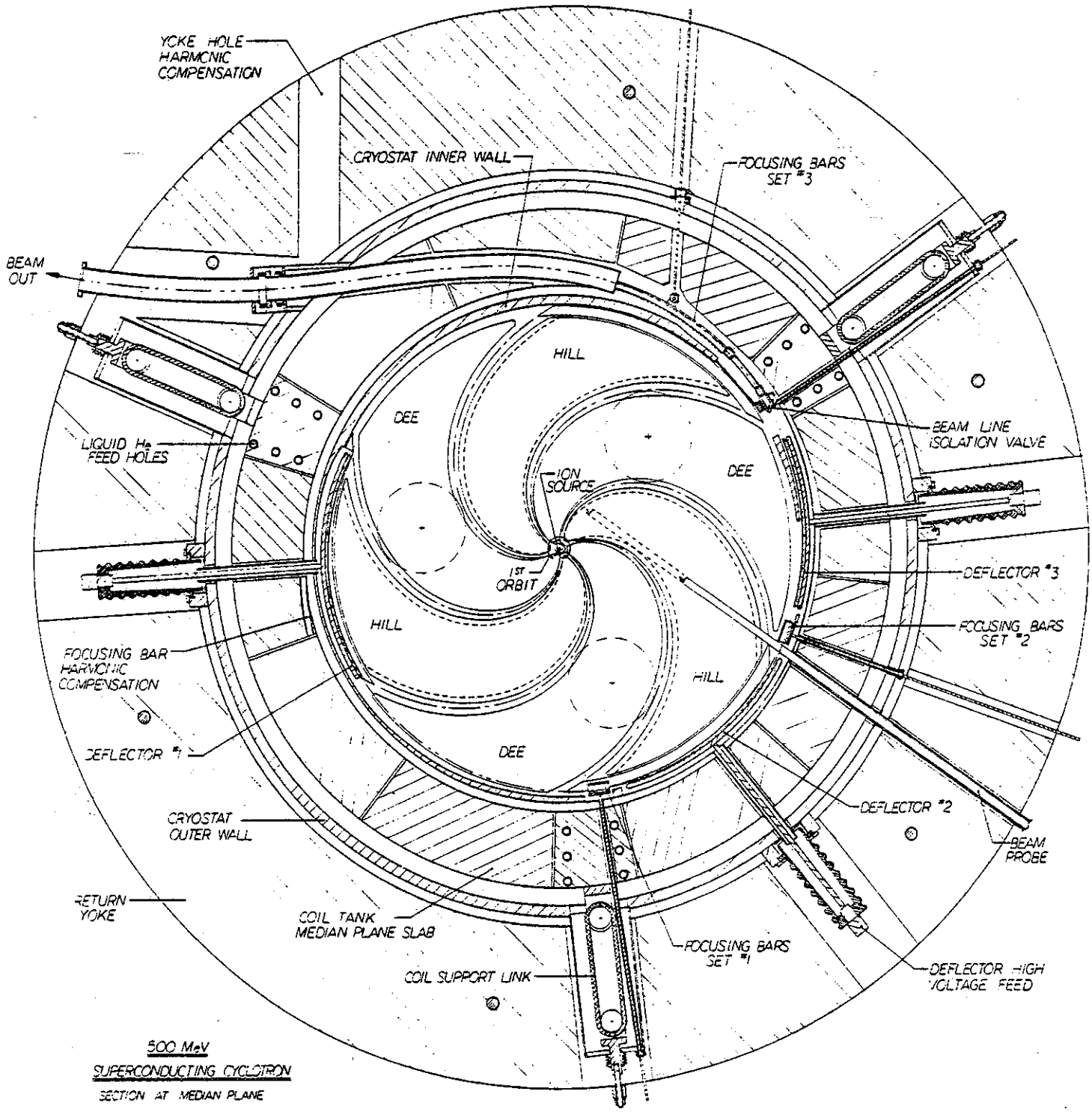

Fig. 6(IV.1).--Median plane section view of the 500 MeV cyclotron. The extraction system utilizes three electrostatic deflectors and three magnetic focusing elements as described in Sec.IV.1.4.

etc., give a total power of 180 kw. This is approximately 25% below the rf power for the present MSU Cyclotron even though the 100 kV dee voltage is significantly higher than the 70 kV used in the present cyclotron.

In both the K=500 and the K=800 cyclotrons, the vacuum system has three independent regions, namely 1) an insulating vacuum for the superconducting coil, 2) an ultra-high vacuum in the acceleration region, and 3) a roughing vacuum in the region of the trim coils. (The trim coils are hollow, water-cooled copper windings wound around the pole tips in a fashion such that each turn forms an approximate rectangle in the vertical (θ,Z) plane.) The acceleration chamber and the coil insulation space could in principle be connected, except that one would have to warm the coil in order to open the acceleration chamber, which would be excessively time consuming. With the separated vacuum chambers, the coil can stay continuously cold for long periods (most probably years at a time). The acceleration chamber is pumped by three large cryopanels located inside the dees. This puts the pumping surface as close as possible to the actual beam space (and, in the first cyclotron, to the gas load from the ion source, a point of great importance in obtaining intense beams of high charge state ions as indicated in Sec. IV.1.3).

The acceleration chamber vacuum is isolated from the trim coil vacuum by a continuous formed and welded copper liner covering hills and valleys and joined to the pole base at the upper and lower inner corner of the cryostat. It is not clear

at this time whether diffusion pumps will be needed in addition to the cryopanels. A key unknown is the quantity of hydrogen which will be produced by the large surfaces of exposed copper. A small diffusion pump might be needed to pump this hydrogen. Another possible hydrogen pumping system is to use hydrogen-getting surfaces on the cryopanels. This is at present a rapidly developing technology and may well be a totally adequate solution at the time the cryopanel design is fixed. Another pumping unknown hinges on whether helium beams will be in demand for the experimental program. If so a diffusion pump will be required for the source gas. If a diffusion pump is not initially included the design will provide for easy later addition of such a pump. Gaskets in the acceleration chamber will be mainly metal to reduce out-gassing loads.

One new and intricate element in the 800 MeV machine is the injection stripping foil. A detailed conceptual design of this system has been developed.[6] The design provides a 50 foil magazine with in-vacuum handling of foils at all points, and quick change (~30 sec) from foil to foil. There is also capability for changing magazines with magnetic field on. The structure encompasses all needed features and easily fits constraints set by the magnet gap, the magnet center hole, etc. The system now appears to be substantially overdesigned for presently anticipated intensity levels, i.e. recent information on foil lifetimes from tests at a number of laboratories[9] indicates an almost indefinite foil durability at energies corresponding to injection into the 800 MeV cyclotron. Depending on

source developments (see Sec. IV.1.3), the intensity realm of the CSC system may well ultimately extend to intensity levels significantly above those now expected and we therefore continue to include the foil magazine and rapid change system as a likely important and valuable feature at these higher intensity levels.

We then terminate our discussion of mechanical features of the two cyclotrons. The design of the 500 MeV machine is in an advanced stage with conceptual plans now complete for virtually all elements; details for the 800 MeV cyclotron are less advanced but in most respects the concepts involved in the 500 MeV cyclotron can be directly carried over.

Addendum to Sec. IV.1.1

Figure A is a photograph of the 500 MeV magnet in its temporary location at the east end of the Cyclotron Laboratory experimental area. The top of the magnet is raised in this photograph in order to display the spiral pole tips. Comparison of this photograph with Fig. 3 (IV.1) of the original text gives an immediate qualitative feeling as to progress in the period since the previous proposal. Results of magnetic studies on the 500 MeV magnet are presented in the addendum for Sec. IV.1.2.

Trimming of the magnetic field to match the mass increase of the broad variety of ions to be accelerated is accomplished by use of the two independent sections of the main coil and of a set of room temperature trimming windings wrapped around each pole tip; the arrangement of these room temperature correcting windings can be seen in Fig. B which shows a prototype set of windings assembled on one of the pole tips of the full scale wooden model. Results of trial calculations with these coils are also presented in the addendum for Sec. IV.1.2.

The design of the rf systems for the two cyclotrons has changed considerably from that described in the original proposal in order to avoid problem areas which turned up in detailed studies of the systems proposed. The CSC proposal for example speaks of an rf system in which the 500 MeV cyclotron operates on the 3rd and 9th harmonics of the rf, and the upper rf frequency is 84 Mhz. Detailed studies uncovered two relatively serious difficulties with this system, namely 1) at 84 Mhz, the physical size of the

500 MeV dee is too large a fraction of a quarter wave length and a severe voltage gradient along the dee then results, and 2) central region studies of acceleration on the 9th harmonic show a difficulty due to transit time effects between the source and puller, forcing the use of a DC bias on the source, a technique which is felt to be a likely source of maintenance difficulty. Both of these problems have been eliminated by shifting the design frequency range for the coupled cyclotron system to a much lower band, namely 9-27 Mhz.

With the 9-27 Mhz frequency range, operation of the coupled cyclotron system is excellent. High energy particles run on the 3rd harmonic in the injector cyclotron which is the peak energy gain harmonic, and geometry, clearances, and focusing on the early turns are all good. Low energy particles run on the 4th harmonic which has reduced energy gain, but because the final energy is also lower, turn clearances are larger than on the third harmonic. Major operating parameters for the coupled cyclotron rf systems are summarized in the upper lines of Table A (the entries labelled "long resonator").

The 9-27 Mhz frequency range does involve long dee stems, namely 200 inches at 9 Mhz. In the injector cyclotron, such long stems might be a source of difficulty due to mechanical vibration of the dees; on the first turn, the beam is extremely sensitive to geometric details of the electrode configuration and mechanical vibrations would modulate this geometry. To avoid this difficulty, dee stem insulators have then been introduced in the 500 MeV design.

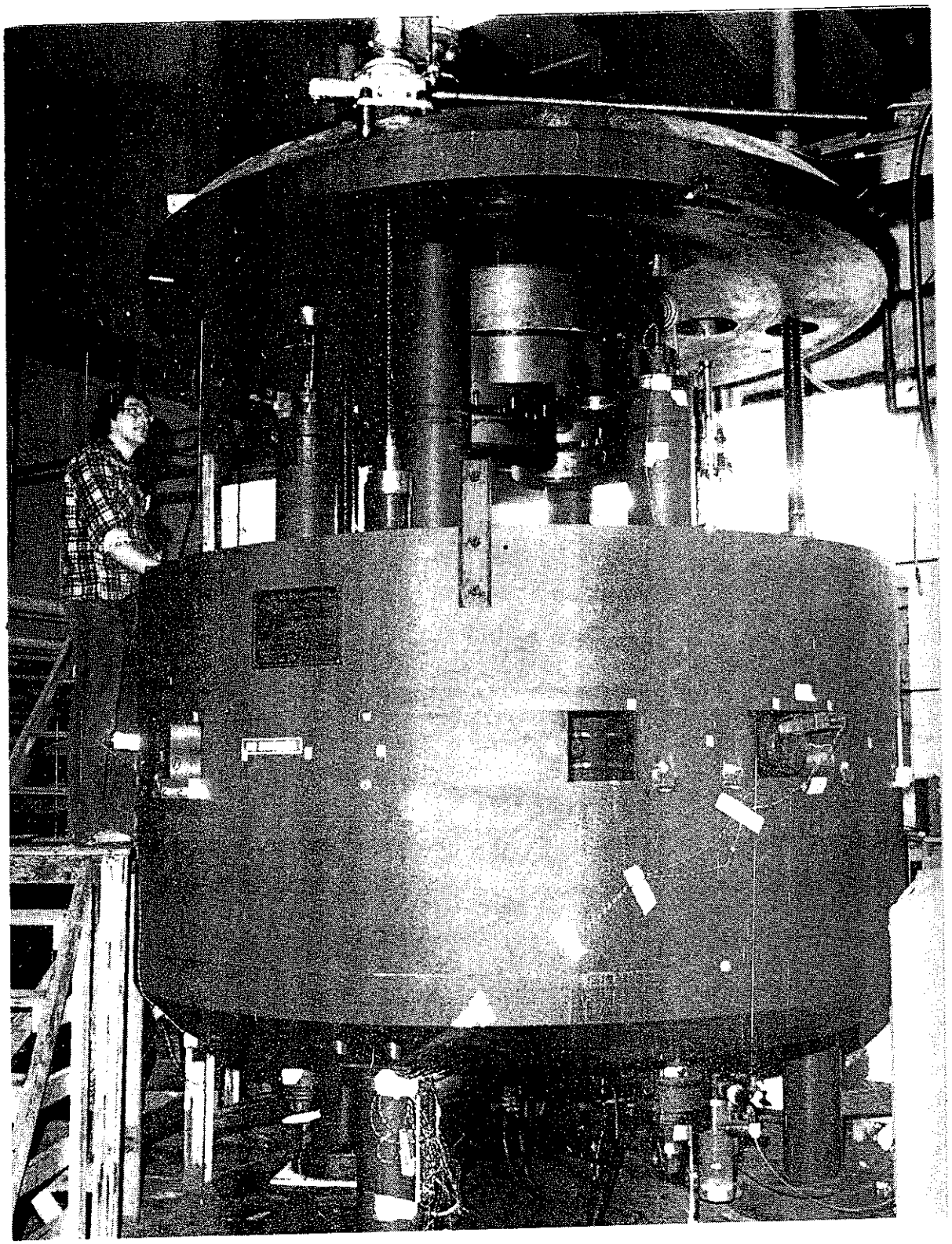

Fig. A (IV.1.1). Photograph of 500 MeV superconducting magnet with top raised.

Table A (IV.1.1). Frequency range, acceleration harmonic (ω_{rf}/ω_o), and energy range for "short" and "long" resonator systems.

Resonator	freq. range / short position	Acceleration harmonic		Energy Range MeV/A
		K=500	K=800	
long (coupled 500-800 operation)	9 — 27 Mhz / 200" — 66"	3	1	18 — 200
		4	2	4.2 — 40
short (stand-alone 500 operation)	30 — 65 Mhz / 60" — 18"	2		21 — 125
		3		9.2 — 45
		4		5.2 — 24

The insulators to be used are identical to insulators used on the main ring rf cavities at Fermi Lab. These insulators operate at Fermi Lab at voltages up to 70 kilovolts and no electrically caused failures have been experienced. This voltage range is completely adequate for the 500 MeV cyclotron when it is operating in the injector mode. A photograph of an insulator is shown in Fig. C.

When the 500 MeV cyclotron is operating as a stand-alone accelerator, the 9-27 Mhz frequency range is unfortunately not well matched to beam requirements. In particular, high energy light heavy ions such as C^{4+} would run in the first harmonic mode and detailed studies of central region orbits in this mode show a real difficulty, namely that when central electrodes are shaped to put particles in a region of strong electric focusing, as needed for good beam quality, a very narrow clearance is left between source and dee which would be only marginally adequate for holding the required dee voltage. Figure D is a view of the electrolytic tank facility which is used to obtain detailed

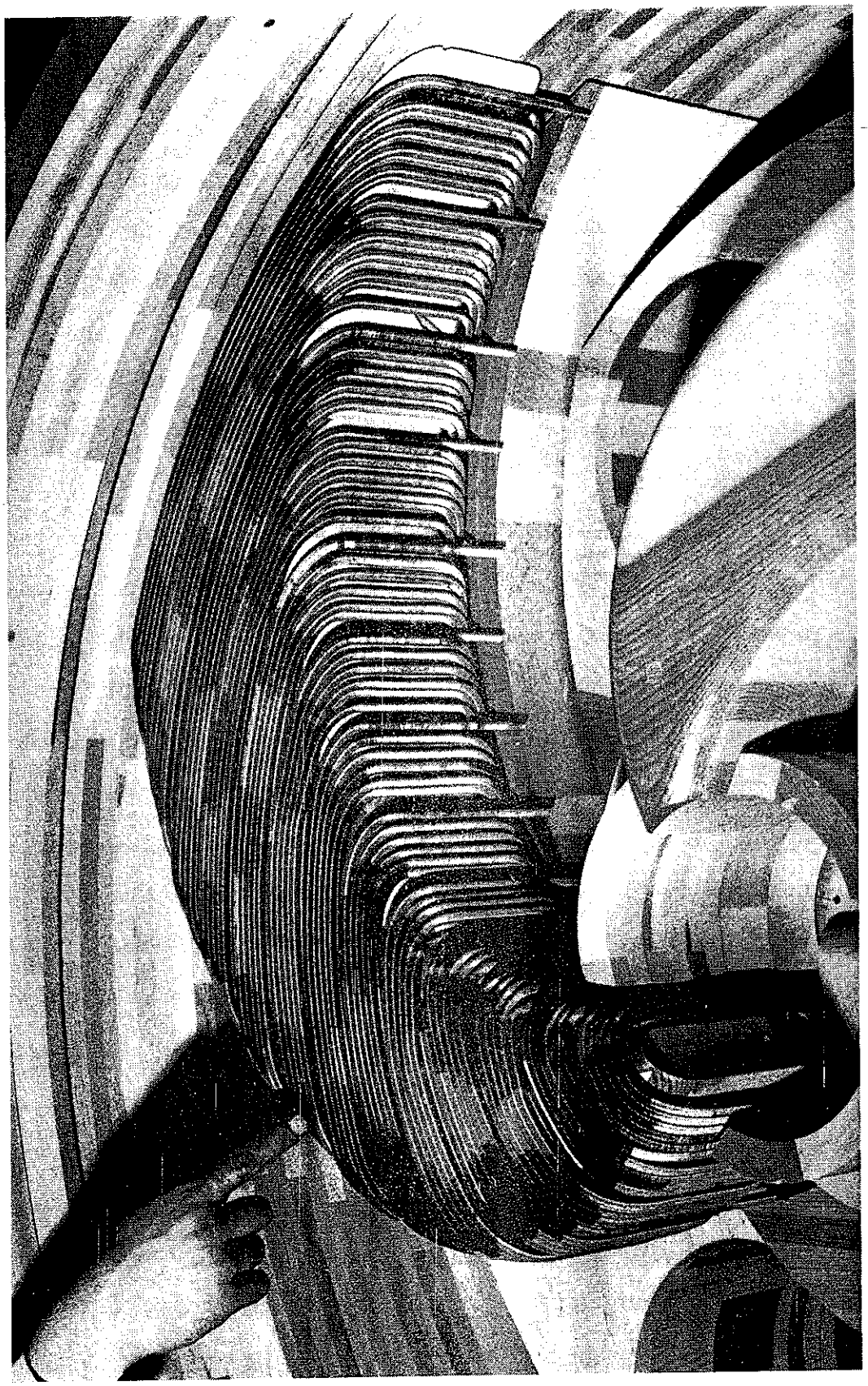

Fig. B (IV.1.1). Photograph of prototype set of trim coil windings wrapped on pole tip of full scale model.

electric field maps, and in the figure the tank is set up with electrodes in first harmonic position. The marginal clearance occurs between the puller electrode and the #3 dee in the photo. The difficulty is further exacerbated by the fact that particles for which the first harmonic central region problem is most severe are exactly those whose research potential is considered most interesting when the 500 MeV cyclotron is operating in the stand-alone mode. To eliminate this difficulty, we have then introduced an alternate second resonator into the design which we refer to as the "short" resonator.

Characteristics of the "short" resonator are shown in the lower part of Table A. These characteristics in general give an excellent match to requirements for the stand-alone operation. Figure E for example shows two typical central region orbits running on harmonics 2 and 3. The orbits are superimposed on voltage contours obtained from the electrolytic tank and overall have very desirable characteristics. The complete rf system plan is then to utilize the short resonator structure in the years when the 500 MeV cyclotron is operating as a stand-alone accelerator, and to shift to the long resonators at the time the coupled system comes into use.

The resonator for the 800 MeV cyclotron will be basically identical to the long resonators for the 500 MeV cyclotron since the dee systems in the two cyclotrons will always run at the same frequency. Dee stem insulators will however not be needed in the 800 MeV system since particles at the point of injection

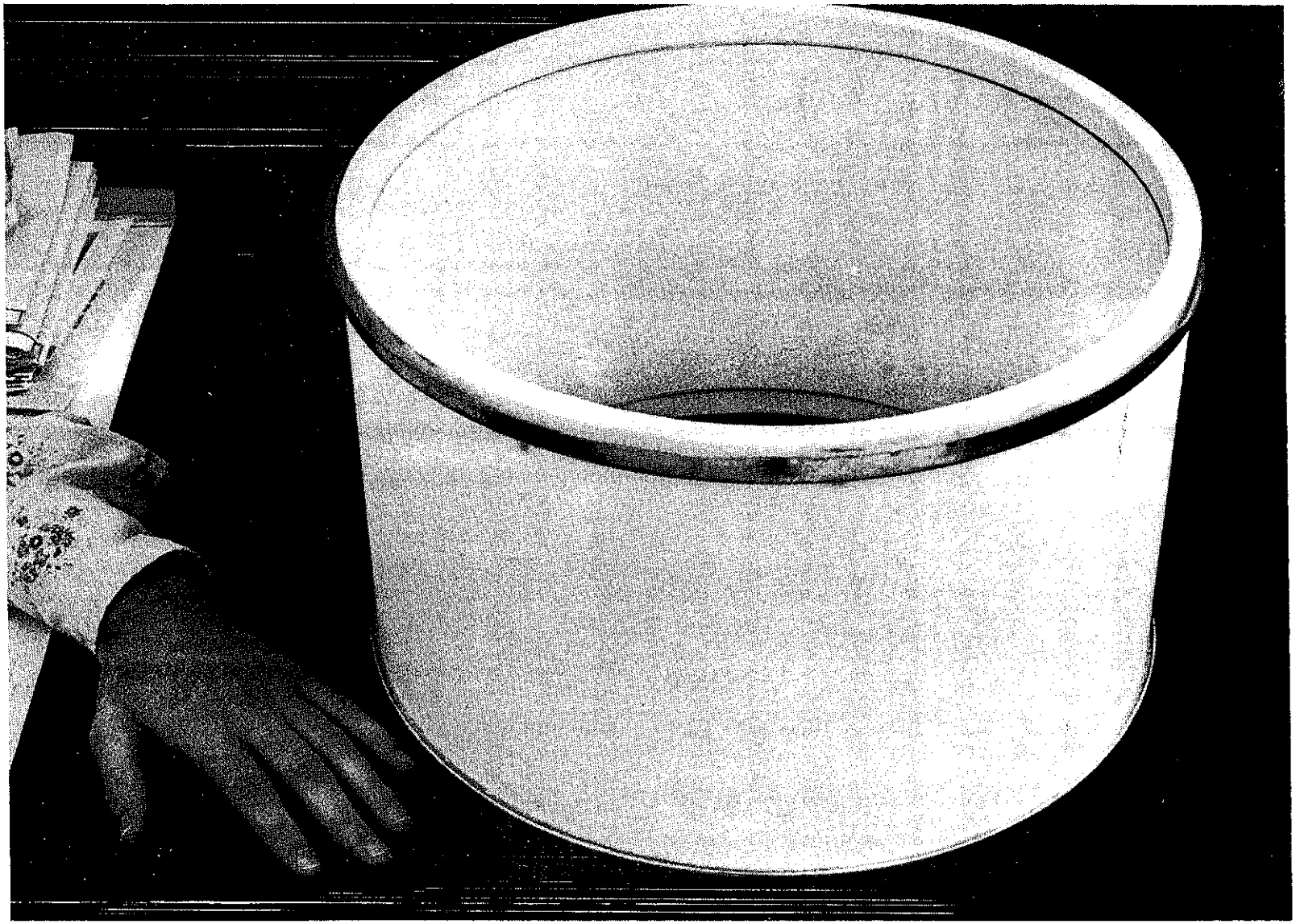

Fig. C (IV.1.1). Photograph of high purity alumina insulator of the type which will be used on the dee stems of the "long" resonator. (Insulator on loan from FNAL.)

will already be extremely rigid and will have no sensitivity to fine details of the electric field, and hence no sensitivity to possible mechanical vibrations of the dees.

The use of harmonics 1, 2, 4 etc. for acceleration brings a relatively novel rf requirement, namely the necessity to operate the dees in a three-phase mode as well as in the customary in-phase mode. Only one example of a cyclotron operating on the three-phase mode is known to us, and in view of this relatively brief experience, we constructed an rf model to provide a realistic test of the tuning system for three-phase operation. This model is shown in Fig. F. The stem structure in the model is the same as will be used in the 500 MeV cyclotron; dees and dee-to-dee coupling are included as lumped capacitances. The Q of the model is accurately the same as the Q expected in the actual resonators, and the tuning servoes and servo logic are the actual units we plan to use on the cyclotron. After a period of development, a logic system was obtained which reliably and accurately controls both phase and amplitude in all the needed modes; we then expect the three-phase modes to be completely equivalent to the in-phase mode in both stability and accuracy.

Figure G is an overall cross section view of the 500 MeV cyclotron and updates the corresponding figure on p. 112 of the original proposal. The rf system is shown in this figure with long resonators.

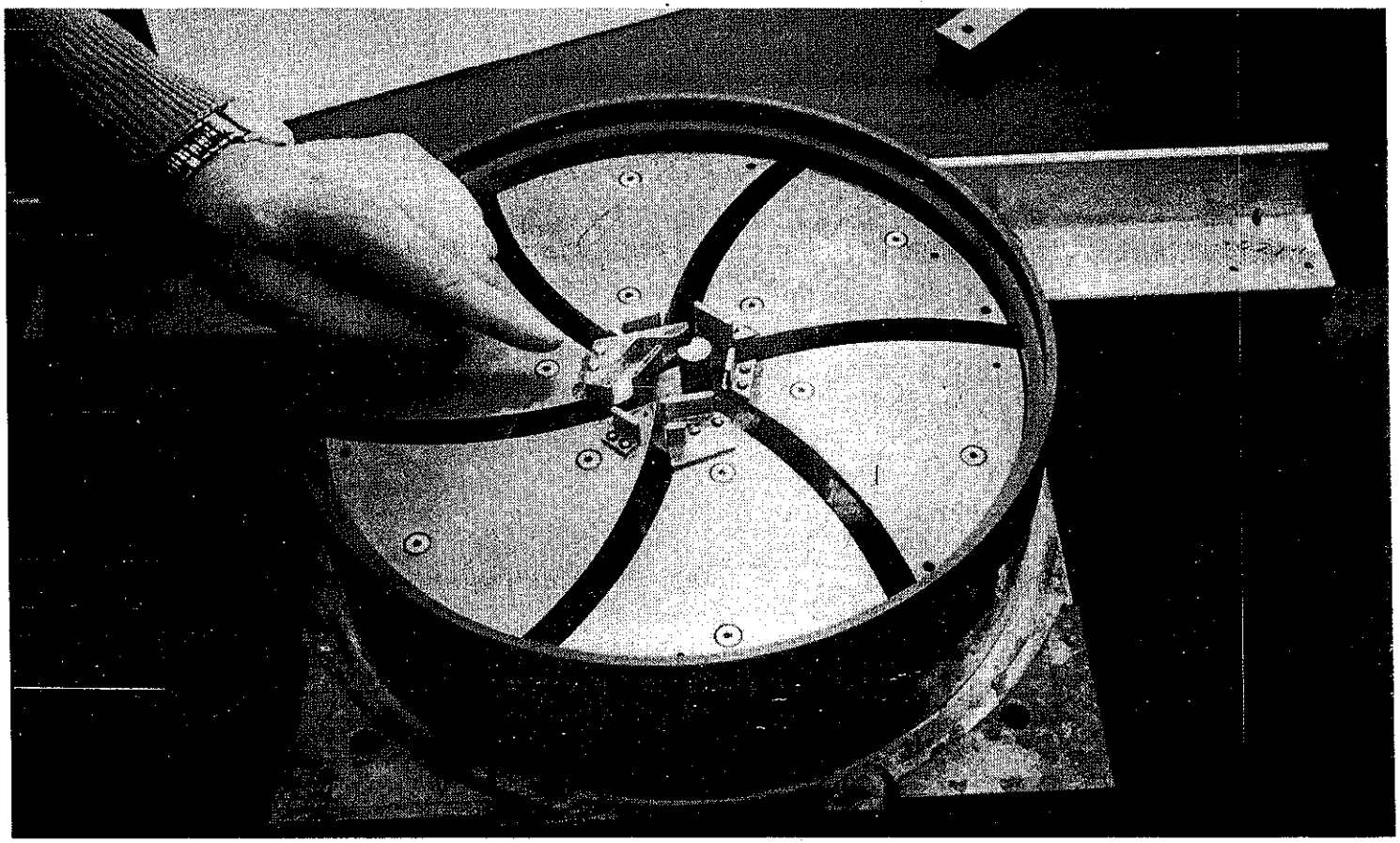

Fig. D (IV.1.1). Photograph of three dimensional electrolytic tank used to obtain central region electric field maps. The forefinger points to the extraction electrode (the "puller") on dee #1 and the cylinder near the puller represents the source. The top surface of the central electrodes corresponds to the median plane of the system. (To simplify construction and data-taking, the mirror image of the electrode system relative to the median plane is omitted; placing the water surface at this plane imposes the proper boundary condition.) Electrodes in the tank are full size and the electrode system in the photo is set up for cyclotron operation on the first harmonic mode.

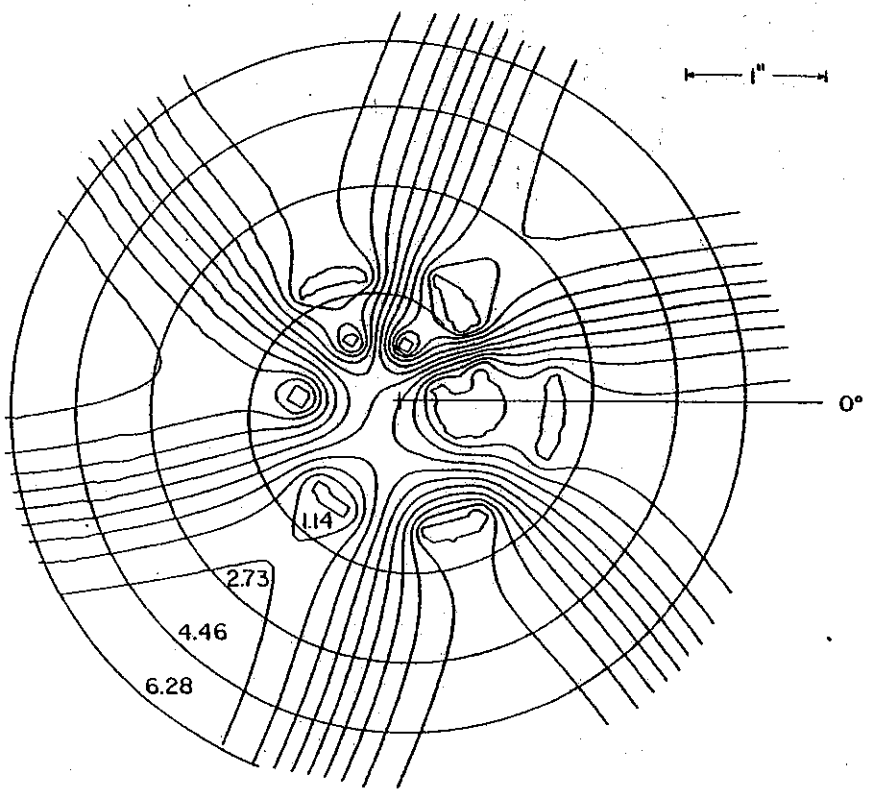

N=2, q/A=.286, B_0=4.81 tesla, V_D=100 kV,

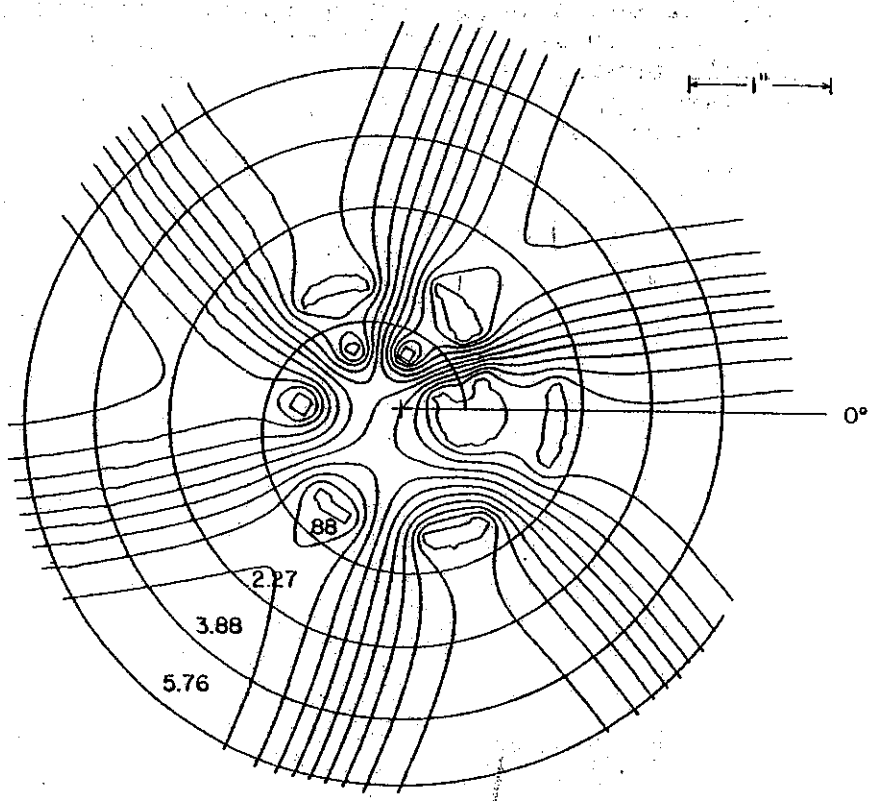

N=3, q/A=.286, B_0=4.81 tesla, V_D=100 kV,

Fig. E (IV.1.1). Two typical central region orbits superimposed on central region voltage contours from the electrolytic tank.

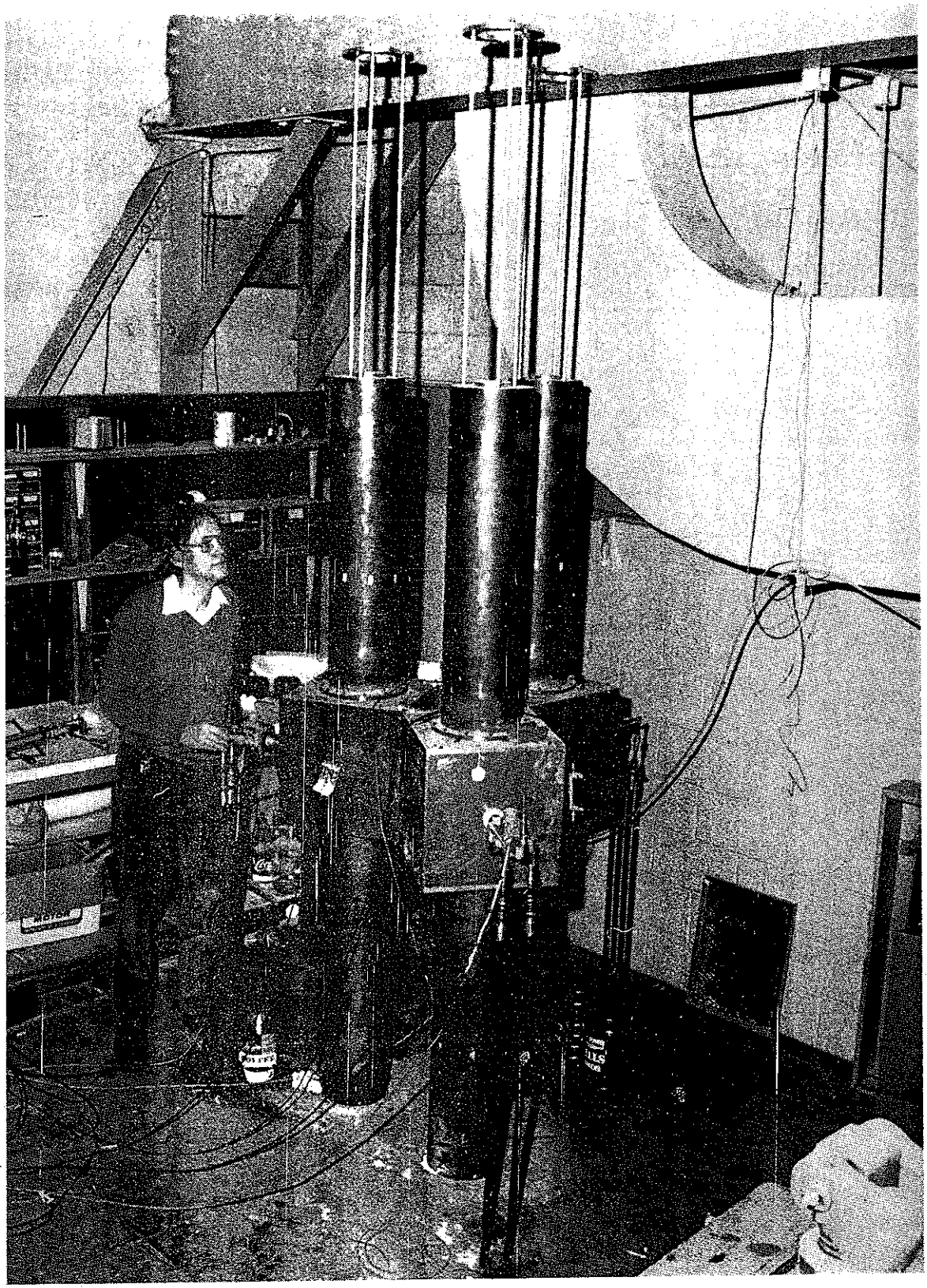

Fig. F (IV.1.1). Photograph of three phase tuning model. The six dee stems are actual size and the hydraulic servos and logic boards are the actual units which will be used in the cyclotron. Dee capacitances are incorporated as lumped elements.

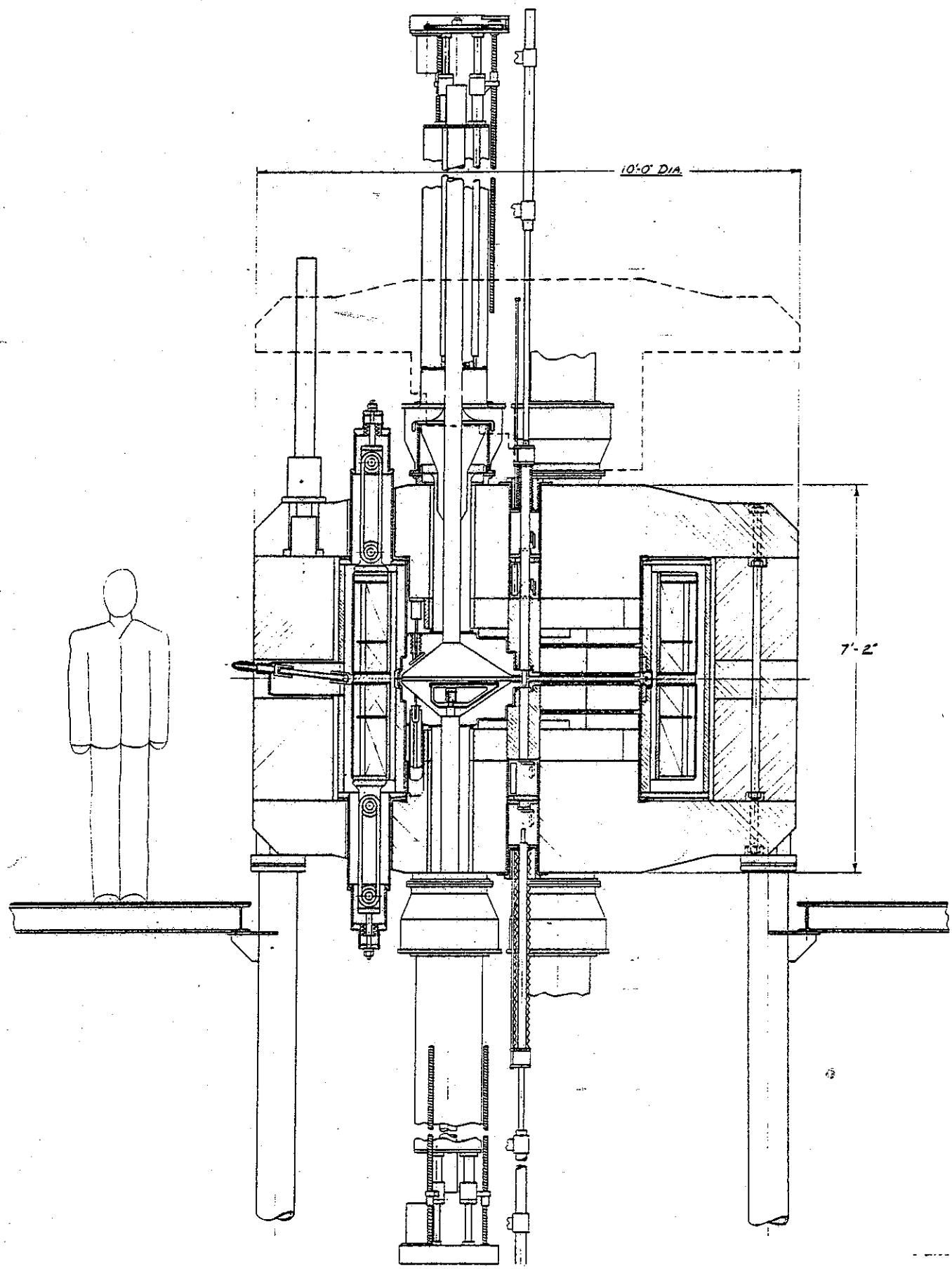

Fig. G (IV.1.1). Updated copy of the drawing given on page 112 of the CSC proposal, vertical section view of the 500 MeV cyclotron showing major components.

IV.1.2 The superconducting main coil

The design of the superconducting main coil was reviewed in June for an external committee[10] consisting of prominent experts on large DC superconducting coils. Documents prepared as a part of the presentation for this committee are available as is the committee's report. (Generally the committee felt that all important design points had been appropriately investigated and their expectation is for the coil to perform as planned.) The basic design of the coil utilizes a layer-type winding tightly packed in the Z coordinate and with a picket fence lattice between radial layers to provide helium cooling. The coil will be directly wound on a large stainless steel spool which will be its permanent mounting. This spool with a welded-on stainless steel outer cover then becomes the helium can. The spool is unfortunately delayed in fabrication as a consequence of welding errors but is now nearing completion. It is shown in Fig. 7 in the process of final machining. While waiting for delivery of the real spool we have proceeded to develop and test coil winding equipment using a dummy wooden spool as shown in Fig. 8. A highly automated system has evolved which will wind the complete coil in about four weeks.

Conductor for the coil was fabricated by Intermagnetics General Corporation and has all been received. In tests at the National Magnet Laboratory[11] the conductor exceeded critical current specifications by 40%.

The helium liquifier-refrigerator unit has also been received and is at present being connected for trial operation.

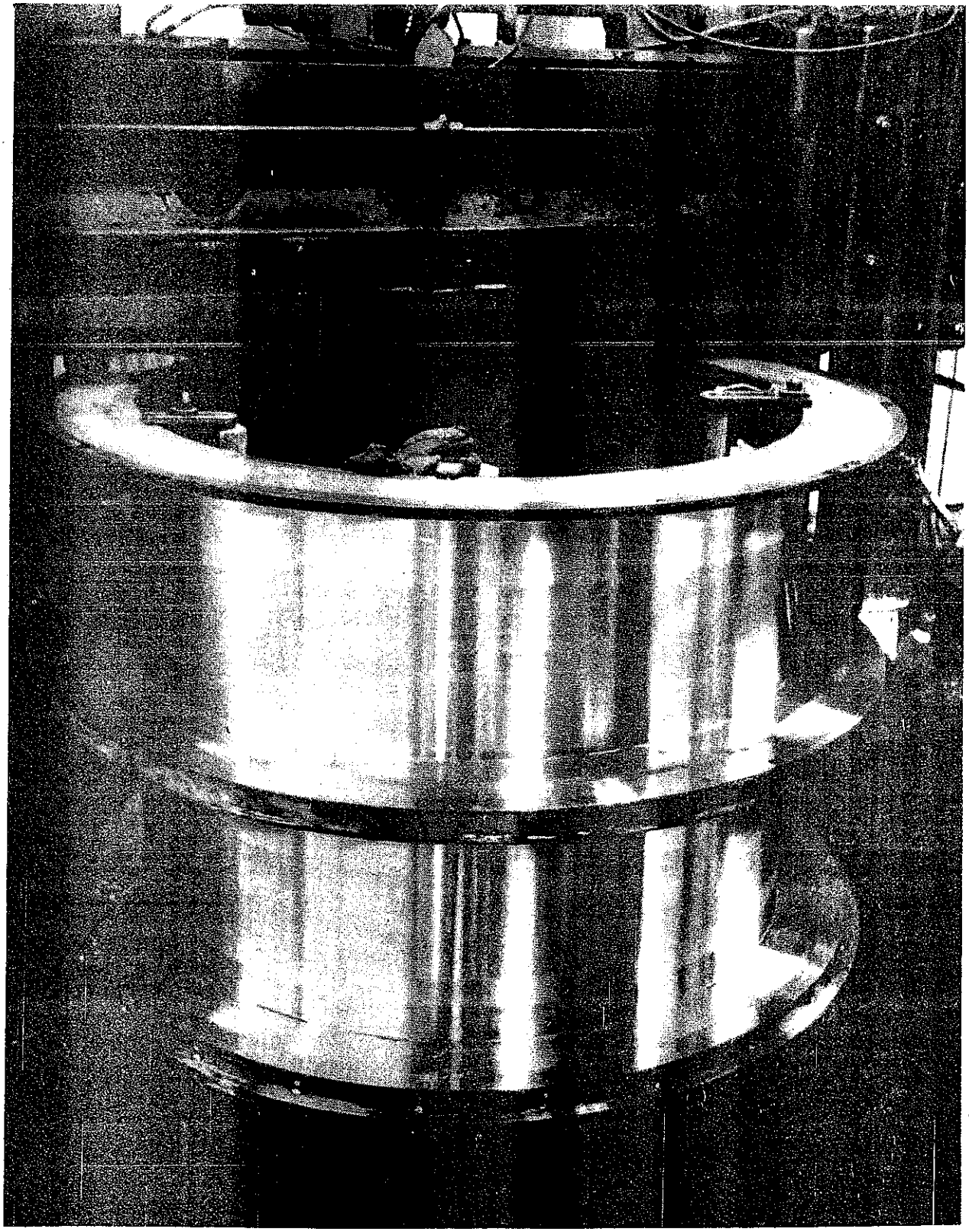

Fig. 7(IV.1).--Photograph of the stainless steel spool for the superconducting coil in the process of final machining. The spool is inverted in the photograph; the open lattice (at the bottom in the photograph) is a liquid helium reservoir. The spool becomes the liquid helium container with the addition of a welded stainless steel outer cover.

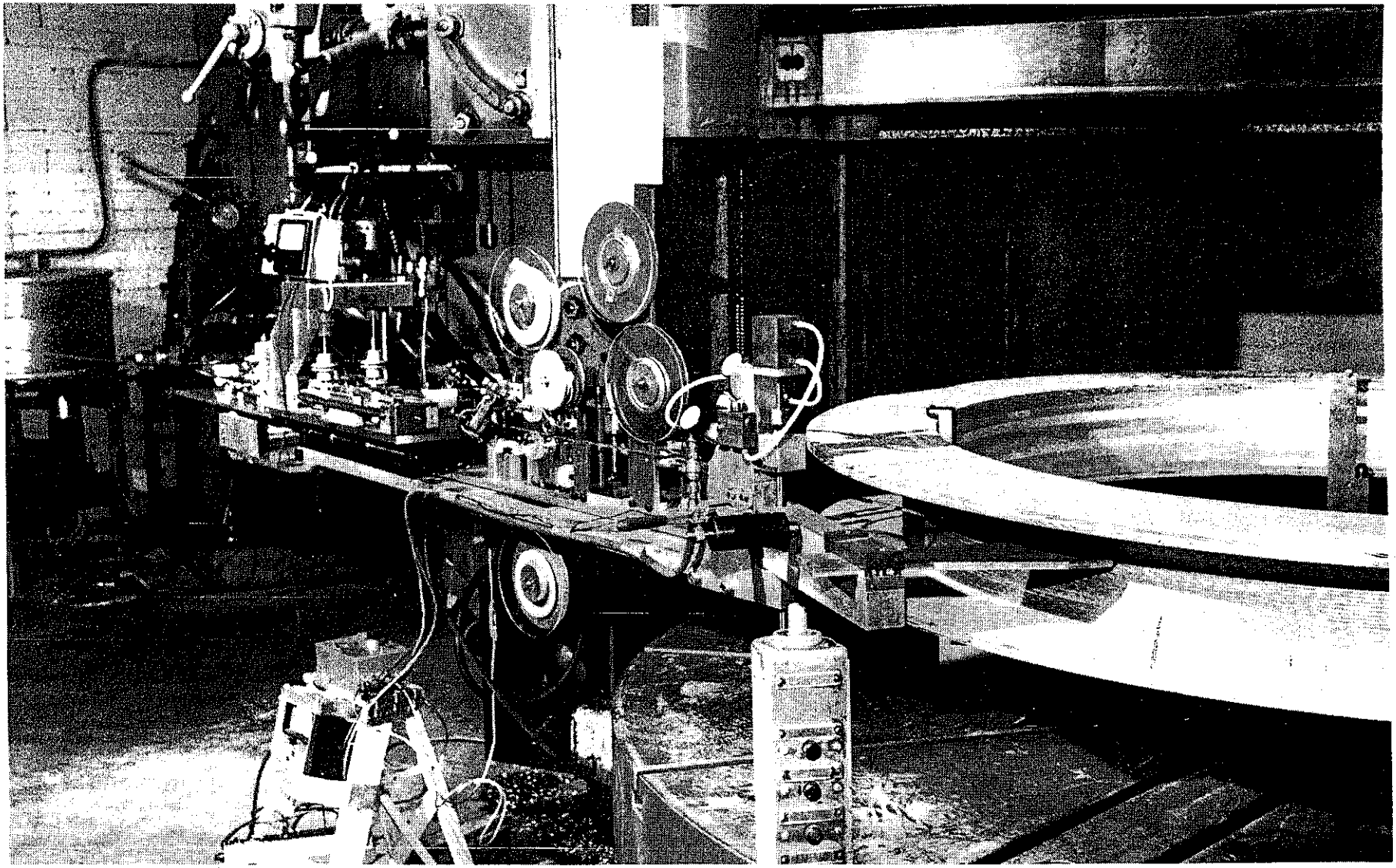

Fig. 8(IV.1).--Photograph of the coil winding machine set up for test operation. A spool of 750 ampere conductor is at the far left and feeds through straightening rolls, tensioning device, and insulation applicator to the dummy winding spool at the right. As the wire touches the spool, a pneumatically pressurized pusher arm places each turn tightly against the preceding turn. The winding machine uses a 96" vertical lathe obtained for the purpose from federal surplus property listings.

In factory tests the unit substantially exceeded its design specifications, producing 30 liters per hour of liquid helium versus the specified value of 26.

We expect to turn on the magnet for the first time in January 1977 and will quickly thereafter be making definitive tests of all aspects of the coil and magnet design. Tests of our field calculation procedure against existing magnet data lead us to expect that the magnetic field will be correct as the magnet is first turned on. We hope to have funding available to proceed with construction of other components so as to complete and test the 500 MeV cyclotron in the ensuing year. (Section V contains additional information on the anticipated schedule.)

Addendum to Sec. IV.1.2

The winding of the superconducting coil took somewhat longer than anticipated at the time the September 1976 proposal was written. Primarily this was due to unexpected delays in the coil winding as a result of manufacturing defects in the cabled conductor. (At more than 1000 locations, the conductor failed to meet mechanical requirements of the specifications due to a pushing out of one or another strand from the body of the cabled conductor.) These defects posed a hazard of possible layer-to-layer shorts and therefore had to be dealt with carefully. As a result, the coil winding took somewhat over three months and first operation of the magnet occurred in May, with first full current operation on May 26.

Gratifyingly the operating tests were outstandingly successful. Sensing devices designed to pick up possible mechanical movement of individual turns in the coil gave no indication of movement, implying that the design goal had been achieved, namely producing a tightly compacted winding with sufficient pretension to outweigh large magnetic stresses.

The field of the magnet has been mapped on a 9900 point polar grid for a range of excitations from 200 to 700 amps. Results are in excellent agreement with design requirements. Table B gives a Fourier analysis of the 700 amp field. Results from the field mapping were immediately in agreement with prior design calculations* to an accuracy of 1%. In addition, deviations between the predicted field and the measured field accurately correlated with geometric simplifi-

*Blosser and Johnson, Report MSUCP-28 (April 1977).

R	BAV	B3	PH3	B6	PH6	B9	PH9
-3.0	4.44536	.12215	2.646	.01920	5.079	.00307	6.546
.0	4.30705	.00000	48.036	.00000	8.820	.00000	9.827
.5	4.31166	.00008	78.822	.00029	.671	.00020	.850
1.0	4.32013	.00363	63.124	.00009	-27.413	.00011	-18.245
1.5	4.33602	.01228	63.178	.00043	-55.907	.00009	.746
2.0	4.36069	.03154	63.117	.00185	-55.019	.00009	-11.678
2.5	4.39642	.06713	63.018	.00673	-54.349	.00077	-13.474
3.0	4.44819	.12361	62.780	.02012	-54.876	.00291	-12.513
3.5	4.50748	.20218	62.220	.04270	-55.534	.00868	-13.838
4.0	4.56837	.28714	61.179	.07087	-56.803	.01607	-15.226
4.5	4.61936	.36473	59.717	.09707	-58.534	.02242	-17.009
5.0	4.66089	.42933	57.966	.11987	-60.529	.02568	-18.969
5.5	4.69215	.48231	56.064	.13776	-62.626	.02680	-20.956
6.0	4.71434	.52538	54.099	.15272	-64.716	.02573	-22.922
6.5	4.73420	.56286	52.087	.16465	-66.843	.02343	-24.754
7.0	4.74918	.59422	50.054	.17465	-68.931	.01996	-26.427
7.5	4.76075	.62076	48.056	.18273	-70.954	.01592	-27.844
8.0	4.77052	.64424	46.017	.18947	-72.995	.01175	-28.783
8.5	4.77816	.66598	43.996	.19505	-75.051	.00822	-28.295
9.0	4.78365	.68437	41.948	.19945	-77.084	.00682	-26.236
9.5	4.78836	.70130	39.880	.20321	-79.145	.00855	-24.340
10.0	4.79225	.71595	37.829	.20578	-81.177	.01176	-24.436
10.5	4.79528	.72945	35.745	.20783	-83.238	.01522	-25.493
11.0	4.79713	.74186	33.636	.20949	-85.357	.01859	-26.920
11.5	4.79924	.75270	31.516	.21025	-87.485	.02141	-28.655
12.0	4.80028	.76185	29.353	.21049	-89.681	.02374	-30.549
12.5	4.80330	.77034	27.191	.21043	-91.911	.02557	-32.553
13.0	4.80010	.77710	24.980	.21009	-94.217	.02687	-34.705
13.5	4.80262	.78321	22.756	.20979	-96.573	.02789	-36.998
14.0	4.80699	.78923	20.529	.21025	-98.951	.02916	-39.398
14.5	4.80516	.79555	18.321	.21148	-101.340	.03077	-41.818
15.0	4.80874	.80328	16.102	.21393	-103.744	.03288	-44.230
15.5	4.81252	.80988	13.942	.21645	-106.108	.03538	-46.424
16.0	4.81562	.81485	11.805	.21914	-108.430	.03770	-48.691
16.5	4.81858	.81794	9.704	.22194	-110.701	.03999	-50.872
17.0	4.82152	.82037	7.624	.22499	-112.942	.04214	-53.016
17.5	4.82471	.82080	5.537	.22776	-115.158	.04456	-55.172
18.0	4.82897	.82234	3.511	.23185	-117.303	.04580	-57.179
18.5	4.83318	.82251	1.447	.23549	-119.455	.04729	-59.255
19.0	4.83622	.81987	-.569	.23834	-121.539	.04882	-61.264
19.5	4.84073	.81907	-2.610	.24217	-123.615	.04961	-63.329
20.0	4.84440	.81659	-4.649	.24532	-125.675	.05051	-65.365
20.5	4.84828	.81254	-6.677	.24788	-127.705	.05108	-67.371
21.0	4.85414	.80900	-8.698	.25066	-129.705	.05141	-69.460
21.5	4.85853	.80329	-10.735	.25266	-131.700	.05164	-71.541
22.0	4.86311	.79578	-12.792	.25380	-133.726	.05119	-73.558
22.5	4.86823	.78700	-14.803	.25406	-135.657	.05133	-75.706
23.0	4.87169	.77458	-16.854	.25317	-137.634	.05033	-77.811
23.5	4.87486	.75882	-18.890	.25008	-139.539	.04918	-79.987
24.0	4.87747	.73724	-20.918	.24295	-141.382	.04802	-82.307
24.5	4.87726	.70612	-22.933	.22963	-143.104	.04774	-84.899
25.0	4.87558	.66336	-24.901	.20575	-144.571	.05180	-87.745
25.5	4.87377	.60713	-26.764	.16558	-145.582	.06492	-90.218
26.0	4.87064	.54293	-28.457	.11787	-146.064	.08281	-91.839
26.5	4.84679	.46211	-29.806	.07862	-146.144	.08958	-92.801

Table B (IV.1.2). Fourier analysis of measured magnetic field at an excitation of 700 amps. Radius is in inches, amplitudes (BAV, B3, B6, etc.) are in tesla and phase angles (PH3, PH6...) are in degrees.

cations introduced in the calculations to save computing time. Subsequent refinement of the computed geometry to include these details brings the result of measurement and calculation into agreement to a level of 0.2%! The field calculation model, which consists of calculating a cylindrically symmetric magnet with relaxation techniques, and superimposing noncylindrical components with a saturation approximation is then beautifully accurate. The model also remains accurate to a surprising degree as the field is lowered, still being good to within 1% at an excitation of 200 amps where the average magnetic field is about 25 kilogauss.

The accuracy with which the saturation approximation holds implies that air core calculations of the effect of trimming windings give an accurate representation of the effects of the actual coils. Exercises are presently in progress using a set of computed trim coil fields in order to evolve an optimized trimming strategy. Some interim results from this study are shown in Tables C and D which give closed orbit properties for two typical trimmed fields corresponding to ions at extremes of the trimming range. Orbit properties for the two fields are excellent, and trim coil powers are respectively 131 kw and 56 kw. It also appears that some "rolling-off" from ideal orbit properties will further reduce the trimming power and also add to the energy range. Trim coil studies exploring the effective limits of this type of strategy are in progress.

The fractional first harmonic error is the principle quantity determining the magnitude of orbit imperfections in a cyclotron. This coefficient is plotted in Fig. H. As a point of reference

E	RAV	PHASE	R	PR	NU R	NU Z	NT	F(E)
8.0000	11.423217	.000226	11.228612	-.247749	1.018636	.136103	2	.000
9.0000	12.102472	-.000076	11.881228	-.185652	1.024224	.122375	2	.470
10.0000	12.741976	-.000443	12.497912	-.114076	1.021761	.157983	2	-1.161
11.0000	13.358993	-.000006	13.097566	-.033058	1.012990	.213738	2	-2.571
12.0000	13.947788	.000421	13.673417	.054930	1.029446	.151766	2	-1.257
13.0000	14.495681	-.000257	14.210861	.146197	1.040083	.090437	2	-.751
14.0000	15.025146	-.000632	14.734677	.239903	1.024995	.192335	2	-3.543
15.0000	15.549181	-.000059	15.258994	.335268	1.015559	.238983	2	-5.714
16.0000	16.054650	.000447	15.768652	.431983	1.026576	.200978	2	-4.497
17.0000	16.537077	.000528	16.258317	.529312	1.033626	.172662	2	-1.435
18.0000	16.999093	.000292	16.730457	.626896	1.041490	.134906	2	1.139
19.0000	17.441347	-.000267	17.185381	.725152	1.049751	.074716	2	1.216
20.0000	17.870511	-.000818	17.630339	.822959	1.043223	.134778	2	-2.193
21.0000	18.297862	-.000806	18.077678	.917229	1.024042	.233378	2	-7.295
22.0000	18.727670	-.000087	18.531857	1.006007	1.020429	.254969	2	-10.099
23.0000	19.145824	.000532	18.977049	1.092747	1.030147	.229358	2	-8.701
24.0000	19.545817	.000697	19.405773	1.179080	1.042098	.184289	2	-4.842
25.0000	19.931523	.000598	19.822095	1.263231	1.047700	.160183	2	-.775
26.0000	20.304106	.000280	20.227121	1.344350	1.056861	.106905	2	1.983
27.0000	20.665179	-.000189	20.622324	1.420656	1.064186	.059456	2	2.268
28.0000	21.018031	-.000670	21.010833	1.489242	1.059691	.117509	2	-.433
29.0000	21.371315	-.000784	21.401924	1.543427	1.041338	.214824	2	-5.001
30.0000	21.728445	-.000409	21.798357	1.577298	1.027287	.274049	2	-8.749
31.0000	22.086934	.000306	22.196747	1.587814	1.030799	.271446	2	-9.073
32.0000	22.431443	.000661	22.580681	1.582334	1.044820	.220909	2	-6.036
33.0000	22.762052	.000660	22.950120	1.558619	1.057491	.161408	2	-1.887
34.0000	23.083431	.000508	23.308616	1.516991	1.062895	.132335	2	1.781
35.0000	23.398674	.000329	23.658776	1.457938	1.059681	.135639	2	4.410
36.0000	23.708025	.000125	24.000328	1.384515	1.065907	.063833	2	5.836
37.0000	24.012641	-.000065	24.333499	1.301018	1.062646	.077216	2	6.025
38.0000	24.312024	-.000272	24.657341	1.207876	1.058268	.058556	2	4.967
39.0000	24.614395	-.000176	24.978373	1.102230	1.040260	.188559	2	3.561
40.0000	24.925178	.000417	25.299577	.983617	1.010368	.295624	2	4.320
41.0000	25.246822	.001578	25.621724	.853180	.989055	.384222	2	10.590
42.0000	25.580658	.003336	25.944731	.718329	.973505	.437555	2	26.028
43.0000	25.916181	.005273	26.262238	.588867	.950852	.500336	2	53.074
44.0000	26.297759	.009062	26.609909	.450730	.857364	.727397	3	98.109

Table C (IV.1.2). Closed orbit properties for an ion with Q/A=0.3 in the 700 amp field. E is in MeV/nucleon, radii and radial momentum are in inches, F (E) is in keV/nucleon, and phase and focusing frequencies are dimensionless.

E	TRAV	PHASE	R	PR	NU R	NU Z	NT	F(E)$_1$
•0800	10•993412	-•000611	10•811336	-•246526	1•005115	•200604	3	•000
•0900	11•666250	-•000068	11•459429	-•187656	1•003846	•220592	3	-•021
•1000	12•301091	•000269	12•072847	-•120058	1•007149	•219254	2	-•015
•1100	12•901553	•000305	12•655356	-•045362	1•013402	•205760	2	•003
•1200	13•468512	-•000159	13•207580	•033213	1•019587	•191339	2	•008
•1300	14•014290	-•000430	13•743003	•116362	1•008865	•244341	2	-•011
•1400	14•549329	-•000002	14•272950	•203087	1•003276	•271585	2	-•024
•1500	15•063961	•000278	14•786162	•291635	1•012371	•246643	2	-•016
•1600	15•554554	•000076	15•278147	•380660	1•018292	•227643	2	-•005
•1700	16•030643	-•000073	15•759213	•469180	1•012443	•252141	2	-•005
•1800	16•496650	•000012	16•233948	•556948	1•009537	•265551	2	-•006
•1900	16•950528	•000127	16•699758	•643999	1•010768	•264669	2	-•002
•2000	17•391869	•000189	17•155936	•730032	1•010732	•267231	2	•008
•2100	17•822007	•000228	17•603710	•814602	1•011229	•268916	2	•021
•2200	18•241160	•000217	18•043061	•897606	1•014847	•262773	2	•035
•2300	18•648963	•000103	18•473316	•978899	1•016208	•263944	2	•045
•2400	19•048840	•000040	18•898068	1•057282	1•013918	•275295	2	•049
•2500	19•443096	•000112	19•319726	1•131569	1•009229	•292759	2	•054
•2600	19•830616	•000233	19•736916	1•201570	1•009384	•295300	2	•065
•2700	20•209242	•000273	20•147027	1•267292	1•016168	•281856	2	•081
•2800	20•577279	•000136	20•547883	1•328287	1•020329	•274647	2	•094
•2900	20•937333	-•000063	20•942148	1•382274	1•019981	•277336	2	•096
•3000	21•292602	-•000190	21•333111	1•425909	1•014539	•296062	2	•088
•3100	21•645375	-•000157	21•722533	1•455144	1•012753	•309246	2	•077
•3200	21•994371	-•000043	22•108616	1•467989	1•011345	•316577	2	•071
•3300	22•335833	-•000029	22•487206	1•464063	1•014975	•304954	2	•069
•3400	22•670014	-•000111	22•857865	1•441220	1•019433	•297107	2	•064
•3500	22•998892	-•000209	23•221696	1•399844	1•019058	•298079	2	•054
•3600	23•322010	-•000353	23•577932	1•341631	1•017815	•295471	2	•037
•3700	23•640026	-•000520	23•926397	1•270039	1•024298	•275099	2	•009
•3800	23•951411	-•000781	24•264924	1•190168	1•022755	•270777	2	-•032
•3900	24•253077	-•001065	24•594863	1•100556	1•021840	•259399	2	-•090
•4000	24•565633	-•001152	24•920325	1•002635	1•006562	•306768	2	-•159
•4100	24•879233	-•000856	25•244416	•892960	•982860	•364088	2	-•222
•4200	25•201401	-•000098	25•567979	•774701	•967774	•419560	2	-•252
•4300	25•533877	•001169	25•891306	•651060	•948766	•474870	2	-•219
•4400	25•866651	•002625	26•209578	•531829	•933338	•517005	2	-•100
•4500	26•244465	•005729	26•555386	•407632	•842364	•717574	3	•163

Table D (IV.1.2). Closed orbit properties for a particle Q/A=0.03 in the 700 amp field.

one can immediately note that the B_1/B_0 in Fig. H is everywhere better than the corresponding fractional error in our 50 MeV cyclotron field* and the 50 MeV cyclotron is itself exceptional among cyclotrons as regards beam precision. Furthermore, major features of the first harmonic in Fig. H correlate with known alignment details of the magnet. The dashed curve at 25" for example shows the calculated first harmonic which would result from a 1 mil center shift of the steel inner wall of the main coil cryostat. Correlating the shape of this curve with the observed first harmonic peak at 25", one infers a coil tank alignment error of 2.5 mils. A position shift of this amount can certainly be made, although it is pointless to make such a fine correction at this time, since the magnet must be fully disassembled for moving to its final location and for installation of extraction components and the fine position adjustment would then have to be repeated. We do feel however that with reasonable care, we can center the coil tank in the final alignment to better than 1 mil and thus greatly reduce the B_1 at this radius.

Other major peaks in the first harmonic data similarly correlate with major geometric details of the magnet and can likewise be reduced with a moderate amount of careful adjustment work in the final assembly. Such corrections are "gilding the lily" in the sense that orbit errors are already totally negligible at the first harmonic level presently achieved. Nevertheless it seems that a significant further reduction in the error component can be achieved with relatively modest effort, and we intend

*Berg, Blosser, Johnson, Report MSUCP-22 (August, 1966).

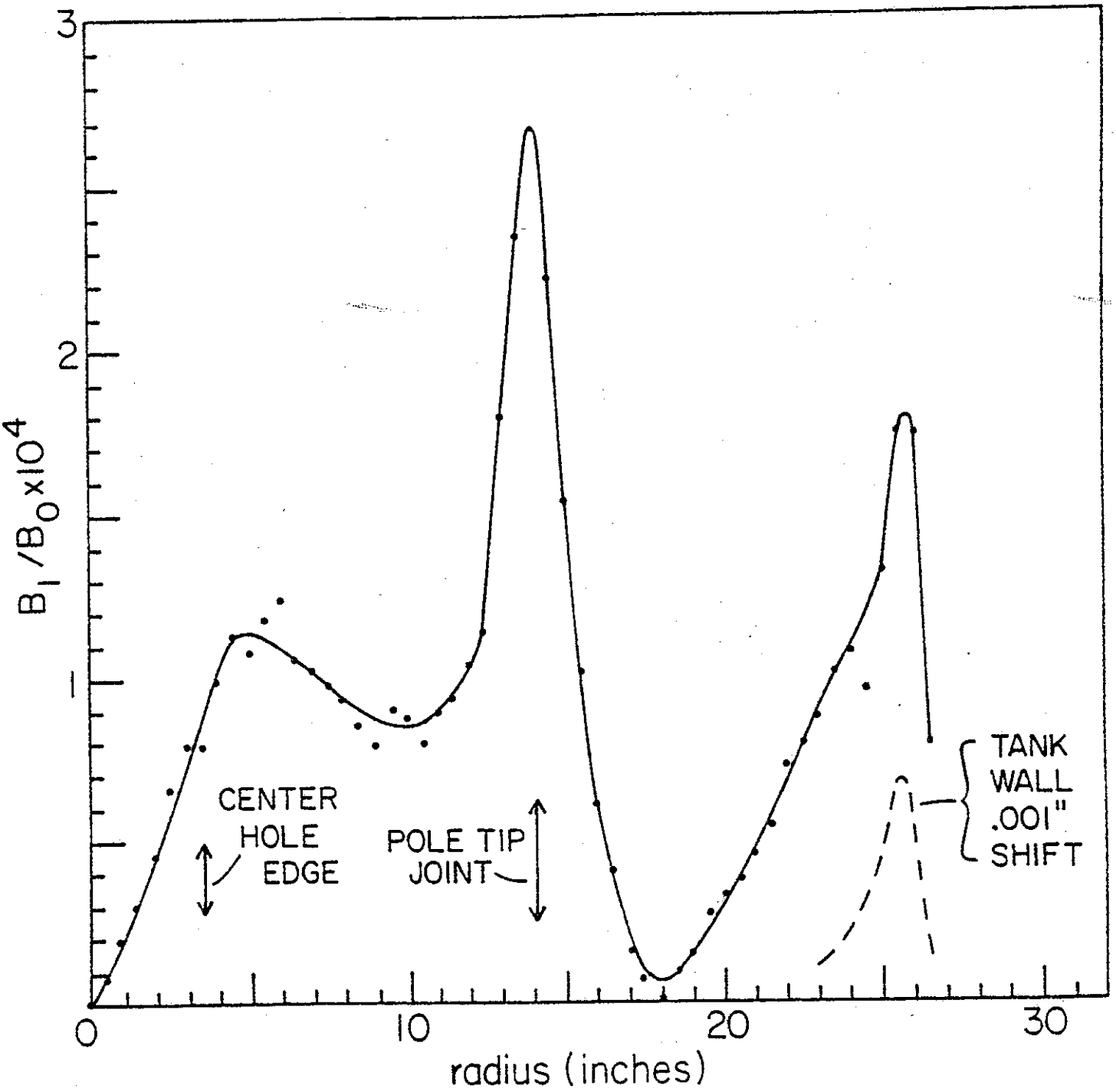

Fig. H (IV.1.2). First harmonic amplitude vs. radius. Points show the measured value; the line is inserted as a visual aid. The point-scatter at a level of about 1 part in 100,000 is mostly due to small calibration errors. The dashed curve is a computation of the first harmonic induced by a 1 mil shift in the position of the inner wall of the coil cryostat.

to make such adjustments, following up on our basic feeling that it is always good to do things as well as one easily can, even when the results give a product significantly exceeding requirements.

The overall integrity of the superconducting coil was unintentionally further verified through the fall months of 1977 as a result of three accident situations which subjected the coil to severe conditions. The first of these came about during a full current test of the energy dumping system for the magnet. A faulty water level controller in the "dump" resistor allowed the stainless steel resistance element to protrude from its water bath. The element consequently melted giving an open circuit on the coil and a very high voltage which led to arcing at two points, one point being in a coil lead and the other being in the power supply. The arc in the coil lead melted through the vacuum wall, thereby breaking the insulating vacuum, and throwing a heat load estimated at 200 kilowatts rather instantly onto the coil. This heat load in turn caused a helium blow-off through the helium can safety valve, leading to a rapid temperature change in the whole coil structure. The power supply was significantly damaged in this accident and required a month of repair, but there was no detectable change in any characteristic of the coil. (The incident was certainly for all of us a vivid and educational demonstration of the punishing capabilities of large stored energy and the ensuing demand for perfection in all aspects of a large coil system.)

The second and third accident situations involved a tension break in one of the support links for the coil; the unstable spring

constant associated with the magnetic forces then banged the coil against the housing but again without damage of any kind to the coil proper. An ensuing careful experimental study of this problem showed that the magnetic spring constant is greatly increased when the spiral pole tips are in place, to a level significantly larger than had been estimated. (In the process of unravelling this puzzle, the accident was inadvertently again repeated.) The survival of the coil through these several unplanned abuses then conveys a message of ruggedness and reliability; we hence look forward to an indefinite lifetime in routine use in the cyclotron.

IV.1.3 Ion sources

Since July 1 of this year our ion source program has been under the direction of M.L. Mallory, an outstanding heavy ion source expert with us on a two-year leave from Oak Ridge. Since Mallory's arrival we have been moving rapidly with design of sources for the 500 MeV cyclotron.

The general mechanical layout of the cyclotron's central region is shown in Fig. 4. An important feature of the design is the use of automatically removable 7"-diameter plugs in both the top and bottom of the magnet. Ion sources will be built-in to one or both of these plugs and will be easily removable through the two center plug vacuum locks without disturbing the machine vacuum and without warming up cryopanels. The plug design is a direct take-over of a feature which has been in use on our present cyclotron for the past three years and which has been exceedingly valuable in providing easy direct access to central region components. The automatic removal system includes vacuum locks, pumps, and a hydraulic ram to move the fairly heavy plug. (Fig. 9 is a photograph of our present center plug in its lowered position; the ion source and the radial selection slit are seen at the top of the plug.) The 7"-diameter center plugs are substantially larger than needed for presently planned sources and give a capability for adapting to future alternate source designs if performance improvements can thereby be achieved. The plugs are also large enough to allow installation of an external axial injection system at a later time if some external source with clearly superior performance is developed or for possible polarized beam sources.

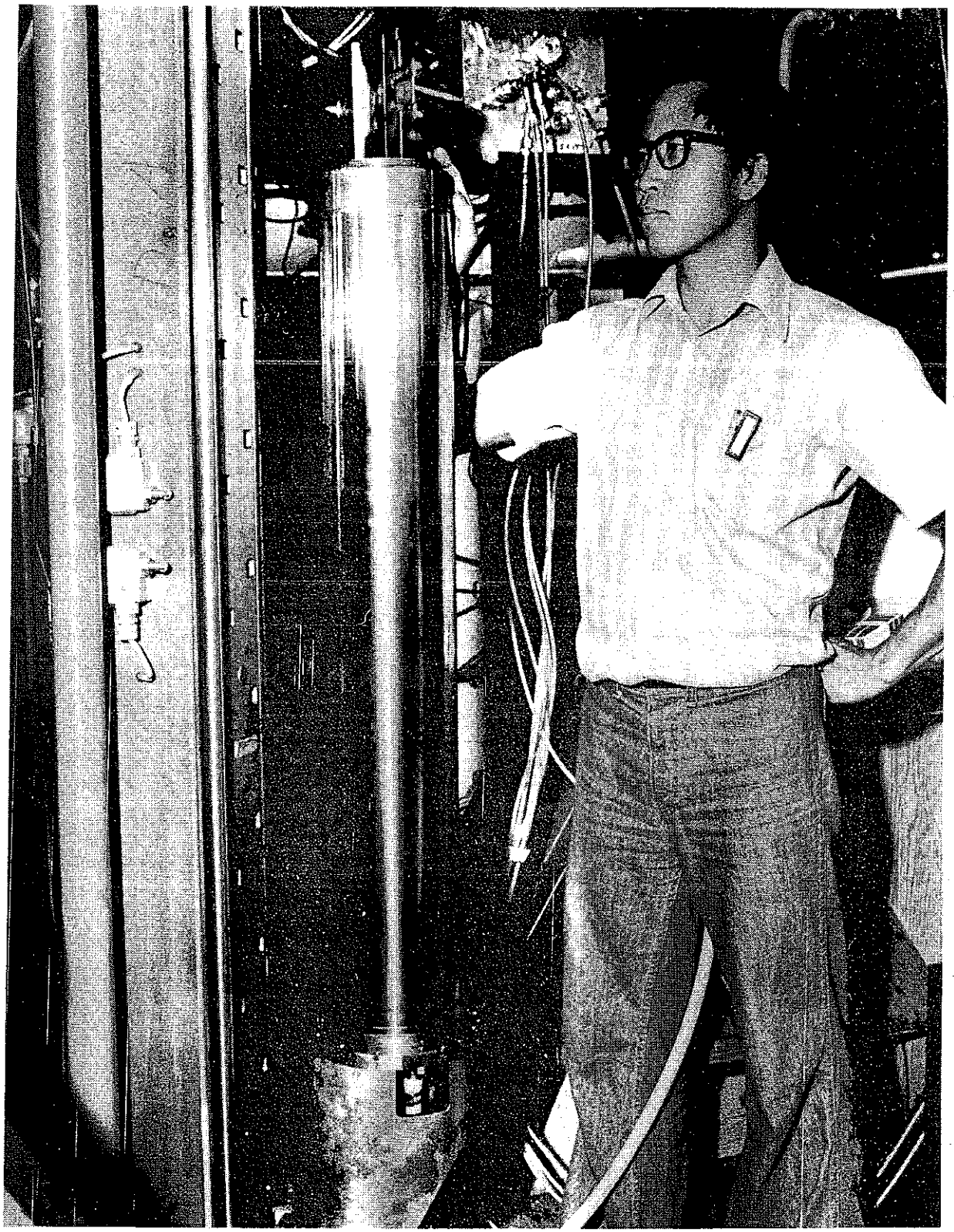

Fig. 9(IV.1).--Photograph of the automatically removable source plug on the MSU cyclotron. The ion source and first turn selector slit are on the top of the plug just to the upper left of Dr. Chien's right hand, and are easily available for servicing without disrupting the cyclotron vacuum. A similar plug system will be utilized in the 500 MeV cyclotron.

Detailed planning for the 500 MeV cyclotron ion source is now focused on the Phillips Ionization Gauge or PIG source, which is at present the best performing cyclotron heavy-ion source. A number of striking performance improvements have been introduced in these sources in recent years. Perhaps the most significant is the development of sputter systems[12] which have broadened the application of the source to include essentially all elements. The sputtering process is illustrated diagrammatically in Fig. 10. With this technique sputter beams approach the intensity of traditional gas-fed beams as is indicated in a later table of examples.

Another major area of recent PIG source improvement has centered on reduced maintenance. Traditionally, PIG sources have been hampered by relatively short cathode life, typically about four hours. When the cathode failed the source had to be removed, the deposited cathode material cleaned from the anode, and the cathodes replaced. Even with good handling devices and practice, the running time lost in this process typically amounted to 10% of total heavy-ion running time (according to records at Oak Ridge for example). A recent Oak Ridge source design, the rotating cathode source,[13] is an important step forward. This design allows the cathode to be remotely changed without removing the source and the limiting lifetime factor is then the build-up of cathode material on the anode which finally reaches a size which shorts the arc as sketched in Fig. 11. With this rotating cathode design, the interval between source maintenance has been extended to about eight hours. The proposed axial source insertion system in the

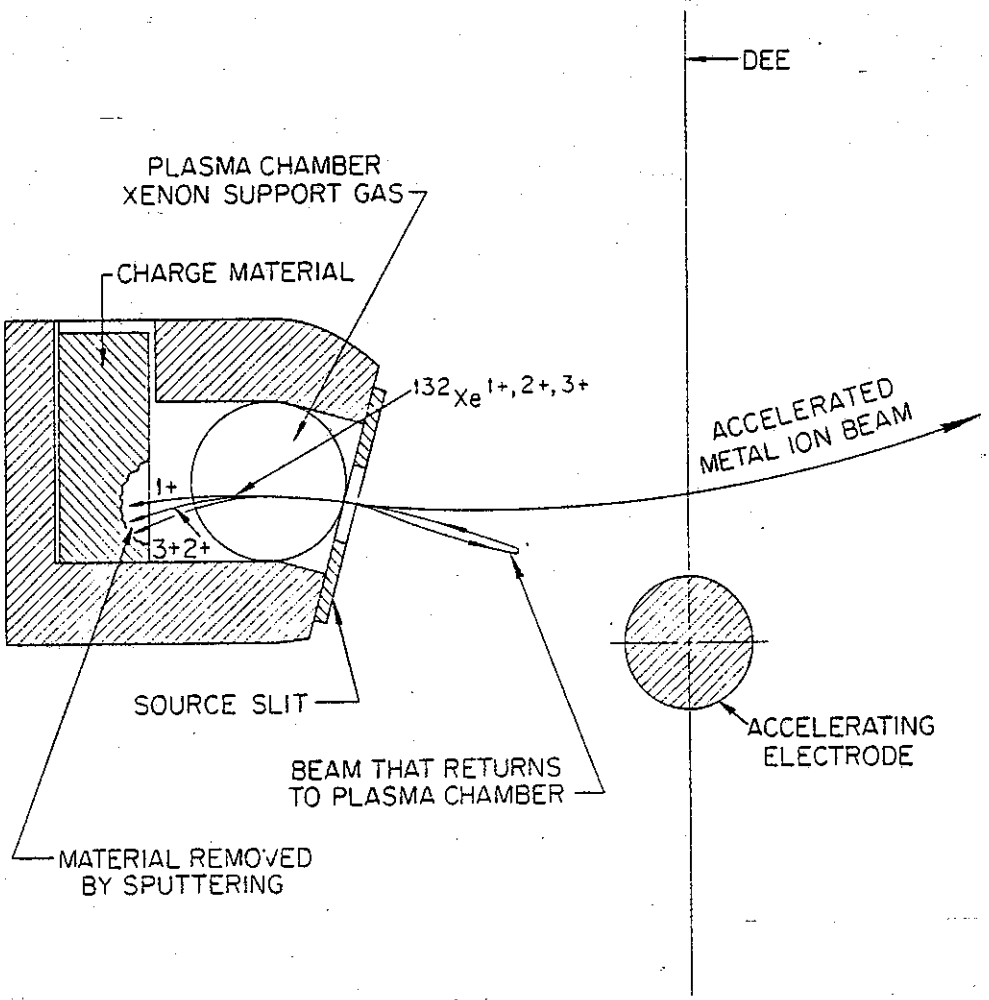

Fig. 10. Section view through the ion source showing basic features of the back-bombardment sputtering process. In such a source a conventional arc is maintained using a heavy feed gas such as Krypton or Xenon. Low charge state ions from this gas, if emitted late in the acceleration cycle, move too slowly to cross the rf gap during the remaining part of the acceleration cycle. They are therefore deaccelerated in the reverse half of the cycle, slow down, reverse, and return to the source as indicated. These relatively energetic ions then hit the rear of the source and sputter any material inserted in the "charge material" pocket. These sputtered ions then drift and diffuse to the front of the source and are extracted. Relatively intense beams (in the microamp range) can be produced with this technique.

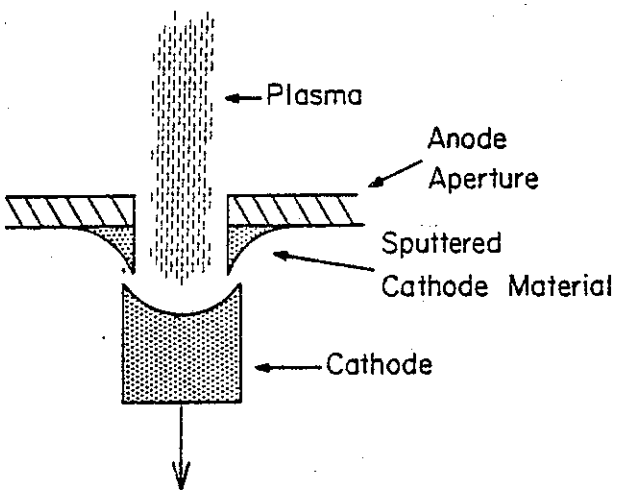

Cross Section View of

Cathode Lifetime Effect

Fig. 11(IV.1).--Schematic drawing of eroded cathode and sputtered cathode material. The latter builds up in a volcanic cone and eventually shorts the cathode causing the arc to "drop out". The 500 MeV PIG source will have axially movable cathodes. When the arc shorts, the cathode will be backed out of contact with the sputtered material so that the arc can restrike and continue to operate, thereby increasing the interval between maintenance periods.

500 MeV cyclotron naturally leads to an additional new cathode feature which should further enhance source lifetime, namely the cathode will be constructed from a long tantalum rod which can be remotely moved axially. With such a cathode it will be possible to break a short caused by sputtered material by backing the cathode out a few millimeters, hopefully thereby gaining an additional factor of two in lifetime before one must finally remove the source to clean out sputtered cathode material.

The rod-type cathode also matches with another novel feature which we plan to include, namely an rf induction coil to provide supplementary heating of the cathode. Source studies at Dubna[14] report significantly higher yields of high-charge-state ions when supplementary cathode heating is used (provided at Dubna by an electron beam). The key mechanism involved in this enhancement is not definitively understood but is involved with the fact that supplementary heating allows the source to operate at lower gas flows, and could in fact be mainly due to reduced charge-exchange losses in the region near the ion source. In any case significant intensity gains (about a factor of two) are obtained with supplementary heating.

A major recent source-related improvement in heavy ion beam intensity has come from recognition of the key importance of charge-exchange collisions near the source. Cross section information for the charge pick-up process is now available;[20] for highly charged ions this cross section is enormous ($\sigma \sim 10^{-14} cm^2$)

on the early turns where the energy is low. The loss of beam due to this process, and also due to the charge loss process which takes over at larger radii, puts a major premium on achieving as good a vacuum as possible. Improved vacuum involves both reduced gas feed (from features such as supplementary cathode heating) and improving pumping. At Oak Ridge for example a supplementary cryopumping system installed near the source[15] improved heavy ion beam intensities by a factor of four. This information immediately sets excellent vacuum as a maximally important design goal for the CSC system. This then leads to the metal gasketing, large cryopanels, etc. described in the previous section. Fortunately this extra pumping is not expensive. The coil refrigerator has a much greater capacity than has previously been used in cyclotrons and approximately three-quarters of this capacity is not needed for the coil except in the cooldown cycle and is therefore available for cryopumping.

The much stronger magnetic field of the superconducting cyclotron will clearly affect the performance of the PIG source and we expect the effect to be strongly favorable. The qualitative basis for this expectation comes from the ninefold increase in the magnetic pressure confining the plasma. The trapping time in the discharge should then be lengthened and the multi-step ionization process thought to produce high charge states will be enhanced. Existing data at low fields[16] support the expectation that yields of high charge states

increase with field, but the results are over a narrow range of field and are clouded by possible changes in extraction geometry as the field shape changes (a phenomenon known to be extremely critical in PIG source output). Quantitative knowledge as to the extent to which the high field improves PIG source performance must then await actual testing of sources in the superconducting magnet. (We have submitted a proposal asking for support for such a study; this proposal is now under review.)

Turning to the question of likely beam intensities in the CSC accelerator system, it is most conservative to simply estimate intensities based on present heavy-ion performance at existing cyclotrons, i.e., not to include any allowance for possible improvement in performance from any of the factors discussed in preceding paragraphs. Even with this assumption the situation is far from simple and the smooth curves presented in the intensity figures in Sec. I are a substantial oversimplification. Factors contributing to the complexity include:

1) The current obtained in a given accelerator run is always influenced by the needs of the experiment then running. To judge the maximum output which a particular cyclotron can produce at some point in time, one must then scan the cyclotron logbook for high values. There is however an immediate sparcity of data since the large number of available ions makes runs with any particular ion an infrequent occurrence.

2) Even when the influence of scheduled experiment goals is removed, a basic irreproducibility in PIG output of about a factor of two appears to remain, depending on unidentified subtle points of geometry, materials, accelerator conditions, etc.

3) Cyclotron heavy-ion technology has been rapidly evolving and logbook entries must be keyed to whether various elements of improved hardware were or were not in use. Thus at Oak Ridge, data without cryopanels give a very different inference than data with cryopanels in use. Also in the spring of this year Oak Ridge introduced a technique for enhancing intensities of many light ion beams by a factor of ten using a partial mixture of xenon as a source support gas; logbook entries using this technique are then totally different from entries based on previous procedures.

4) The total energy required to ionize an atom to a given level is not a smooth function of atomic number when one looks in detail. Sizeable shell effects remain, particularly for light ions. These can lead to unusual steps in intensity between adjacent charge states or between adjacent elements. Such effects are neglected in going to a smooth intensity distribution as for the figures in Sec. I.

5) The design of the cyclotron central region has an important impact on the fraction of the beam which is accepted; the relevant features are strongly dependent on the acceleration harmonic number. If the central region has been optimized for some harmonic number, acceptance can be orders of magnitude higher than for unoptimized harmonics. Optimized design is generally more difficult the higher the harmonic because of

transit time effects, but these can be substantially offset by use of a DC grid on the source.[17] Results on high harmonics therefore vary greatly depending on whether such a grid was in use.

With thought for all of the above factors we list below a selection of observed entries from the ORIC logbook,[18] as typically illustrative of present cyclotron heavy-ion performance. The list contains both the observed external beam at ORIC and the current inferred for the given ion from Fig. 2 of Sec. I of this proposal. Also a ratio of these currents is given.

Ion	Total Ionization Energy (ev)	ORIC harmonic	ORIC External Beam particles/sec	Intensity from Fig. 2 Section I	ratio	Comment
$^{16}O^{5+}$	320	1	4.2×10^{13}	2×10^{12}	21	with Xe
$^{20}Ne^{7+}$	783	1	3×10^{11}	4×10^{11}	.8	with Xe
$^{40}Ar^{8+}$	627	3	9×10^{11}	10^{13}	1/10	
$^{40}Ca^{7+}$	476	3	6×10^{11}	4×10^{13}	1/70	sputter with Xe
$^{64}Zn^{6+}$	367	3	1.5×10^{12}	10^{14}	1/70	" " "
$^{129}Xe^{12+}$		3	6×10^{8}	10^{11}	1/170	26% isotope

This list immediately indicates the intensity estimates in Sec. I to be conservatively sound for the lighter ions and perhaps overly optimistic for heavier particles. Part of this is due to the central region design of ORIC which is optimized for first harmonic and has reduced acceptance on the higher harmonics; unfortunately there is no quantitative estimate of this factor but it could easily be an order of magnitude. Even with this effect included it appears likely that actual intensity contours

will have a steeper slope than our Sec. I estimates, i.e. favoring the lighter ions and disfavoring the heavier ions, the likely shift being of the order of one contour interval in the figure. This is however a relatively minor difference in terms of impact on the physics program. Further the many likely improvement factors reviewed above in our opinion make the intensity estimates of Sec. I a reasonable smoothed representation of the likely beam status at the initial turn-on of the facility.

Addendum to Sec. IV.1.3

As noted in the proposal, accurate assessment of performance to be expected from the Penning ion source is difficult. (A main Penning characteristic unfortunately is lack of reproducibility -- intensity variations of factors of 2 or more from run to run are common even in the best of conditions.) In spite of these difficulties, the Penning source nevertheless continues to rank as the most effective device for producing intense CW beams of highly charged positive ions, and is at present used on all heavy ion cyclotrons as well as on the heavy ion linear accelerators at Berkeley and Darmstadt. (Darmstadt has in fact recently shifted from dual use of Penning and duoplasmatron sources to sole use of the Penning.)

Two main sources of data can be used to estimate currents which one might expect from a cyclotron equipped with a Penning source, namely 1) DC test stand data on the source itself, and 2) surveys of beams obtained from accelerators using these sources. The table on Page 131 of the CSC proposal is representative of data on beams obtained from cyclotrons, the particular data being from the ORIC cyclotron at Oak Ridge. Heavy ion beams from our 50 MeV cyclotron are also very like the Oak Ridge data (which is not surprising in view of the design by M. Mallory), and also tables of accelerated beams from the 88" cyclotrons at Berkeley and Texas A&M are very similar. Reasonable summary statements from a review of all these data are, 1) best performance is obtained with gaseous feed materials; 2) even with gases, significant elemental effects remain which give fluctuations of factors of 2 to 4, depending on electron shell effects

and binding energy; 3) solid materials can be readily introduced into the Penning by use of a sputtering electrode, but yields are generally reduced as compared with gases by factors of 2 to 4; and 4) external beams tend to exceed the estimates in Sec. I of the CSC proposal by factors of 10 to 20 for light elements ($A \leq 20$), and tend to fall below these estimates for medium weight elements by factors of 10 to 100. The crucial issue then in interpreting these data is whether the fall-off relative to our estimates at medium mass will exist in the superconducting cyclotron, and whether an even more severe fall-off might exist for the heaviest elements (which no existing cyclotron presently accelerates).

Our intensity estimates in the figures on pages 2 and 6 of the CSC proposal assume that the yield of the source for a particular charge state does not depend on the mass of the ion (except that a rolling-off is included for light elements as Q approaches Z). Ion source test stand data generally support this assumption. Table E is for example taken from a GSI report on Penning source development. The significance of chemical and shell effects shows strongly in this table, but there is no indication of a significant fall-off in the yield of a particular charge state for heavy elements. (The charge 6 column for example might even be said to evidence an increasing yield at large A.) These test stand results then suggest that the observed fall-off in medium mass currents from present cyclotrons is a cyclotron transmission problem rather than an ion source problem.

Two factors dominately determine heavy-ion transmission in

Test Specimen	Arc Parameters			Ion Current (μA_{el}) (peak)											Part. % Metal	Support Gas	Slit Dimens. mm^2
	V	A	P/cw	1^+	2^+	3^+	4^+	5^+	6^+	7^+	8^+	9^+	10^+	11^+			
Si	420	10	25 % 5 ms	35	660	730	220								40	Ar	0,5x20
Ca	600	8	25 % 5 ms	60	--	1150	--	85	--						25	Ne	"
Ti	520	5	CW	--	280	290	270	80							80	Ar	"
V	500	8	25 % 5 ms	--	90	100	120	--	15						20	"	"
Cr	350	12	"	--	240	370	440	370	130	10					45	"	"
Mn	350	10	"	--	950	1000	870	325	65						70	"	"
Fe	300	12	"	--	280	400	400	200	50	--					60	"	"
Co	400	13	"	--	280	--	340	140	--						40	"	"
Ni_{58}	400	12	"	--	120	130	120	50							40	"	"
Cu^{65}_{63}	380	4	CW	--	90 220	80 190	65 155	15 40	~ 2 ~ 5						75	"	"
Zn_{64}	300	14	25 % 5 ms	--	120	190	145	--	10						75	"	"
Ga	350	10	"	--	220	410	280	90	20						30	"	"
Ge_{74}	450	8	"	--	95	120	170	70	35						30	"	"
As	350	10	"	--	110	330	280	150	40						25	"	"
Se	650	10	15 % 1.5ms	--	45	165	200	145	145	75	25				--	--	"
Sr	350	10	25 % 5 ms	--	170	530	600	330	90	15					55	Ar	"
Sn_{120}	360	3	CW	--	--	--	60	25	--						?	"	"
I	650	12	25 % 5 ms	--	--	200	300	440	420	500	270	80	20		90	"	"
Ba	350	10	"	--	--	145	180	250	270	--	115	30			35	"	"
Ce	600	14	"	--	--	--	80	100	95	--	85	70	50		20	"	"
Nd	350	9	25 % 5 ms	--	40	80	160	260	220	--	80	40			25	"	"
Sm	400	8	"	--	20	65	115	155	120	70	--				25	"	"
Tb	400	8	"	--	--	70	--	360	295	200	--	50			20	"	"
Er	500	10	"	--	--	--	85	120	95	70	35				~ 15	"	"
Au	490	6	CW	--	--	--	--	--	15	12	8	3			15	"	"
Hg	600	8	25 % 5 ms	--	--	--	100	140	170	175	140	100	50	20	45	"	"
Pb	400	9.6	"	--	--	--	30	60	80	80	60	33	10		25	"	"
Bi	300	10	"	--	--	--	--	21	36	33	21	8	4		15	"	"
U	350	13	"	--	--	--	--	--	--	26	34	36	40	20	~ 5	"	"

Table I: Ion currents measured at the PIG source test stand.

Table E (IV.1.3). From article, "Penning Ion Source Development at GSI 1976-77", by H. Shulte, W. Jacoby and B. Wolf (reproduced from Report GSI-P-3-77, page 14).

a cyclotron, namely 1) the focusing conditions on the first orbits and 2) the vacuum. The focusing is an effect which can vary greatly depending on precise details of the early orbits, and is also likely to change by large factors depending on the harmonic number of the beam relative to the rf. If the cyclotron beam for example passes through a region of electric defocusing, enormous attenuation factors can be introduced as compared with the situation for well optimized central orbits. This could easily be the case in presently operating heavy-ion cyclotrons, since these machines were originally designed for light ions, reflecting the research interests of the period, and generally have been adapted for acceleration of heavy ions in an ad hoc, seat-of-the-pants way, often with severe restricting constraints imposed by features of the original design. Heavy ions in a cyclotron also generally require operation on higher harmonic numbers than is the case for light ions -- in fact the heavier the ion, the higher the harmonic number that must be used, and high harmonic numbers are certainly likely to give poor transmission. This argument unfortunately remains qualitative since careful studies of heavy ion central orbit conditions have not been made for any of the existing cyclotrons. We have however carefully studied the central orbits in the K=500 cyclotron (some typical results were presented in the addendum to Sec. IV.1.1). These studies show good focusing in all the accelerating modes which will be used in the CSC system, and the techniques employed in these studies, namely detailed mapping of both electric and magnetic fields and numerical integration in

these fields are known to give definitive results. The K=500 cyclotron should then be free of special central region losses for even the heaviest ions.

The other major attenuation mechanism is charge exchange of accelerated ions in the residual vacuum. For given vacuum, present information on charge-exchange cross sections indicates these vacuum losses to be larger, the heavier the accelerated ion, but the calculated losses are also for the CSC much smaller than for existing cyclotrons due to the much more effective pumping system. Numerical calculations of vacuum losses in the CSC indicate a relatively minor beam loss due to these processes.*

In total then, it appears that performance for medium mass and high mass ions in the CSC will be comparable to performance for light ions, and overall intensities then seem most likely to be significantly higher than the estimates given in the figures on pages 2 and 6 of the original proposal.

A further significant question relative to Penning sources is the matter of source maintenance. Cathodes in the Penning sources used in present cyclotrons fail frequently, lifetimes generally being in the range 2 hours to 8 hours. When the cathode fails, the source must be removed, the cathodes changed and the source reinstalled; use of the cyclotron is interrupted for 10-30 minutes in this cycle. In contrast, at GSI, typical Penning source cathode lifetimes are 40-50 hours for light and medium elements, and 25 hours for the heaviest elements. Since the basic geometrical

*M. Mallory, B.A.P.S. 8, 1015(1977).

structure of the GSI source (15 cm high and 8 mm x 8 mm square chimney) is essentially identical to a typical cyclotron source, it seems most likely that the longer cathode lifetime at GSI dominately reflects the relatively low power at which the source is operated. The low source power operation at GSI in turn reflects the fact that the linear accelerator is designed for a constant Q/A ratio, and charge states needed by the Unilac for light mass and medium mass ions are very easy to obtain. This is in contrast with present cyclotrons where the energy increases as Q^2, and cyclotron users then tend to work at the highest possible charge state in order to be on the energy frontier. The coupled cyclotron system will however be much more like the linac, at least with the lighter elements. Thus a C^{2+} ion from the source will give full energy from the coupled cyclotron system and there is no gain from use of higher charge states. A Penning source optimized for charge two would undoubtedly have a long cathode lifetime.

Runs with heavy elements will nevertheless continue to place heavy demands on the Penning source, and typical cathode lifetimes for these elements are likely to be in the 2 to 4 hour range. Easy maintenance capability is therefore emphasized in the design of the source system for the 500 MeV cyclotron. The design thus involves two totally independent sources, one inserted from the top and one inserted from the bottom of the magnet in 2" diameter iron-free holes. A new source will then be waiting, already pumped out and in a partially heated condition, just off the median plane. When a cathode fails, the rf will be turned off, the burned out source

pulled back, the new source moved up and the rf restarted. This cycle should require no more than one to two minutes. For most heavy ion beams, the source technician will be able to go into the vault with the cyclotron running since the beams will be well below radiation producing levels. The burned out source will be removed through its vacuum lock, replaceable elements will be installed, the source reinserted into the ready position, pumped out and given an initial heating, all while the cyclotron continues in operation. The system is then ready to recycle.

Our overall expectation is then that the accelerator system will be able to produce currents as estimated and that source maintenance operations will be reduced to a level where there is no significant interference with the nuclear physics program.

Turning to the question of future developments in sources, we note first of all that source development in our own laboratory is actively proceeding although on a somewhat smaller scale than anticipated at the time the CSC proposal was prepared. (The portion of our ion source development proposal dealing with a dedicated source testing facility was unfortunately not funded.) Our present source development program consists of construction and utilization of sources in the 50 MeV cyclotron and testing of sources in the 500 MeV magnet. These latter tests are fitted into the magnet schedule in periods when the magnet is not tied up by some other cyclotron construction activity.

The Penning ion source for the 50 MeV cyclotron as previously indicated performs well, basically matching the performance of

similar sources in other present cyclotrons. Tests of sources in the 500 MeV magnet are expected to begin in a few months, and we should at that point begin to obtain real data on the exciting speculations as to likely improvements in peak performance in the high field (as discussed on page 128 of the CSC proposal). We also continue to maintain close contact with the outstanding source development program at GSI. (The GSI program of itself constitutes a major proportion of present world effort on Penning source development.)

At a number of laboratories, major programs are in progress aimed at development of so-called exotic sources, particularly sources which might yield charge states in the 20-30 range. If development of any of these sources proceeds to the point where such charge states can be reliably obtained with good intensity and good duty factor, from a source significantly less expensive than the 500 MeV cyclotron, we would certainly propose to procure such a source for the CSC system. The central iron plug of the 500 MeV cyclotron can be adapted to allow insertion of an axial injection system, as noted in the original proposal. Injection from an external ion source could then be accomplished in much the same fashion as polarized ions are presently injected in many existing cyclotrons. As a point of reference for evaluation of exotic sources, we note that the 500 MeV cyclotron is itself an exotic ion source, i.e. the beams from the cyclotron, after stripping, are in the charge range 20-30 with good intensity and good optics, and are also sufficiently rigid to be easily injected into a following accelerator. If an exotic ion source were then

comparable in cost to the 500 MeV cyclotron, as present exotic source projects tend to be, or if the source had difficulties with intensity or duty cycle, then one would certainly think of an additional cyclotron as a more effective technique for obtaining ultra-high charges (assuming a compelling physics demand for such high charge states had been established).

IV.1.4 Beam extraction

Typically in cyclotrons the extraction system is a critical component involving tighter margins on natural limits of materials and fields than other components and often in the end greatly degrading the beam quality. In the superconducting cyclotron extraction moreover tends to be significantly more difficult since the usual extraction technique is to use electric fields to partially compensate the magnetic force and no technique is available for achieving the threefold increase in electric field strength which would be needed to obtain the same fractional magnetic compensation as in normal cyclotrons. It is then of great importance to carefully study the extraction system for the superconducting cyclotron at an early stage to be sure that extraction is in fact possible. This has then been a principal line of effort of our design studies. The studies have included testing of component mock-ups in our existing cyclotron.

The conceptual guidelines for the extraction system for the 500 and 800 MeV cyclotron are the same as those used in our present cyclotron, namely: 1) use the Q_r=1 resonance to build a coherent amplitude in the focusing oscillation; this amplitude alternately adds or subtracts from the natural turn separation depending on the phase of the precession and gives comfortable turn separation at the deflector entry point. 2) use all available devices to bring the beam across the magnetic field edge as quickly as possible, and 3) distribute focusing elements along the extraction path to offset the natural defocusing of the fringe field, thereby keeping the beam

narrow and avoiding the quality deterioration which the aberrations (from the large nonlinear components of the fringe field) would otherwise induce.

The extraction system for the superconducting cyclotron follows exactly these guidelines. The process begins with the Q_r=1 resonance which excites the coherent focusing oscillation. Perhaps the most striking illustration of this phenomena is an actual turn pattern from our present cyclotron; such a pattern is shown in Fig. 12. The full spatial separation of turns with zero intensity in the region between turns shows clearly in the figure. For the case shown, the discrete structure of the energy spectrum was sharpened by use of a phase selection system in order to enhance the coherence. If a broad interval of phases had been used, the figure would be smeared out but each orbit would nevertheless be experiencing the same enhanced turn separation and its probability of entering the deflector would still be greatly increased, although in the broad phase case some particles will of course always be lost. If the cyclotron is well stabilized the phase interval is the distinguishing difference between clean turn separation at extraction and smeared turns. We plan to include a phase selection system in the injector cyclotron parallelling the system in our existing cyclotron. Our existing system is designed so that it can be either inserted or removed with the flip of a console switch, the choice depending on the relative importance of intensity or precision in a particular experiment. With the Q_r=1 resonance and the calculated field shape, calculations of accelerated

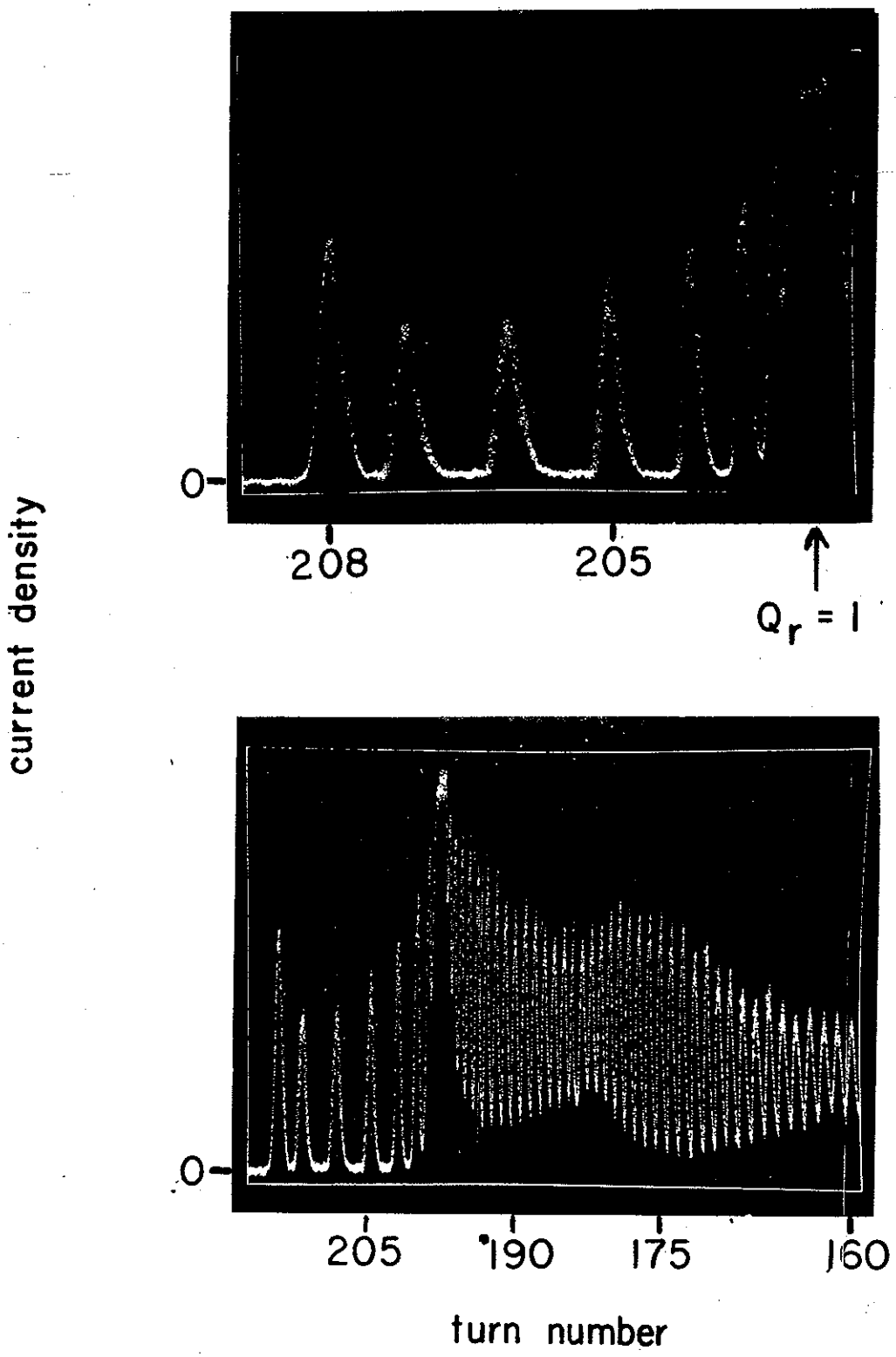

Fig. 12(IV.1).--Particle density versus radius in the extraction region of the MSU cyclotron showing turn structure and showing the build-up of turn spacing following the Q_r=1 resonance. The pattern is taken with the cyclotron's phase selection system in use which gives a sharp energy spectrum and therefore a sharp turn spectrum.

orbit behavior preceding the deflector entry give 4.5 mm as the turn separation in the most severe case, which makes clean deflector entrance comfortably easy.

Once the beam has entered the deflector the difficult problem begins, namely cleanly transporting the beam through the edge region of the magnetic field. At the very early stages this problem was a dominant consideration in the design of the 500 MeV magnet; the main criterion in selecting the superconducting coil shape was to provide a sharp field edge to make extraction easier. With the field edge as sharp as constraints allow, the remaining problem is to find feasible combinations of electric and magnetic fields which will pull the beam out of the cyclotron as quickly as possible and at the same time offset the defocusing of the fringe field. Originally our extraction plans involved a superconducting shielding tube as one of the important elements in accomplishing the desired goal.[6] Such tubes were originally developed at Stanford[19] and have been used successfully in a number of important applications. The supertubes do however involve critical elements of technique which are difficult to reproduce and which lead to wide variations in the performance of given tubes. After testing several tubes loaned to us by Stanford, we developed substantial concern as to whether supertube reliability was really adequate and therefore turned primary attention to extraction systems utilizing more conventional devices.

The system finally selected uses very conventional elements, namely three electrostatic deflectors as the prime

bending element. These deflectors are shown in Fig. 6. The deflectors are adequate to break the beam free with the field edge achieved but give no assistance in offsetting the fringe field defocusing. For this latter purpose we plan to utilize arrays of iron bars which in the saturated condition produce a linear, strongly focusing field gradient, as has been known for some time by synchrocyclotron designers. The idea was newly brought to our attention as well matched to the needs of the superconducting cyclotron by Clarence Hoffman of the Chalk River Group. Figure 13 presents the results of orbit calculations for the full extraction system, namely deflectors and focusing bars, and shows beam width superimposed on a contour map of the magnetic field in a convenient distorted projection where the polar angle theta is plotted as a linear coordinate. The set of initial conditions used for the calculation of the figure involves the highest velocity full-field beam, which is the most difficult extraction situation. The 2 mm turn width assumed at the deflector entry point matches the value expected in the actual beam. As the figure shows, the beam comes out of the cyclotron in a tight narrow pencil and when the set of rays are inspected in phase space the distribution is found to be highly linear so that the lenses of the beam transport system can proceed to linearly reshape the phase space distribution in any way desired. The performance is in fact excellent in every respect.

Two of the three deflectors in the system are located in hills of the magnet where the clearance between poles is relatively restricted. We have confirmed that the design clearances

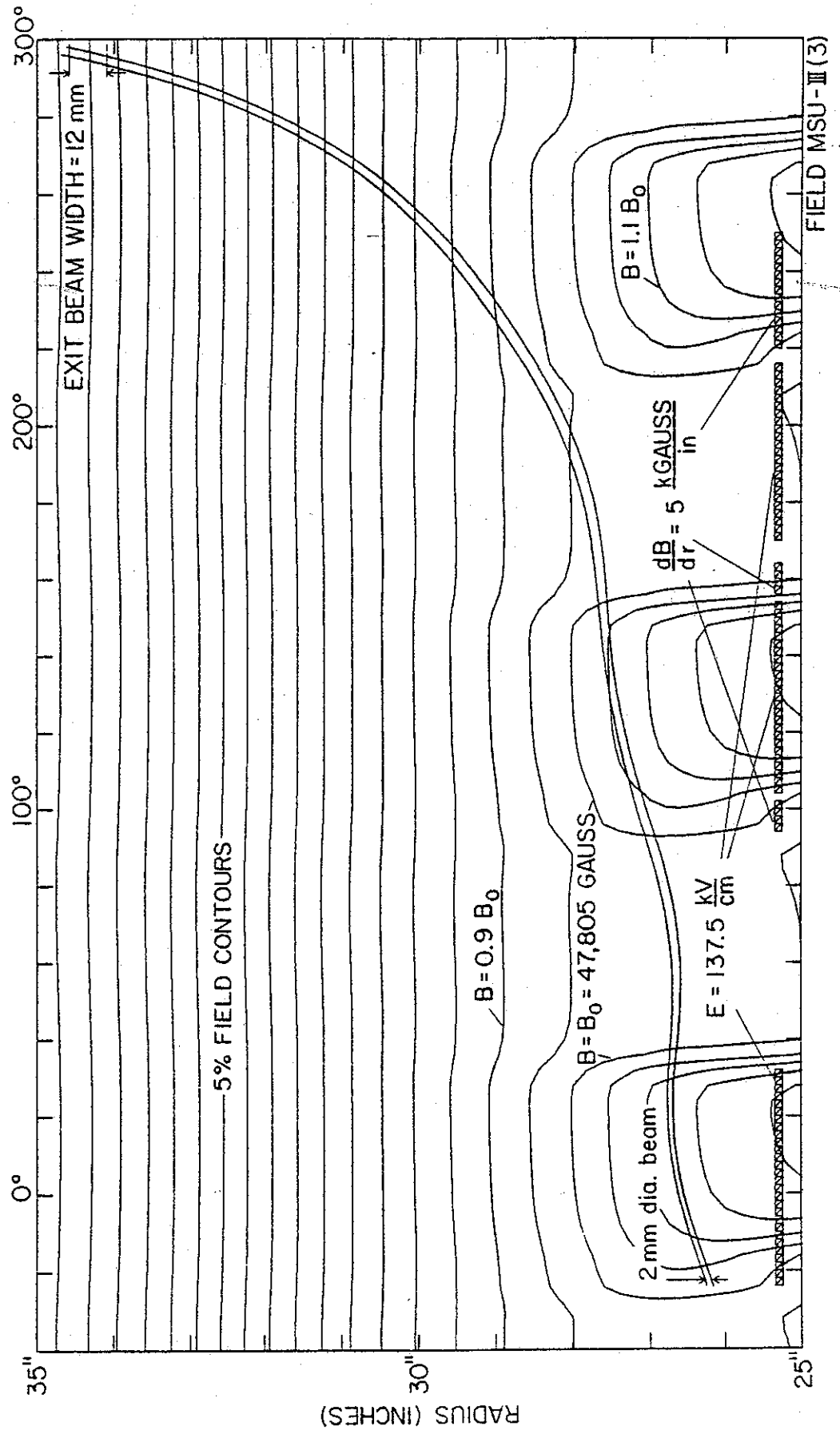

Fig. 13(IV.1).--Computed beam envelope from deflector entrance to exit port for the 500 MeV cyclotron shown in a distorted projection where radius and azimuth are plotted as linear coordinates. The deflection elements act over the azimuth intervals indicated by the cross-hatched bars near the bottom of the figure. The orbits are superimposed on a magnetic field contour map which gives 5% contour intervals relative to the central field value of 47,805 gauss. The magnetic focusing bars largely offset the fringe field defocusing so that the beam width remains narrow.

are adequate by modifying the existing deflector in our present cyclotron so that the various clearances are the same as assumed in the new design. This modified deflector has worked very satisfactorily. As in our present cyclotron, all electrostatic deflectors will be mounted in fixed position without remote adjustment. For variable energy operation, the orbit shape in the new cyclotron shifts substantially, since the percentage azimuthal variation increases inversely with field strength as the field is lowered and this percentage is linearly related to the amplitude of orbit scalloping. The three-deflector system contains an effective compensating element for the change in scalloping in that the voltages on the three deflectors can be independently adjusted. Also, the magnetic focusing elements are provided with spatial adjustments and sensing elements will be provided at several points along the deflected beam path. Computer studies utilizing these controls verify the capability for adapting to changes in orbit scalloping with the fixed position deflectors.

In summary the extraction system as now designed consists entirely of known elements, the detailed design of which has been confirmed by testing in the existing cyclotron, and the system leads to excellent characteristics in the extracted beam.

Addendum to Sec. IV.1.4

The beam extraction system for the 500 MeV cyclotron is basically as shown in Fig. 13 on page 138 of the CSC proposal, namely three electrostatic deflectors plus a system of inert focusing bars. Several details have however changed as a result of "polishing" studies on the system. The arrangement of focusing bars is thus somewhat different than that shown on page 138, the first bar now being omitted, the second lengthened and the third divided into a series of shorter elements of greater total length. The focusing bars are also now positioned radially so that the beam central ray follows the geometric center of the focusing bar aperture rather than following the zero field contour which is sizeably shifted from the center.* These changes give an even better beam envelope than that shown in Figure 13. The exit beam width is now 7 mm and the electric field required for the three deflectors is reduced to 110 kV per centimeter. Field measurements in the edge region of the superconducting magnet also confirm that the magnet field shape assumed in the extraction calculations is accurately realistic. The extraction system overall is then in excellent shape. Electric field requirements are 30% lower than the corresponding requirement for our 50 MeV cyclotron and optical properties are significantly superior. (The 50 MeV extraction system is of course itself very good -- as far as we know the best that has been accomplished in cyclotrons thus far.) The 500 MeV cyclotron we then feel should operate routinely and

*Gordon, Herrlander, and Johnson, MSU Cyclotron Laboratory Annual Report 1976-1977, p. 115.

smoothly, and preserve beam quality in an outstanding way.

In the 800 MeV cyclotron, the extraction system should run with basically the same electric field levels as in the 500 MeV machine. The maximum ion velocity is somewhat higher in the 800 Mev machine (200 MeV per nucleon vs. 80 MeV per nucleon), and this acts to make electric deflector extraction more difficult. This difficulty is however almost evenly balanced by compensating factors coming from the lower average magnetic field (44 kilogauss rather than 49) and by the larger orbit radius (1 meter rather than 65 centimeters). The final important factor, the sharpness of the edge in the magnetic field, is essentially the same in the 800 MeV cyclotron since the magnet gap and coil radial width are the same.

IV.1.5 Coupled-cyclotron matching requirements

The requirement that the two cyclotrons operate as a coupled system imposes a number of operating restrictions. The essential features of the problem can be understood by thinking of the time dependence of the beam as it passes from one cyclotron to the other. The beam from the first cyclotron, or from any cyclotron, consists of a train of short pulses spaced in time according to the period of the rf frequency used on the accelerating system. As each of these pulses enters the second cyclotron it must be timed relative to the rf voltage in the second cyclotron so as to be accelerated. If every pulse from the first cyclotron is to see such an accelerating field, the rf frequency in the second cyclotron must be the same as the frequency in the first and phased relative to the first in a way which compensates for the transit time between the two machines. (The frequency in the second cyclotron could in principle be some integer multiple of the frequency in the first but in practice this is undesirable both because of practical difficulties in the resulting frequency range and also due to the fact that the final energy error for a given initial phase spread would be greatly increased.)

After the ions have entered the second cyclotron, continued acceleration requires that they stay in phase with the radio-frequency voltage, i.e. that their orbital frequency matches the rf frequency or some harmonic thereof. The orbital frequency in a cyclotron is of course proportional to the product

of charge and field (Q and B) and for given Q, the match between accelerating frequency and orbital frequency is achieved by appropriately adjusting the B of the second cyclotron. If this can be done by lowering the magnetic field, there is no difficulty except that the final energy will be less than one would infer from simply using the K value corresponding to peak field. It may well however happen that the field needed to obtain the desired frequency is higher than the maximum field of the magnet. In this case the only way of achieving the required frequency is to shift to ions with a higher charge state. Such a shift will however involve changing to a charge state which is off of the peak of the stripping distribution and therefore the intensity is reduced. This is then referred to as a "frequency mismatch" between the cyclotrons.

The matching of the time structure of the beams in the two cyclotrons also has the effect of forcing the second cyclotron to act as an energy multiplier for the first. The linear velocity of the particle is unchanged in the transition from one cyclotron to the next -- if the orbital frequencies are to match the same accelerating frequency the length of the last orbit in the first cyclotron must be in an integer relation to the length of the first orbit in the second cyclotron. The ratio of these lengths is the "harmonic ratio", h_1/h_2, of the two cyclotrons. The energy gain in the second cyclotron is proportional to the square of the ratio of final radius to injection radius and we have:

$$E_{2_f} = \left(\frac{r_{2f}}{r_{2i}}\right)^2 E_{1_f} \quad , \qquad \text{but } r_{2i} = \frac{h_2}{h_1} r_{1f}$$

and therefore

$$E_{2_f} = \left(\frac{r_{2f}}{r_{1f}}\right)^2 \left(\frac{h_1}{h_2}\right)^2 E_{1_f} = \gamma_2 \, E_{1_f} \quad , \text{i.e. } \gamma_2 = \left(\frac{r_{2f}}{r_{1f}}\right)^2 \left(\frac{h_1}{h_2}\right)^2 .$$

γ_2 is then the energy multiplier. Note that it does not depend on either B or Q in the second cyclotron. Individually these are not determined; their product must be set to satisfy the orbital frequency matching requirement.

If $K_1 \, (Q_1/A)^2$ is inserted in place of E_1 we have

$$E_2 = \gamma_2 \, K_1 \, (Q_1/A)^2$$

The maximum value of E_2 is then proportional to the square of the charge state in the first cyclotron, i.e. high initial charge states are of key importance. To lower the energy one first lowers K_1 which corresponds to lowering the magnetic field in the first cyclotron; when the energy reaches the value corresponding to using the next lower value of Q_1 at full field, one shifts to this charge state which since it is lower would be more intense. The cyclotron field is then generally used near its maximum value which is helpful in minimizing the scalloping change in the extraction region.

The phenomena are shown quantitatively in Fig. 14 for the cyclotron system proposed here. The solid lines labelled with charge states give the maximum energy of the pair of cyclotrons when the ion source in the first cyclotron is giving the charge indicated. The dashed lines at the upper right of the figure mark the region where the magnetic field of the second cyclotron is incapable of being set high enough to give the required

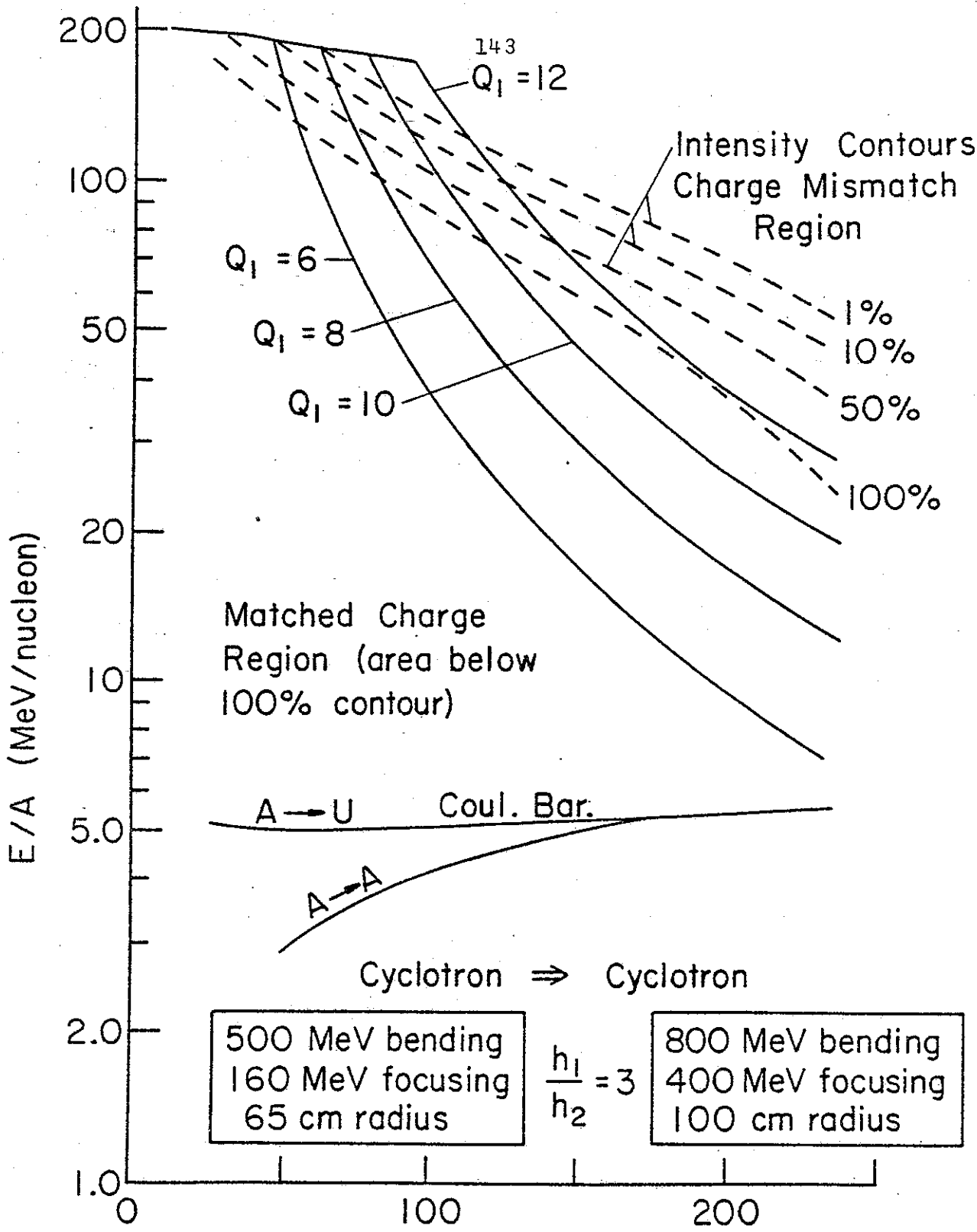

Fig. 14(IV.1).--Energy per nucleon versus mass number for the proposed two-cyclotron system. The maximum energy from the system depends on Q_1, the charge state in the first cyclotron as indicated in the text. The solid curves are the maximum energy for respective values of Q_1 as labelled. The dashed curves at the upper right mark the region where the charge state in the second cyclotron must be above the peak of the stripping distribution leading to intensity loss as noted on the contours. The normal operating region of the two-cyclotron system is generally well below the loss region.

rotation frequency; operation in this region must then use ions in the second cyclotron which are beyond the most probable charge of the stripping distribution and intensity is therefore reduced as indicated by the percentage value on the various contours. The solid lines are seen to be below the mismatch contours over most of the operating region so that there is no significant mismatch problem for the cyclotron system proposed. For comparison, if 4 had been selected for the harmonic ratio, implying that the ions must go four times faster in the second cyclotron, the charge mismatch problem would have been much more severe, and if 2 had been selected the mismatch would have been entirely eliminated but the second cyclotron would be mostly running far below its rated energy. In any case, with three dees neither of these options is allowed.

At this point we terminate the discussion of design features of the cyclotron system even though many points of detail have not been considered. (We assume that persons interested in knowing more about these details will contact us.) It is, in summary, our strong expectation based on our knowledge and experience with cyclotrons that the superconducting cyclotron will measure up in every way to the best standards of cyclotron performance. We know of no points of critical difficulty which would require development of techniques beyond those already in use in precision cyclotrons.

References (Section IV.1)

1. R.E. Berg, Magnetic Coil Design for a Superconducting Air-cored 40 MeV Cyclotron. MSU report MSUCP-14(1963).

2. C.B. Bigham, J.S. Fraser, and H.R. Schneider, Superconducting Heavy Ion Cyclotron, CRNL report AECL-4654(1973).

3. D.J. Clark, Proceedings of Quebec Heavy-Ion Accelerator Symposium, McGill Univ. (1973).

4. Studio del progetto di un ciclotrone superconduttore per ioni pesanti, Istituto nazionale di fisica nucleare (1976).

5. J. Purcell, Superconducting Magnet System for the 12 foot Bubble Chamber, Argonne report ANL/HEP 6813(1968).

6. H.G. Blosser, Seventh International Conf. on Cyclotrons, Birkhäuser Verlag, p. 584 (1975).

7. J.R. Richardson, AIP Conference Proceedings #9 (1972) 126.

8. L. Ruby, M. Heusinkveld, M. Jakobson and B.H. Smith, Rev. Sci. Instr. 27, 490(1956).

9. Sources of information are from foil tests at Chalk River, from positive column stripping foil experience at the Brookhaven MP tandem facility, and from SuperHILAC foil lifetime experience.

10. The committee consisted of J. Purcell, General Atomic (Chairman), Y. Iwasa, Nat. Magnet Lab., M. Leupold, Nat. Magnet Lab., R. Niemann, Argonne Nat. Lab., and W. Young, Univ. of Wisconsin.

11. Y. Iwasa (private communication).

12. E.D. Hudson, M.L. Mallory, R.S. Lord, IEEE Trans. Nucl. Sci., NS-23 No. 2(1976) 1065.

13. M.L. Mallory and E.D. Hudson, IEEE Trans. Nucl. Sci., NS-22 No. 3(1975) 1669.

14. B.N. Makov, IEEE Trans. Nucl. Sci. NS-23 No. 2(1976) 1035.

15. E.D. Hudson, R.S. Lord, M.L. Mallory, J.E. Mann, J.A. Martin and W.R. Smith, IEEE Trans. Nucl. Sci. NS-22 No. 3(1975) 1544.

16. A.S. Pasyuk, et. al., Atomnaya Enerziya 39 (1975) 139.

17. M.L. Mallory, E.D. Hudson and R.S. Lord, IEEE Trans. Nucl. Sci. NS-20 No. 3(1973) 147.

18. M.L. Mallory (private communication).

19. F. Martin, S. St. Lorant and W. Toner, Nuc. Inst. & Meth. 103 (1972) 503.

20. H. Klinger, B. Muller and E. Salzborn, J. Phys. 138(1975)230.

Addendum to Sec. IV.1.5

The use of three-phase rf modes in both cyclotrons (described in the addendum to Sec. IV.1.1) allows the harmonic ratio h_1/h_2 to be shifted to other values in addition to the basic ratio of 3 discussed in the original proposal. Thus $h_1/h_2=2$ will be used for the lower part of the operating range as indicated in Table A of the addendum to Sec. IV.1.1.

Changes in the harmonic matching ratio also have a possible important application in allowing the CSC system to utilize future ultra-high charge state ion sources which for the basic ratio of 3 would be of little help because of taking the operating region into the charge mismatch region (see figure on page 143 of the original proposal). Going to a lower value of the harmonic ratio in particular raises the charge mismatch contours on a graph of the sort given on page 143, and if an ion source capable of making good beams of a charge state in the range of 20 to 30 should become available, one could obtain energies in the 100 to 200 MeV per nucleon range for even the heaviest ions. The CSC system then has a basically unlimited capability for effectively utilizing benefits from future source development programs. (See also discussion in the addendum to Sec. IV.1.3.)

Addendum - New Sec. IV.1.6 - 800 MeV Magnet Design

A number of design features for the 800 MeV cyclotron have been described in previous addendum sections. In general, design features are based on moderate rescaling of the 500 MeV design. Few detailed studies for the 800 MeV machine have thus far been made since the relatively small extrapolation from the 500 MeV design seems reasonably secure and also reflecting a lack of available manpower. (This latter limitation we note has however recently been significantly relieved -- Professor F. Resmini, Director of the superconducting cyclotron project at the University of Milan, and Dr. G. Bellomo of the Milan group have joined our staff on a visiting appointment basis -- Professor Resmini will be undertaking responsibility for detailed design of the 800 MeV cyclotron -- we hope that other laboratories interested in the design of an 800 MeV superconducting cyclotron will be sending collaborators to join in this study.)

The one element of the 800 MeV cyclotron which has already been studied in significant detail is the magnet since this is the item which mainly determines the overall costs of the cyclotron. Our magnet design calculations as mentioned in the addendum to Sec. IV.1.2 involve use of a model combining a cylindrically symmetric relaxation calculation with a fully saturated assumption for nonsymmetric components. The relaxation calculation is carried out with an LBL program "TRIM" which solves the wave equation for the vector potential in a spatial region including both current sources and magnetic materials, the magnetic materials being specified as empirical tables of B vs. H. The program includes

a feature which allows several different magnetic materials to be included, and we utilize this feature of the program to include the effect of the azimuthally varying components such as pole tips, dee stem holes, etc. by putting in a fictitious material whose magnetization is reduced by a factor corresponding to the azimuthal fraction of the particular r-z element occupied by iron. This procedure then has the effect of precisely matching the volume of magnetic material assumed in the calculation with the volume in the real magnet. Tests on the 500 MeV magnet show such calculations to be accurate to about 0.2%, when the geometry is accurately included. Figure J shows the relaxation grid used in studies of this type on the 800 MeV magnet, and Fig. K shows the computed results for the average magnetic field. As in the 500 MeV cyclotron, the main coil is divided into two parts so that the coil can be used to assist with the trimming thereby reducing the power requirement on the room temperature pole tip windings. The lower two curves in Fig. K show that the field shape can be shifted from the 20% rise required for the most relativistic particles to an essentially flat shape by an appropriate shift of main coil ampere turns.

The azimuthal dependence of the magnetic field is calculated assuming full saturation of pole tip steel, and these components are then added to the average field obtained from the relaxation calculations. Again we note that the 500 MeV magnet shows this type of approximation to be highly accurate. Orbit properties are then computed in the combined field.

A possible difficulty in the 800 MeV cyclotron is posed by

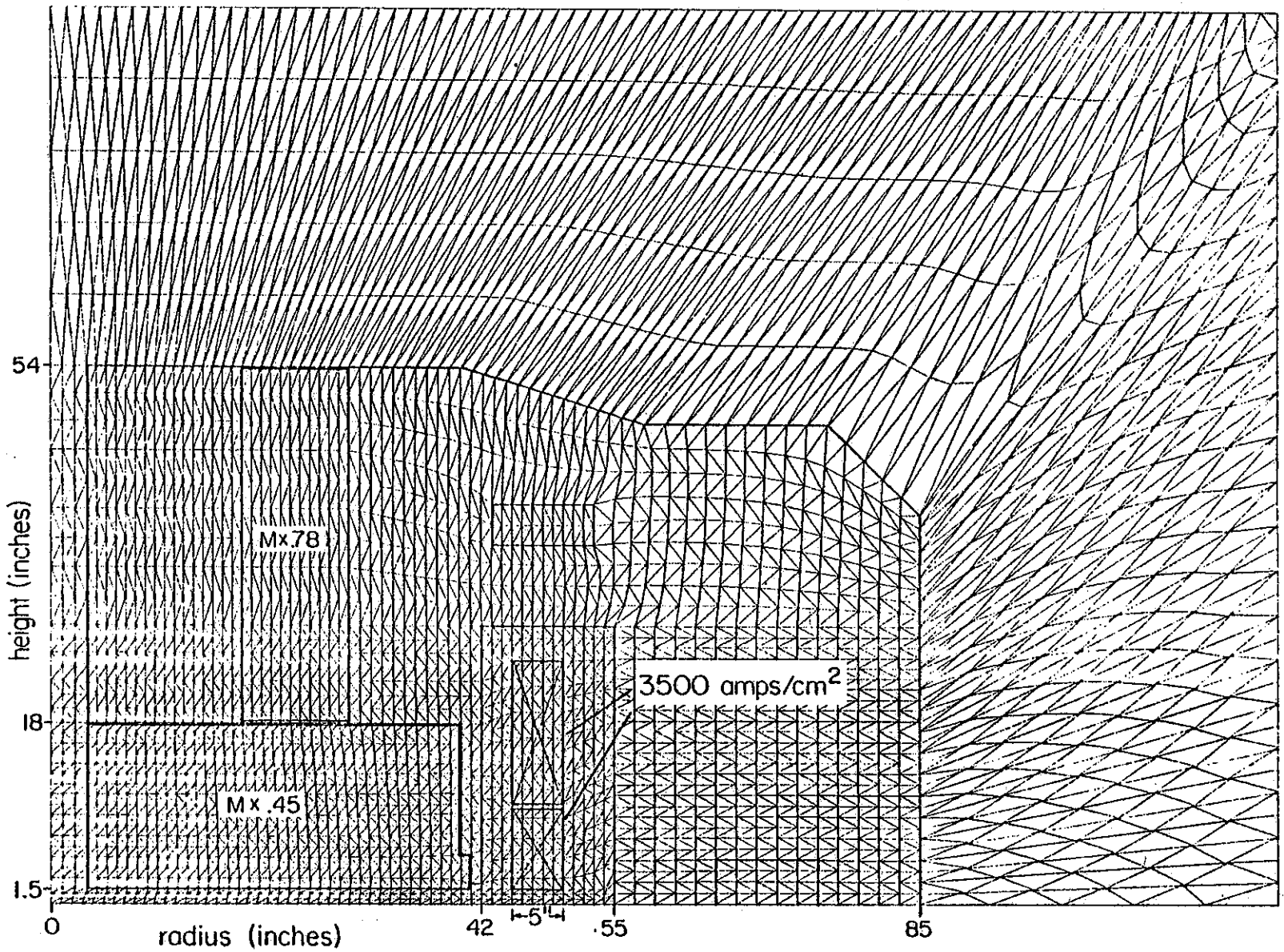

Fig. J (IV.1.6). Drawing showing the relaxation grid used for the cylindrically symmetric part of the field calculations for the 800 MeV magnet. In two regions, labelled "M x .78" and "M x .45", the magnetization is reduced corresponding to the azimuthal fraction of the region which is occupied by dee stem holes and pole tips respectively. Other parts of the magnet are standard 1020 steel.

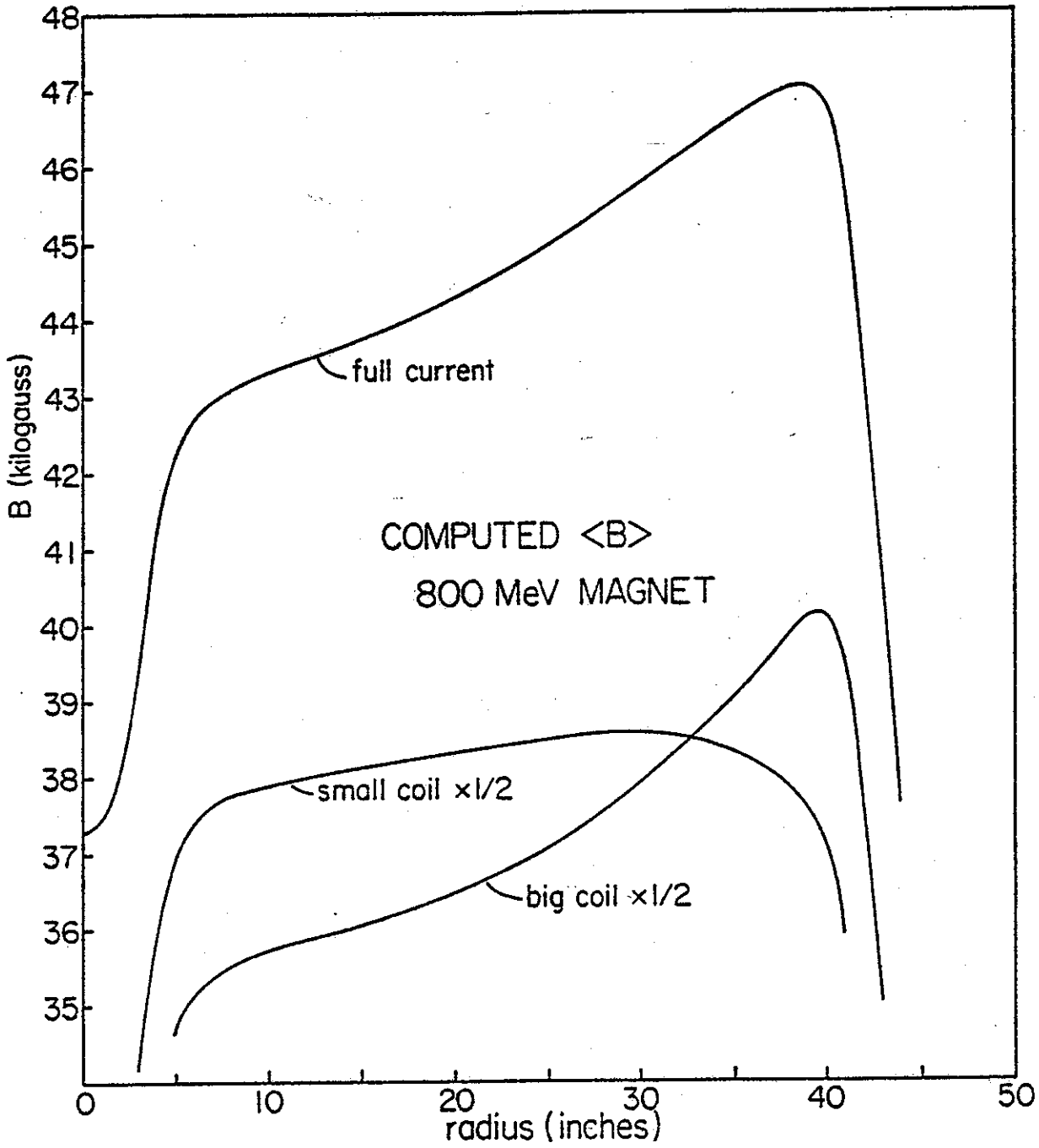

Fig. K (IV.1.6). Computed average field of the 800 MeV magnet, for full current (the upper curve), and for currents reduced to one half in the small coil and large coil respectively. The sharp field fall-off in the edge region closely matches the corresponding fall-off in the 500 MeV magnet, therefore allowing the use of a similar extraction system.

the fact that at 200 MeV/nucleon the radial focusing frequency will approach a major instability known to accelerator physicists as the "3/2's stop band". A series of orbit calculations have then been performed to check the margin of stability relative to this stop band. The first step in these calculations was an exploration of the r,p_r phase plane at an intermediate energy. Results of this study are shown in Fig. L. The closed orbits which define the center of the stable region (the "equilibrium orbit") and the three corners (the "unstable fixed points") are shown as open circles in the figures. These orbits were then tracked in energy and results are shown in Fig. M. In this figure, the stable region at several energies is approximately drawn in as a triangle between the unstable fixed points. At 190 MeV per nucleon, the stable region is seen to be approximately one inch in size which is comfortably adequate for the accurately defined beams which would be injected into the 800 MeV machine although very much smaller than the large stable regions occurring at lower energy. Beyond 190 MeV the field begins to roll off from the isochronous shape in anticipation of extraction and the stable region first enlarges and then quickly shrinks to zero at $\nu_r=1$. From this point, extraction proceeds as in the 500 MeV cyclotron (and also as in most existing lower energy cyclotrons).

Beam injection into the 800 MeV cyclotron has not been studied in detail, but is believed to be straightforward based on results of extensive injection studies at Chalk River. Overall the problem of injection in the coupled cyclotron system should be significantly less complicated than the injection problem for a tandem-cyclotron system in that 1) the cyclotrons are time-locked and all

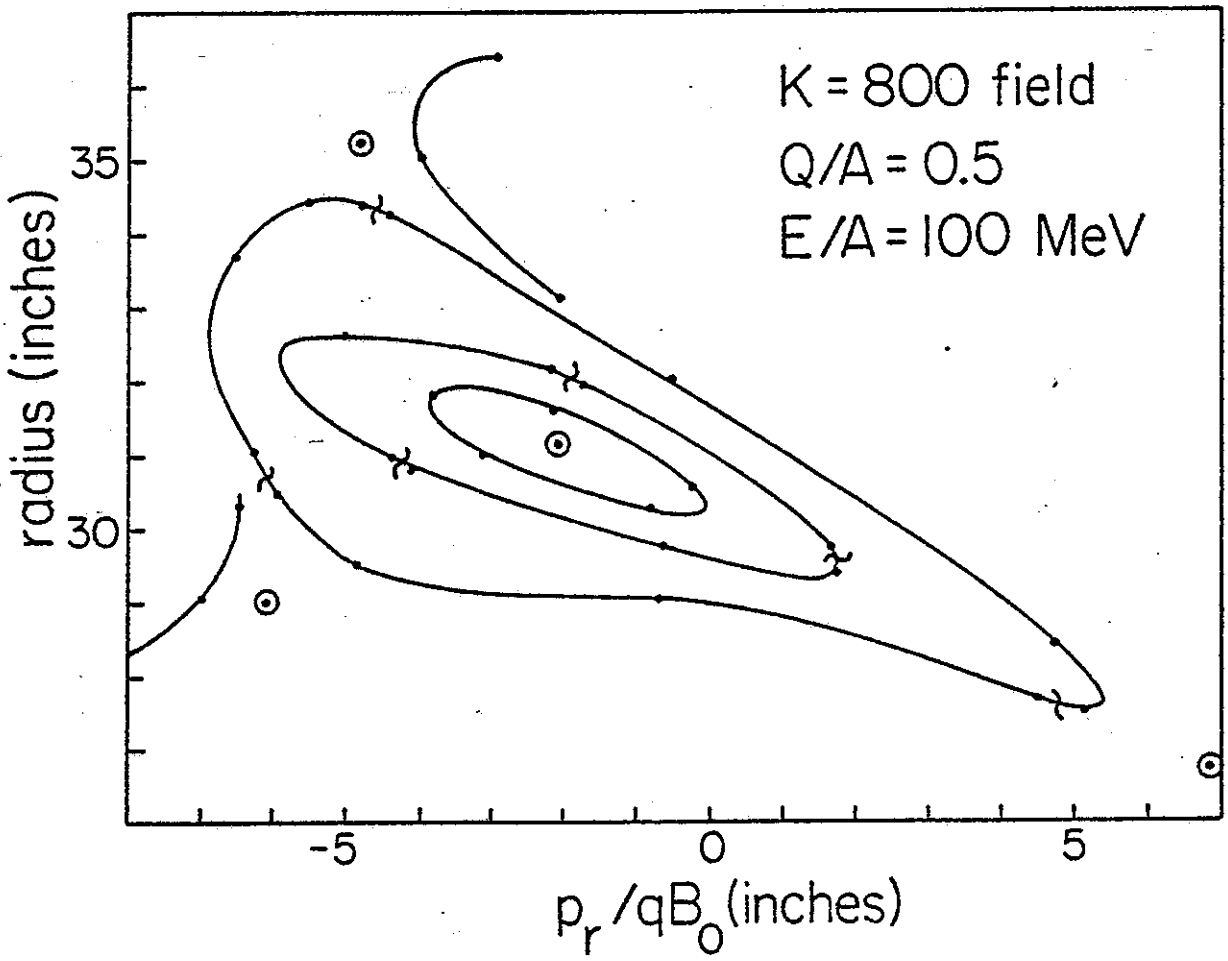

Fig. L (IV.1.6). Results of numerical integrations of ion trajectories in the 800 MeV field. Given a pair of initial values of radius and radial momentum, the coordinates of a trajectory are plotted after each revolution, and points for a given trajectory are connected by a line. The circled dot near the center of the figure corresponds to a pair of coordinate values which repeat, i.e. to an orbit which closes smoothly on itself after one revolution. This orbit is customarily called the "equilibrium orbit". The remaining three circled dots similarly correspond to orbits, which close after one revolution, these being the "unstable fixed point orbits".

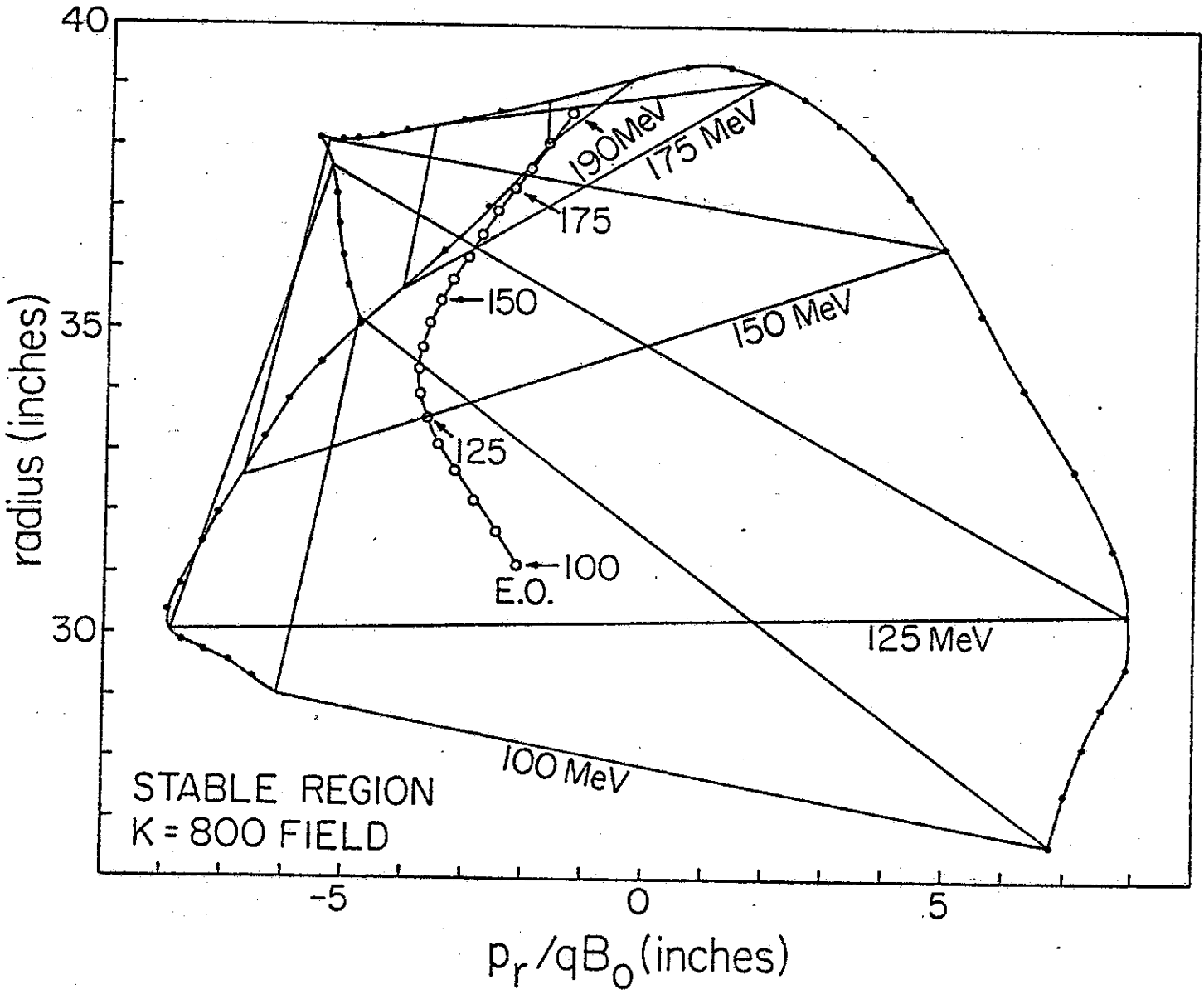

Fig. M (IV.1.6). Plot of r, p_r location of equilibrium orbit (open circles) and unstable fixed point orbits (black dots) as a function of energy per nucleon in the 800 MeV field. A triangle connecting the unstable fixed points at a given energy approximately indicates the size of the stable region. Four such triangles are shown.

timing requirements are automatically controlled by the geometrical length of the transfer line; and 2) the injection orbit is an orbit of fixed radius in the cyclotron-cyclotron case rather than variable radius as in the tandem cyclotron case, and the injection stripping foil can therefore be fixed in position. Studies at Chalk River together with experience at the heavy ion linacs indicate that stripping foil lifetime is not a problem at the energies to be used here.

In summary, design of the magnet for the 800 MeV cyclotron is established on firm ground; other design features appear qualitatively sound; detailed design work on the complete cyclotron will now move vigorously, handled by the group under Professor Resmini.

IV.2. Building additions and experimental layout.

In this section we describe the cyclotron laboratory as it presently exists, the proposed building additions, the proposed experimental areas and beam lines, and the anticipated shielding requirements.

IV.2.1 Building addition and site plan.

Figure 1 is a photograph of the present Cyclotron Laboratory. The tall rear part of the building consists of an 11,000 sq. ft. high bay area which contains five experimental vaults. The remaining approximately 30,000 sq. ft. includes offices, laboratories, library, computer rooms, electronics and mechanical shops, etc. This is in addition to the space occupied by mechanical rooms which service the laboratory.

Internal shielding walls are constructed of stacked concrete blocks which are small enough to be readily handled by one person. Since the initial construction of these walls we have made two major changes in the configuration of this shielding in order to implement important changes in our experimental program. This flexibility feature is retained in our proposed expansion in which most shielding walls will be similarly movable. Roof shielding for the vaults consists of layers of prestressed concrete beams. The whole high bay area is serviced by a 40-ton overhead crane, which can shift roof beams to gain access to any part of the experimental area and is invaluable for installing or relocating heavy equipment.

The proposed expansion of the laboratory as a new heavy ion facility is shown in Figs. 2 and 3. The new areas will increase

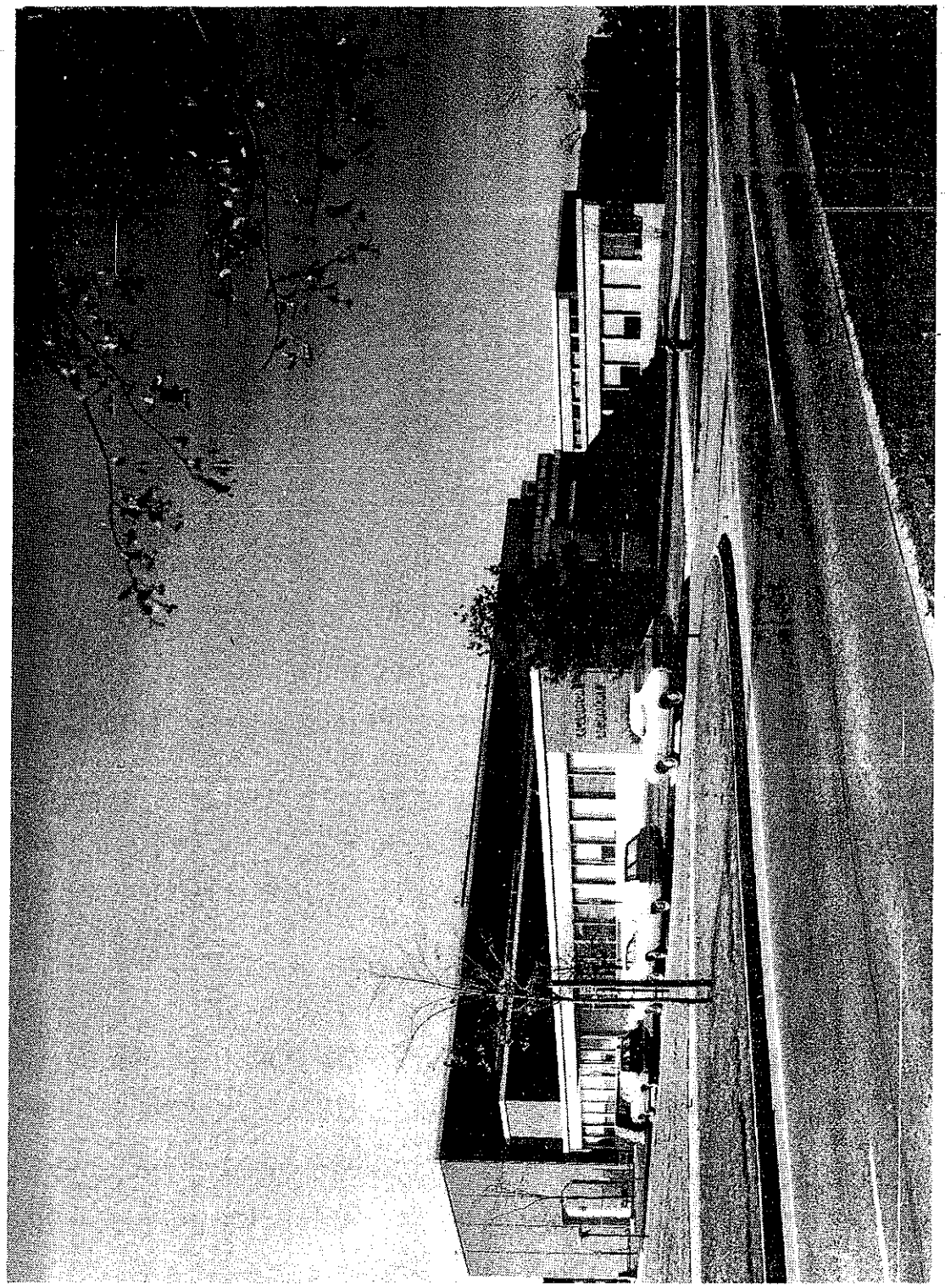

Fig. 1(IV.2.1)--Present Cyclotron Laboratory

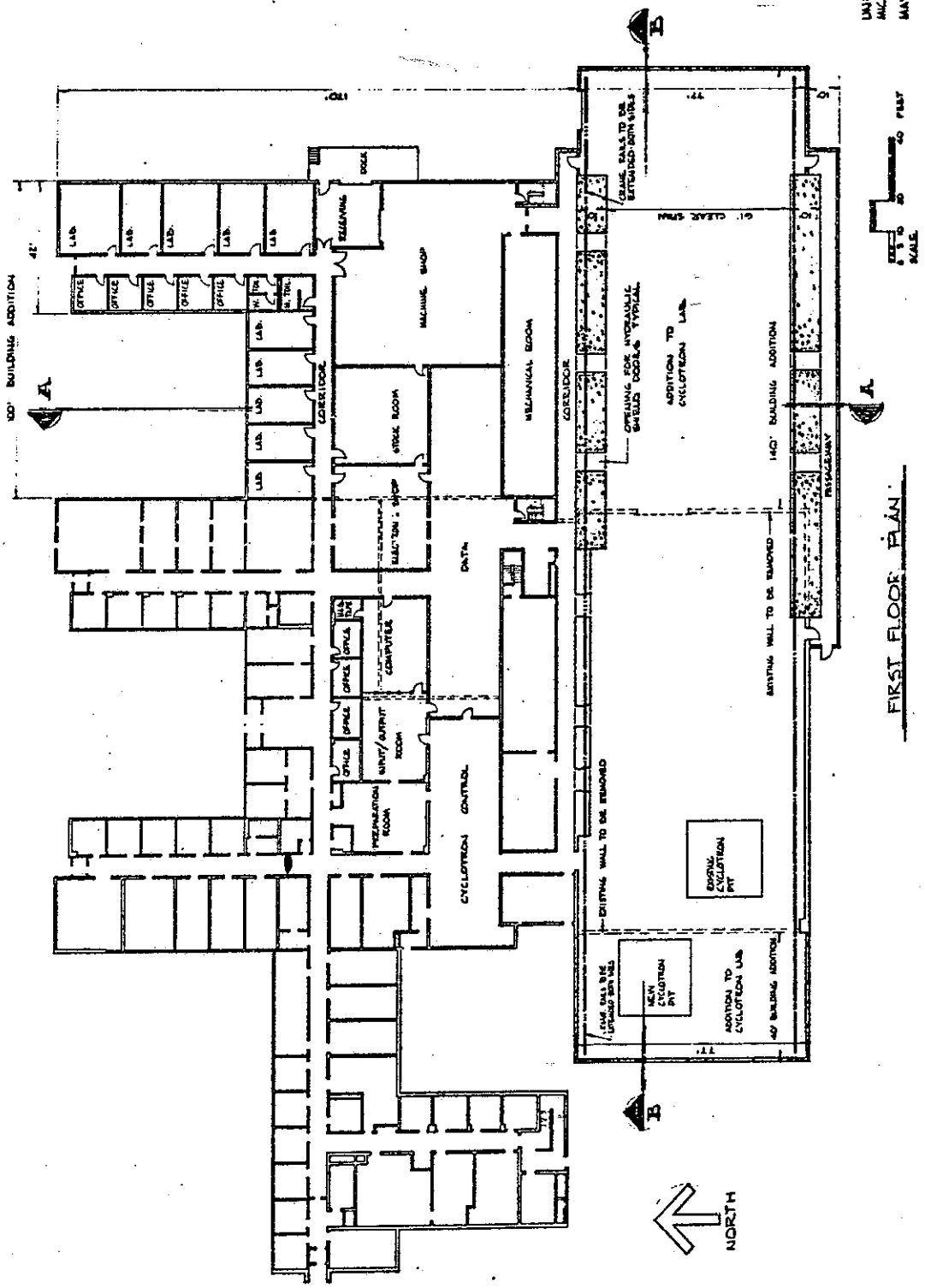
UNIVERSITY ARCHITECT
MICHIGAN STATE UNIVERSITY
MAY 26, 1976
FIRST FLOOR PLAN
NORTH
SCALE
100' BUILDING ADDITION
140' BUILDING ADDITION
MACHINE SHOP
MECHANICAL ROOM
STORE ROOM
CORRIDOR
ADDITION TO CYCLOTRON LAB
EXISTING WALL TO BE REMOVED
EXISTING CYCLOTRON PIT
NEW CYCLOTRON PIT
CYCLOTRON CONTROL
DATA
COMPUTER
UNIT/ SUPPLY ROOM
PREPARATION ROOM
OFFICE
LAB.
DOCK
RECEIVING

Fig. 2(IV.2.1)

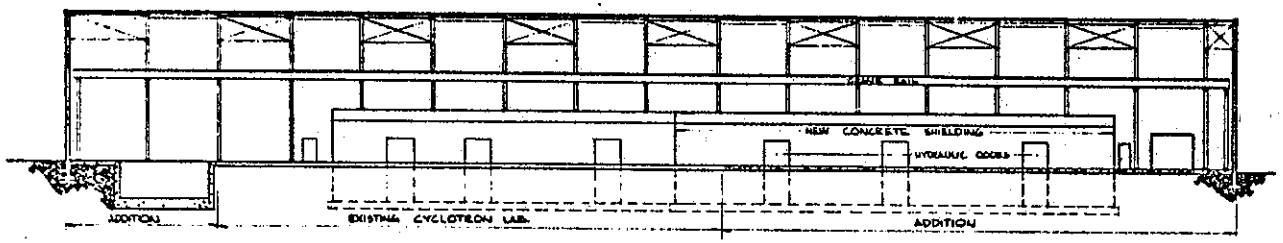

SECTION BB

SCALE 0 5 10 20 40 FEET

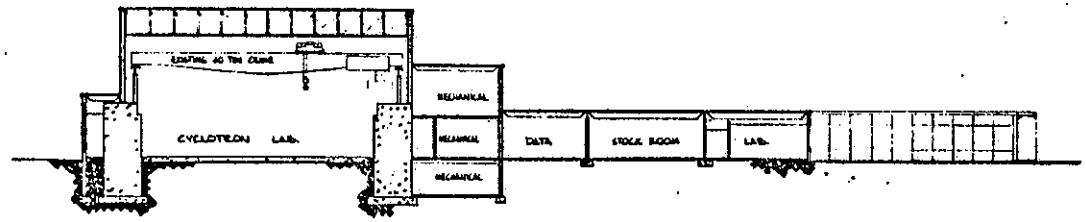

SECTION AA

SCALE 0 5 10 20 40 FEET

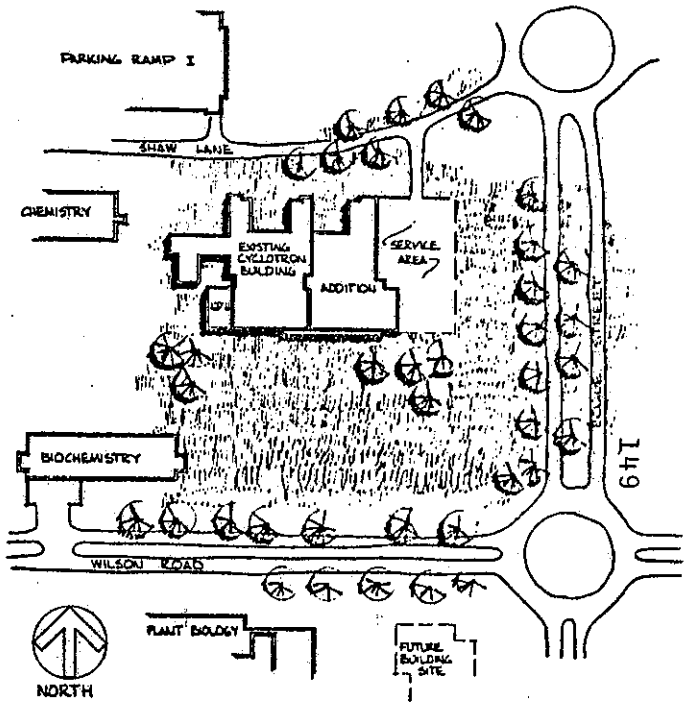

SITE PLAN

SCALE 0 50 100 200 FEET

UNIVERSITY ARCHITECT
MICHIGAN STATE UNIVERSITY
MAY 26, 1976

Fig. 3(IV.2.1)

office and lab space by approximately fifty percent while the experimental areas will more than double. The new plan includes shifting the present machine shop to the new addition and greatly expanding the data room, computer room, and electronic shop. The new high bay areas to the east (≈11,000 sq. ft.) and to the west (≈3,000 sq. ft.) will be serviced by the present 40 ton crane. A large door at the east end of the high bay area will provide excellent delivery access; trucks carrying heavy equipment can drive directly into the high bay and under the overhead crane. There are no buildings either to the south or east of the CSC facility as can be seen from the site plan on the right hand side of Fig. 3, so that further expansion at a later date to the east or south is possible, should it prove necessary or desirable. A graduate residence hall diagonally across the traffic circle at the upper right in Fig. 3 offers snack bar and cafeteria. The laboratory will also reserve a group of rooms for outside users in this residence hall.

IV.2.2 Experimental area

Our present plan for the arrangement of the high bay area is shown in Fig. 1. The layout allows operation of the K=500 cyclotron while the K=800 is being constructed. All of the vaults are accessible to beams from either single stage or two-stage acceleration, with the first cyclotron located in vault A and the second in vault B. Vault #1 is planned for studies which use He-jet or other methods of transport of reaction products. The present split pole spectrograph is in its present position in vault 2, and only the beam line leading to the spectrograph will be changed. Vaults 3, 4, and 5 provide varying size experimental areas, with a large magnetic spectrograph having ample space in vault 5. The small-angle bends in the beam line feeding the spectrograph reflect a qualitative guess for the dispersion-matching requirement of the new spectrograph including the dispersion of the cyclotrons. Detailed design of this beam line will be carried out at a later date. Adequate space is available if stronger dispersive elements should be required to the matching line. Heavy ion reaction product collectors with flight paths on the order of 10 meters can be located in vault 4. The area labeled 6 is the receiving area mentioned above and is serviced by the 40-ton crane which spans the whole experimental hall. An existing beam-rotating device, known as a swinger, is shown in vault 7. This device (refitted with stronger magnets of the standard type used in the transport system) will give a capability for neutron and heavy ion time of flight studies in vault 8 with path lengths

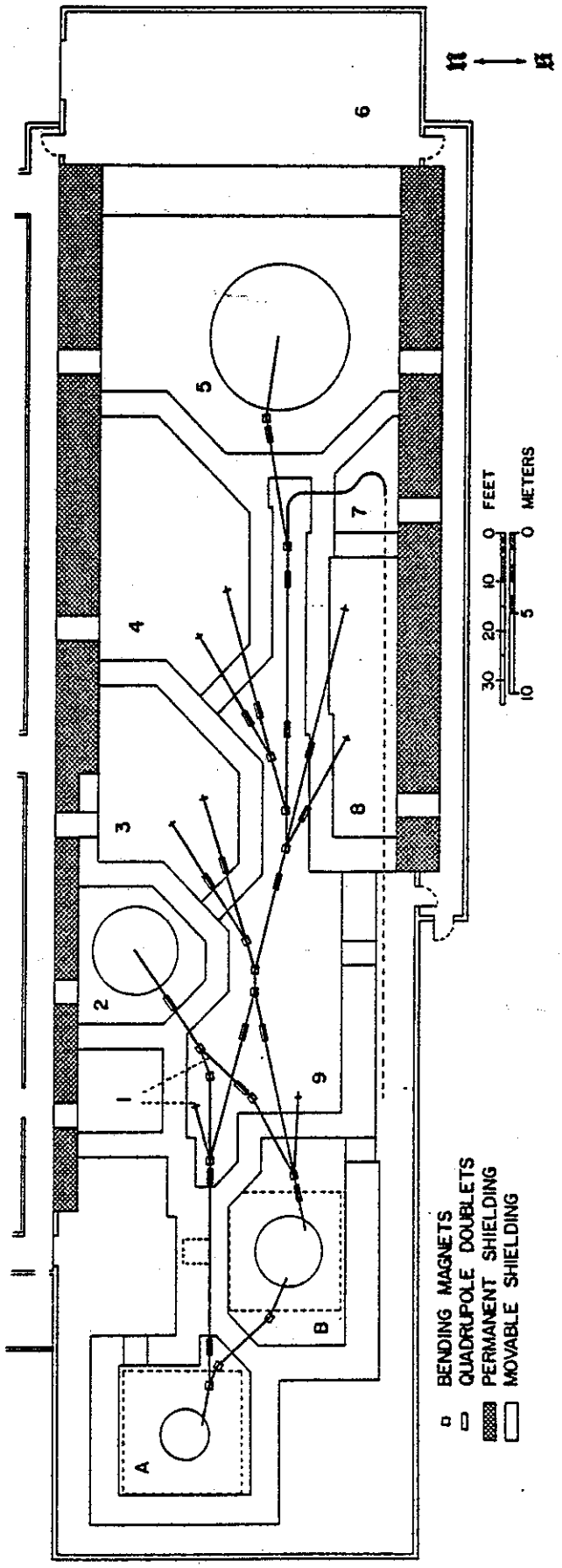

Fig. 1(IV.2.2)--Layout of Experimental Area

from 3 meters to 20 meters. The potential for further expansion to a 60 meter flight path also exists should this be required. Two additional beam stations can be located in vault 8. Vault 9 is the beam switchyard area and provides for a beam station very close to the large cyclotron. In addition to the walls, extensive use of local shielding is planned for slits and beam dumps and will be an integral part of the design of these devices.

The beam transport system includes about 700 feet of beam line, with the beam controlled by 16 bending magnets and 34 quadrupoles. All these magnets will be superconducting and designed in the fashion of magnets now in use in ZGS beamlines at Argonne.[1] Even with superconducting magnets, the high rigidity of the beams mandates relatively small angles of bend, in the present case 17 degrees. The beam rigidities do not necessarily require superconducting quadrupole magnets for adequate focussing in the transport system. Electrical power and cost considerations however favor this choice. A typical first order beam line calculation is shown in Fig. 2 for transporting the beam from the K=500 cyclotron to beam station 3a, the east line in vault 3. Further calculations will include ray tracing studies for beam lines going to the spectrometers.

1. J. Purcell, S. Wong, R. Niemann, K. Malaya, H. Ludwig, J. Biggs, IEEE Trans. on Magnetics, Mag-11, #2, 455(1975).

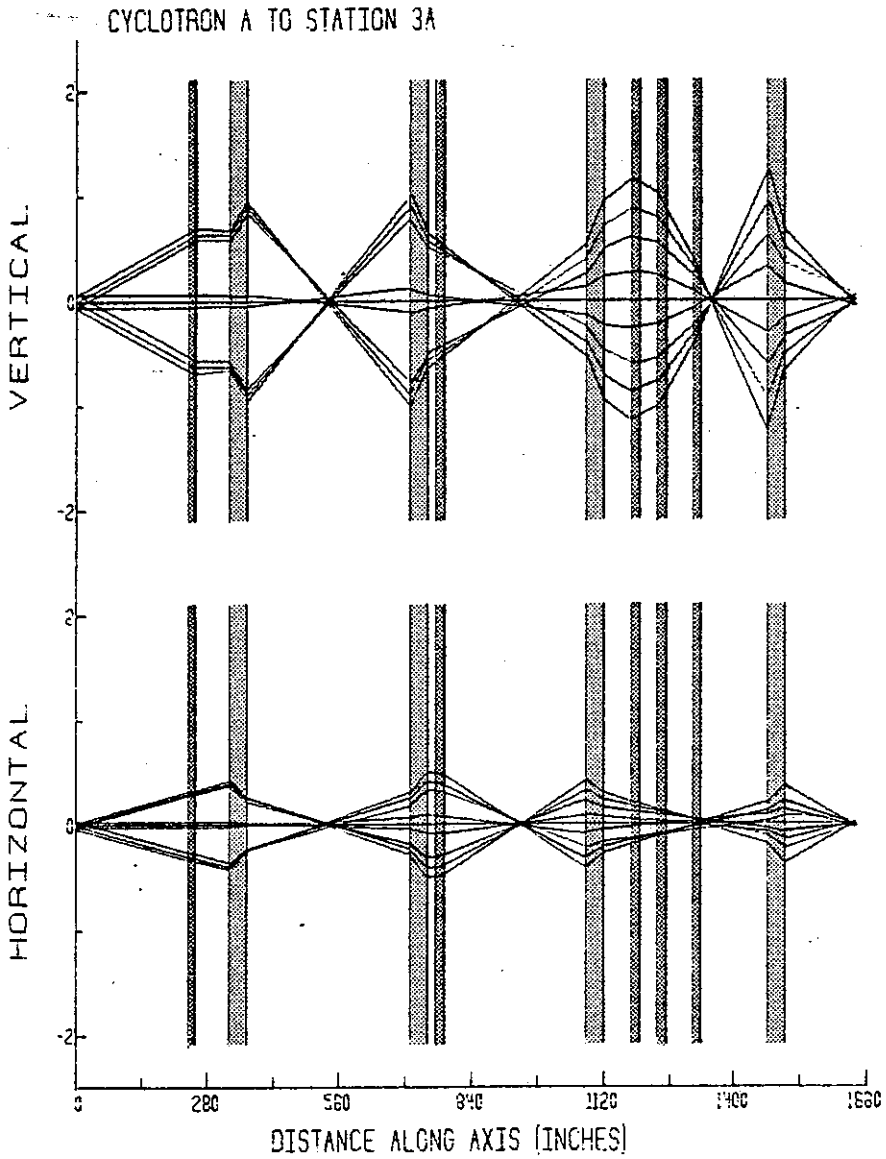

Fig. 2(IV.2.2)--Typical Beam line optics. The narrow strips represent bending magnets and the wide strips are physical limits of quadrupole doublets. The rays inside the quadrupole doublets are not shown in detail in the figure.

IV.2.3 Neutron shielding

Shielding requirements for the facility are determined by the 200 MeV/amu light ions which produce copious fluxes of nucleons, including roughly two neutrons per ion in a stopping target. Shielding requirements have been determined assuming ^{12}C beams with 6×10^{12} ions/sec at 200 MeV/amu stopping in water. [We presently use a recirculating water faraday cup in the scattering chamber of the split-pole spectrograph; this system has sizeable advantages in reducing both prompt and residual radiation hazards.] In estimating shielding requirements we use neutron production cross sections from calculations by Bertini[1] for ^{12}C ions on ^{16}O targets: these are shown in Table 1 and a description of the calculation is contained in Ref. 2. The shielding requirements follow the work of Moyer,[3] using neutron attenuation lengths from Patterson, et al.[4] The calculations assume exponential attenuation in the shielding and inverse square decrease in flux with distance from the beam stop. Neutron yields for ion energies below 200 MeV/amu are interpolated from the 200 MeV calculations, with resulting neutron fluxes similar to those obtained from extrapolation of calculations for 75 MeV/amu ^{12}C ion on Fe.

Fig. 1 shows the calculated neutron flux/MeV after attenuation by various thickness of concrete assuming a source distance of 10 meters, while Table 2 lists the integrated neutron flux emerging at that distance. Considerable use of local steel beam-dump shield is planned. These shields will be of sufficient thickness to bring neutron fluxes at maximum anticipated beam intensities below tolerance outside the experimental area. Most

of the beam lines planned are aimed at angles of 45° or less to the external shielding walls. Thus, a requirement of 8 meters of normal density concrete will be met by local shielding of 1.3 meters of steel and an external 2.7 meter wall of concrete. The water in which the beam is stopped will be contained in closed recirculating systems with shielded holding tanks. Other areas where beam losses may occur, e.g. slit systems, will also be designed with local iron shielding. We plan to make measurements of neutron attenuation using the 200 MeV/nucleon alpha beam of the SREL cyclotron to check assumptions of the calculations and to measure both neutron yields and residual radioactivity of common materials which may be activated by the beams.

References

1. H.W. Bertini (private communication).
2. H.W. Bertini, R.T. Santoro, O.W. Hermann, Phys. Rev. C14 (1976)590.
3. H.W. Patterson, R.H. Thomas, "Accelerator Health Physics", (Academic, 1974) p. 471.
4. Ibid., p. 374.

Table 1(IV.2.3)--Calculated Differential Cross Sections for 200 MeV/Amu ^{12}C on ^{16}O for neutron production (Bertini: Ref. 1).

ANGULAR INTERVALS (DEGREES)	0.0-10.0	10.0-30.0	30.0-60.0	60.0-80.0	80.0-110.0
ENERGY INTERVALS (MEV)	CROSS SECTION MB/SR-MEV	CROSS SECTION MB/SR-MEV	CROSS SECTION MB/SR-MEV	CROSS SECTION MB/SR-MEV	CROSS SECTION MB/SR-MEV
.0 TO 20.0	.1199E 02	.9010E 01	.1037E 02	.1037E 02	.5882E 01
20.0 TO 40.0	.3850E 01	.4352E 01	.6426E 01	.4318E 01	.9775E 00
40.0 TO 60.0	.3230E 01	.3969E 01	.6256E 01	.2422E 01	.4692E 00
60.0 TO 80.0	.4684E 01	.4726E 01	.5907E 01	.1224E 01	.1751E 00
80.0 TO 100.0	.7701E 01	.6978E 01	.4972E 01	.6154E 00	.7361E-01
100.0 TO 120.0	.9350E 01	.8755E 01	.4216E 01	.2762E 00	.3681E-01
120.0 TO 140.0	.2023E 02	.1139E 02	.3136E 01	.1113E 00	.3068E-02
140.0 TO 160.0	.3391E 02	.1343E 02	.1997E 01	.3392E-01	.9180E-02
160.0 TO 180.0	.5610E 02	.1199E 02	.9095E 00	.1938E-01	
180.0 TO 200.0	.7114E 02	.7267E 01	.3714E 00	.1453E-01	
200.0 TO 220.0	.4989E 02	.4955E 01	.1861E 00	.4845E-02	
220.0 TO 240.0	.2465E 02	.2932E 01	.6919E-01		
240.0 TO 260.0	.1063E 02	.1734E 01	.6485E-01		
260.0 TO 280.0	.5202E 01	.1122E 01	.1726E-01		
280.0 TO 300.0	.3017E 01	.6129E 00	.8670E-02		
300.0 TO 320.0	.1453E 01	.3196E 00	.4318E-02		
320.0 TO 340.0	.4165E 00	.2133E 00			
340.0 TO 360.0	.1037E 00	.9350E-01			
360.0 TO 380.0	.1037E 00				

Table 2(IV.2.3)--Number of neutrons/cm^2 - sec at 10 m from beam stop in water as a function of shield thickness in meters of normal density concrete (ρ=2.4 gm cm^{-3}). The numbers in parentheses are powers of ten.

shield thickness (meter of concrete)	0°-10°	10°-30°	30°-60°	60°-80°	80°-110°
0	1.3 (7)	3.1 (6)	9.7 (5)	2.4 (5)	7.0 (4)
1	1.3 (6)	2.5 (5)	3.3 (4)	1.9 (3)	2.5 (2)
2	1.9 (5)	3.4 (4)	3.7 (3)	1.6 (2)	1.8 (1)
3	2.9 (4)	4.9 (3)	4.7 (4)	1.9 (1)	2
4	4.5 (3)	7.3 (2)	62	2.3	0.2
5	7.1 (2)	1.1 (2)	8.5	0.3	
6	1.1 (2)	1.8 (1)	1.2		
7	1.9 (1)	3	0.2		
8	3.1	0.5			
9	0.5				

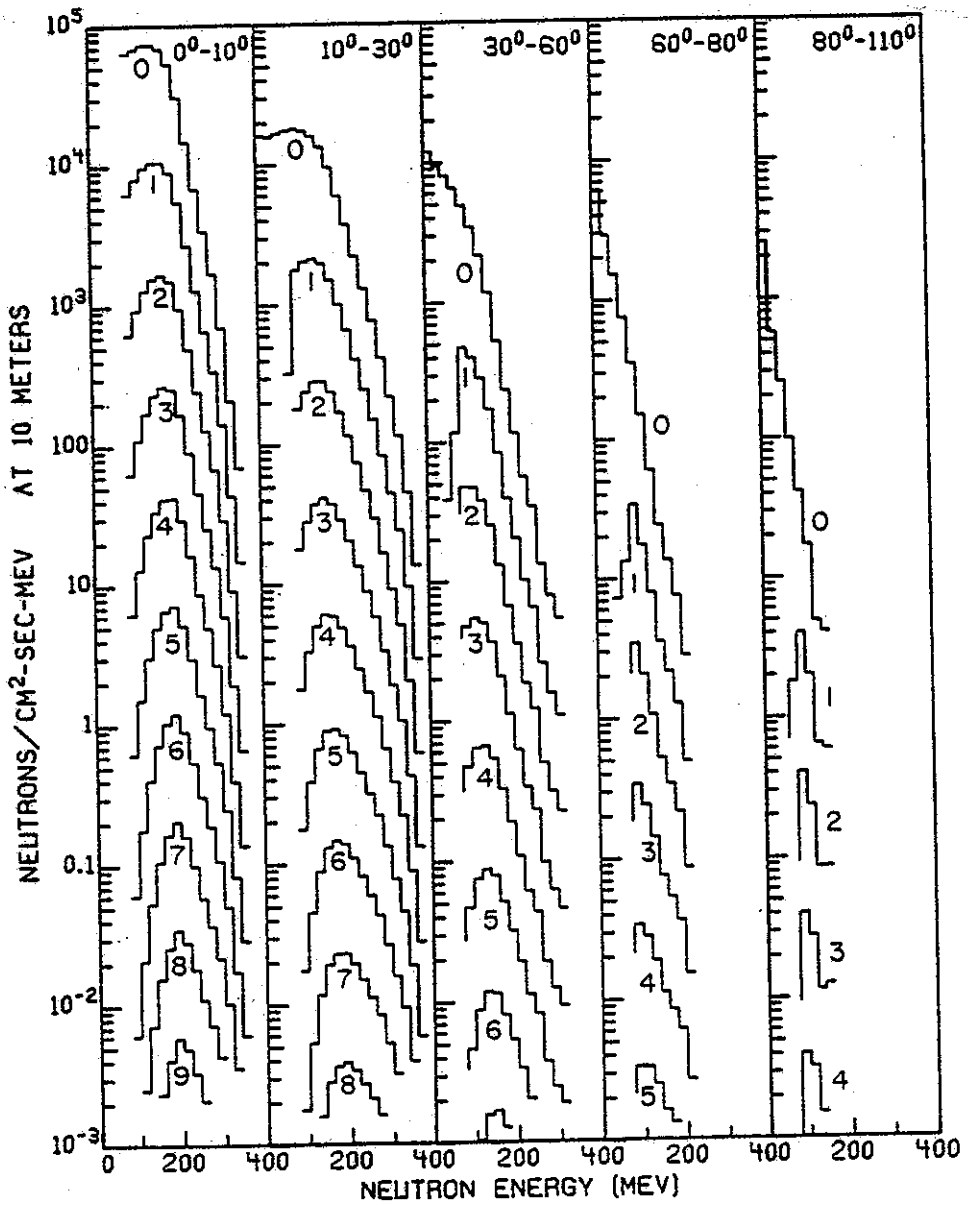

Fig. 1(IV.2.3)--Neutron flux/MeV spectra emerging 10 meters from the source after indicated thicknesses (in meters) of concrete.

Addendum to IV.2

The west addition to the Cyclotron Laboratory high bay area is basically complete and was turned over for occupancy in January 1978. The layout of this addition is as shown on the plan view on page 148 of the CSC proposal. Figure A is a photograph of the addition.

Experiments have been performed as suggested on page 156 of the CSC proposal to check estimates of shielding and activation using the 720 MeV alpha particle beam at the Space Radiation Effects Laboratory. The first of these experiments measured absolute thick target neutron spectra at 180 MeV/A, the measurement being performed in collaboration with a group from Kent State University. As reported[1] at the Rochester APS meeting, spectra were obtained at 9 angles from 0° to 150° for targets of C, H_2O, Fe, and Pb. The data are not very different from that assumed in estimating the shielding, but said design can now proceed from a much firmer foundation.

At another time, an experiment was carried out with the same energy alpha particle beam to predict the levels of radioactivity induced by the direct beam when striking such components as a tungsten septum for an electrostatic deflector. The septum thickness will be 0.5 mm, following existing designs. Thin (3 mm) samples of tungsten were bombarded, and the decay of the radiation dose rate from the induced radioactivity was plotted and analyzed. These data imply that a 0.1 pμA beam striking the target for one day will result in a dose rate, at a distance of 20 inches from the source, of about 2 Rem/hr one hour after the beam is turned off and about 0.1 Rem/hr after one week.

One therefore expects to be able to carry out maintenance procedures without requiring elaborate remote handling equipment or long shutdown periods.

[1]R. Cecil et al., BAPS 22,1006(1977).

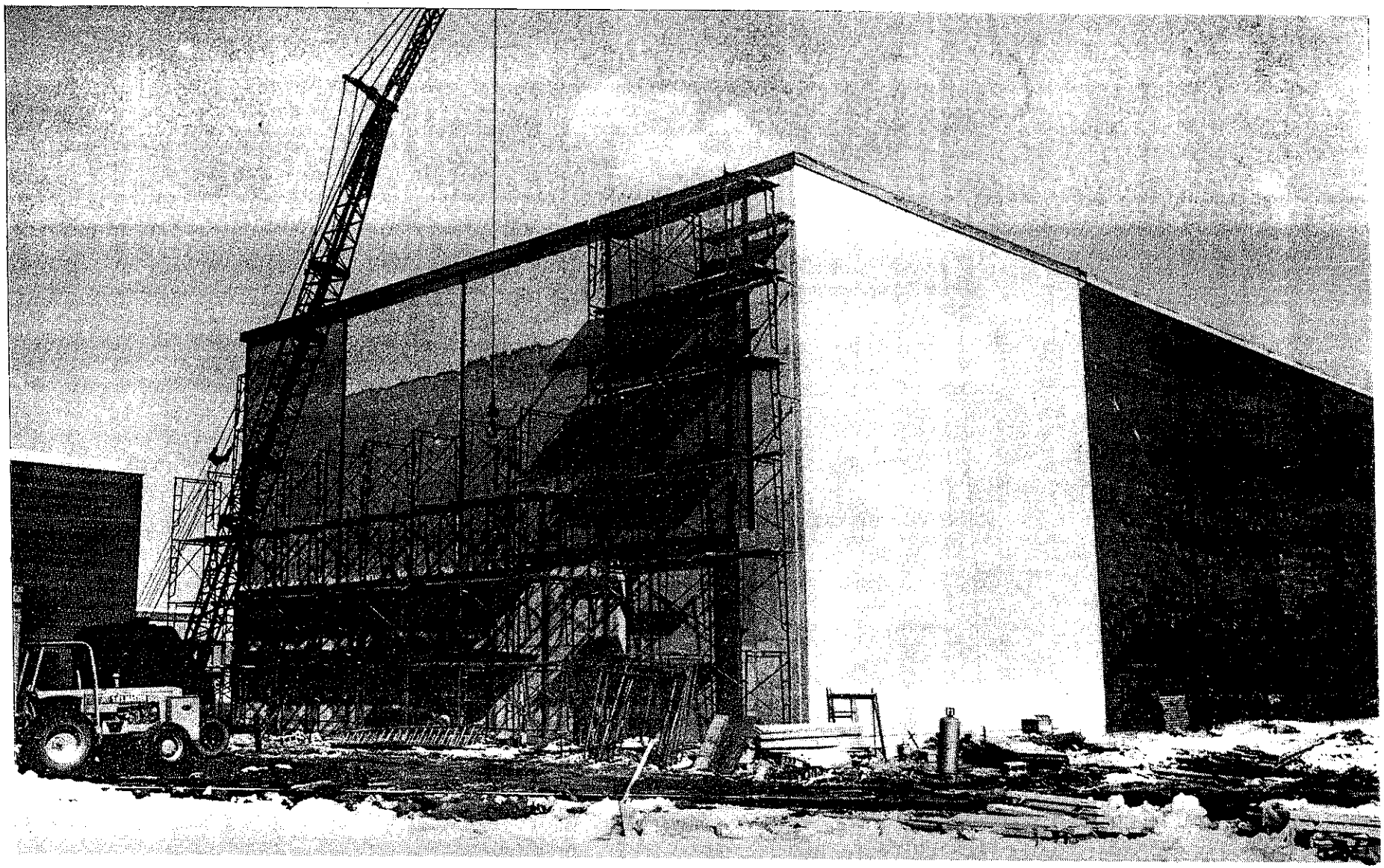

Fig. A (IV.2). Photograph of west building addition in February 1978. At this time, interior work was already completed and the building turned over for occupancy. The principle remaining exterior work involved installation of limestone facing on the west wall.

IV.3 Digital-data processing systems

Experience at nuclear physics laboratories shows that scientific productivity can depend almost as much on the quality of computing facilities as on the accelerator. Days of running on a modern accelerator can lead to months of analysis and interpretation, and this time is primarily spent in various steps of computer-based data analysis. The present MSU Cyclotron Laboratory computer is for example a powerful, versatile and convenient resource of the Laboratory. It handles all computing for the Laboratory as well as on-line and off-line data taking and data analysis and control of a variety of devices located throughout the building. The improved computer system for the new laboratory would ideally come into operation at about the same time as the accelerators. Plans can therefore remain flexible for several more years so as to take advantage of possible technical developments in these years. As with our other items, we base our proposed discussion of computing systems on how we would picture them at this time. This then gives a reasonable basis for a budget estimate.

At the present time, the Cyclotron Laboratory computer group is in fact trying out new working concepts; experience as to the effectiveness of these new concepts will be an important element in assessing the final, most appropriate plan for meeting the computing needs of the heavy-ion laboratory. The principal feature of the new approach to computing needs is a shift from a past status of writing software and constructing interfaces matched to the capabilities of commercial equipment

to a present status of substantially modifying commercial hardware, constructing additional units etc. in order solve or ease software problems. Restated, the group feels that software problems in very complicated multifunctional time-sharing systems are the dominant limiting element; it is thus more effective to tailor hardware to match software than vice versa. Experience with this new, more encompassing approach to the solution of computer problems is now being accumulated. In twelve to eighteen months we should have a very solid basis for evaluating this approach. Our experience up to this time is good, and our detailed plan for expanded computer facilities presented here is therefore based on this approach.

The tentative plan for the new system is an evolution of the present Cyclotron Laboratory computing system; this present system is shown diagrammatically in Fig. 1. The main computers in the system are a Xerox Sigma-7 and a number of PDP-11's. The entire system is under control of our own operating system JANUS, which in computer parlance would be referred to as a multi-tasking system for real-time, batch, background, and time sharing. The JANUS software system was written by our own staff and contains features particularly tailored to the needs of a major nuclear physics laboratory including features not available (or not available until a much later point in time) from manufacturer-generated software. For the past three years our staff has also been directly handling computer maintenance; reliability has been substantially improved compared with the previous years when maintenance was under a standard service contract with the manufacturer. At the present time the computer group is proceeding

with procurement and testing of a replacement main memory bank for the Σ-7 as a first implementation of concepts proposed here, namely to procure hardware matched to existing software. The general specifications are compatible with standard modules from a number of manufacturers. Assessment of the effectiveness of this memory replacement project will be an important guidepoint in determining our final approach to the computer system for the CSC laboratory. When plans are relatively complete but before freezing major commitments, we plan a design review meeting analogous to the review meeting held for the superconducting coil. At this meeting we will present the system plan to a panel of nuclear computer experts for comment and review.

Our present computer system is well suited to the needs of a nuclear physics laboratory; our planning for the new laboratory is therefore in terms of expanded capability of the same basic system. The plan provides hardware compatible with present software (or with easy modifications of this software). We feel this approach reflects an accurate assessment of the relative difficulty of providing tailored hardware versus modifying a major software system. The approach also has the advantage that new hardware elements can be introduced into the system in a phased way with minimal disruption of ongoing laboratory programs.

A block diagram of the new system is shown in Fig. 2. The phased approach to implementation of this system would proceed through the following steps:

1) The first of an eventual pair of new central processors would be installed in parallel with the Sigma-7. In the initial test configuration this processor would function as a calculation-

only unit, and in this mode the configuration is fully compatible with the existing software system.

2) The next new component is a low/high speed interface bus system for terminal/computer intercommunications. This bus system would permit later easy low-cost expansion of time-sharing and data acquisition capability.

3) The present Sigma-7 memory would be replaced by a new mass storage system with state-of-the-art cycle time, built-in error correction, etc.

4) With the bus system in operation, the Sigma-7 CPU would be replaced by a second new CPU. The operating system would be modified so that the two processors would function as equivalent independent systems each with access to the mass storage in the network. The final configuration as depicted in Fig. 2 would operate in the distributed processing mode.

5) Data acquisition units, cyclotron control units, IO processors etc. connect to the bus system and would include both present units and new additional units. Figs. 3, 4, 5 and 6 give likely configurations. For cost estimating purposes we assume three additional data acquisition units. Additional cyclotron control units already exist or are included in the cyclotron cost estimates.

The system described is not a standard computer system but is nevertheless constructed of standard components. The components are available from a number of manufacturers, and we expect this to give real competition in bidding and therefore reduced cost. As mentioned above, the present memory replacement

project is a test of this philosophy. At the time of our final computer review we should have solid information on the effectiveness and viability of the approach described here. This will be compared with the more conventional alternate of procuring a complete computer system from a manufacturer, and we will choose the alternate which seems most likely to serve the needs of the laboratory best. We view effective computing capability as comparable in importance to the accelerators in determining the overall productivity of the laboratory. We therefore plan to proceed with extreme care in finalizing decisions in this very important area.

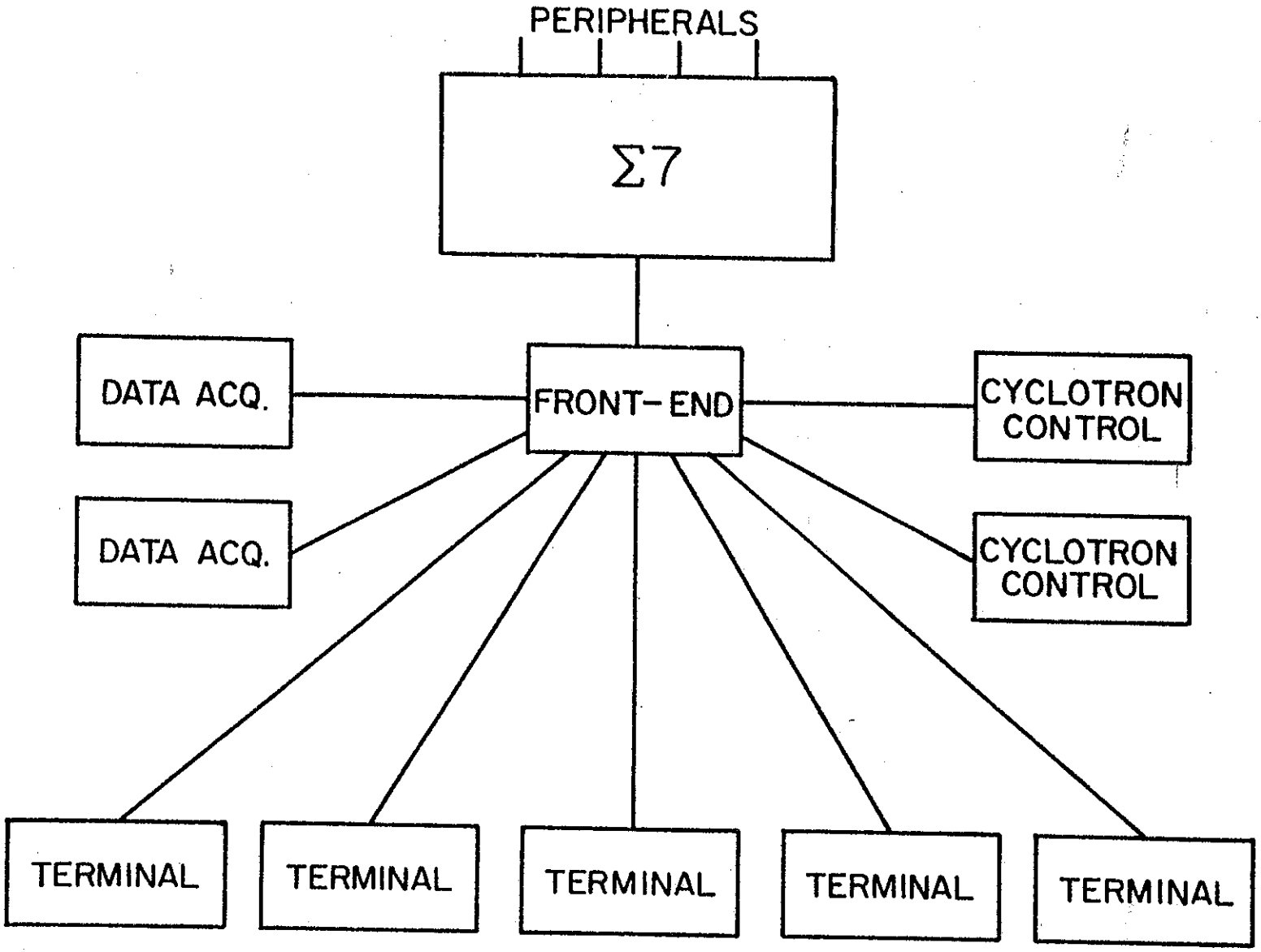

CURRENT CONFIGURATION

FIG. 1(IV.3)

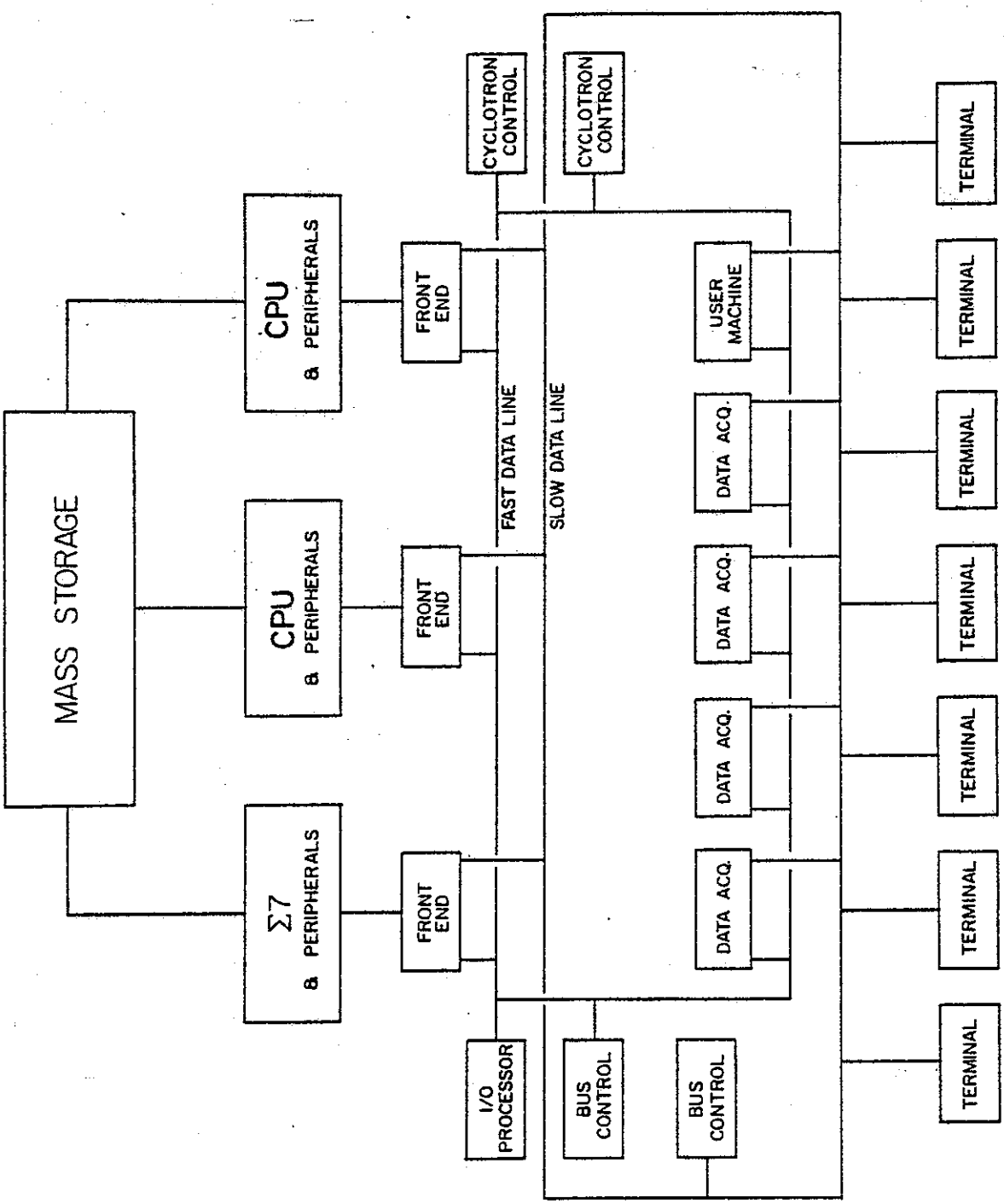

FIG. 2(IV.3)

FINAL CONFIGURATION

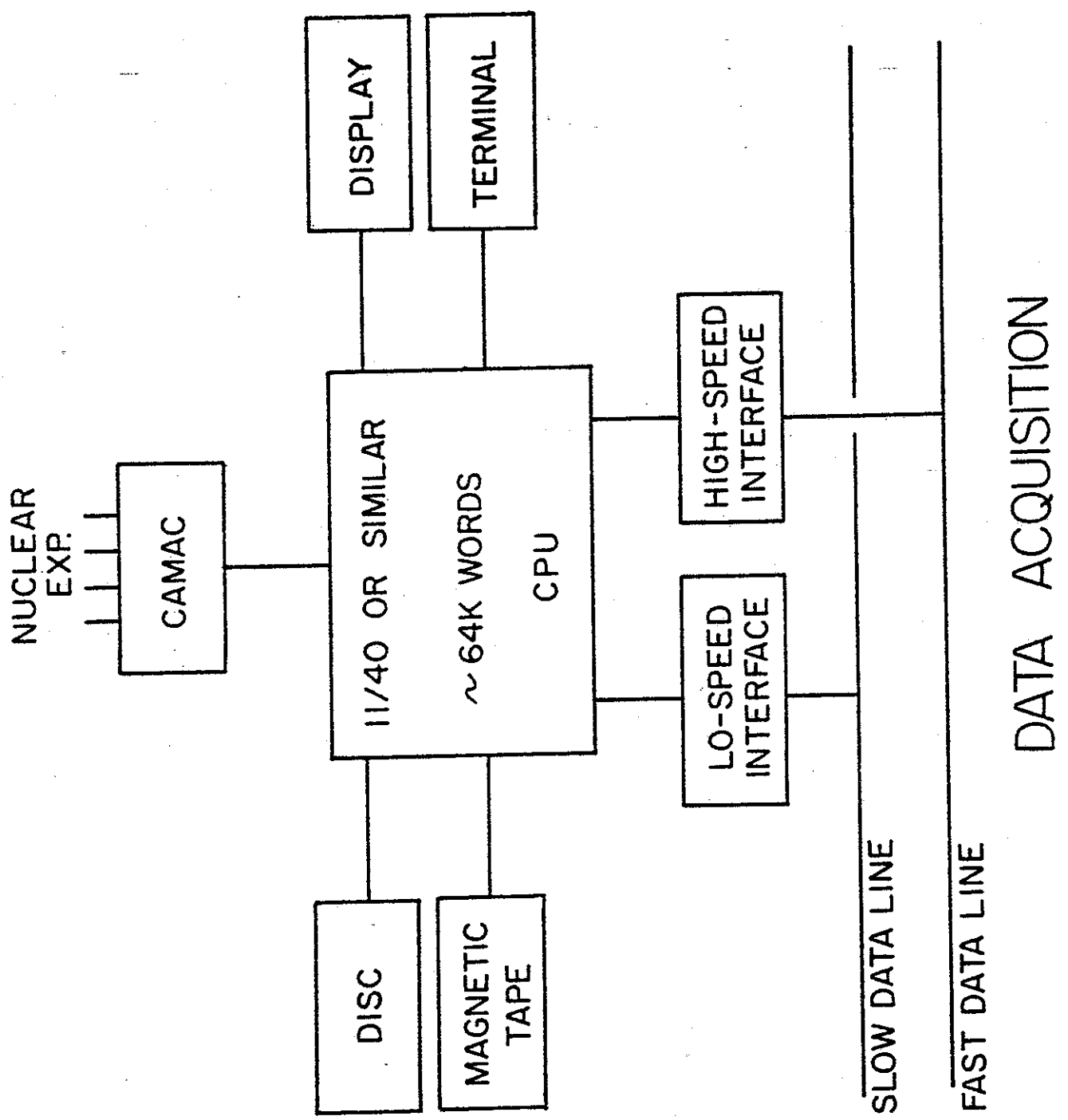
NUCLEAR EXP.
CAMAC
11/40 OR SIMILAR
~64K WORDS
CPU
DISPLAY
TERMINAL
DISC
MAGNETIC TAPE
HIGH-SPEED INTERFACE
LO-SPEED INTERFACE
SLOW DATA LINE
FAST DATA LINE
DATA ACQUISITION

FIG. 3(IV.3)

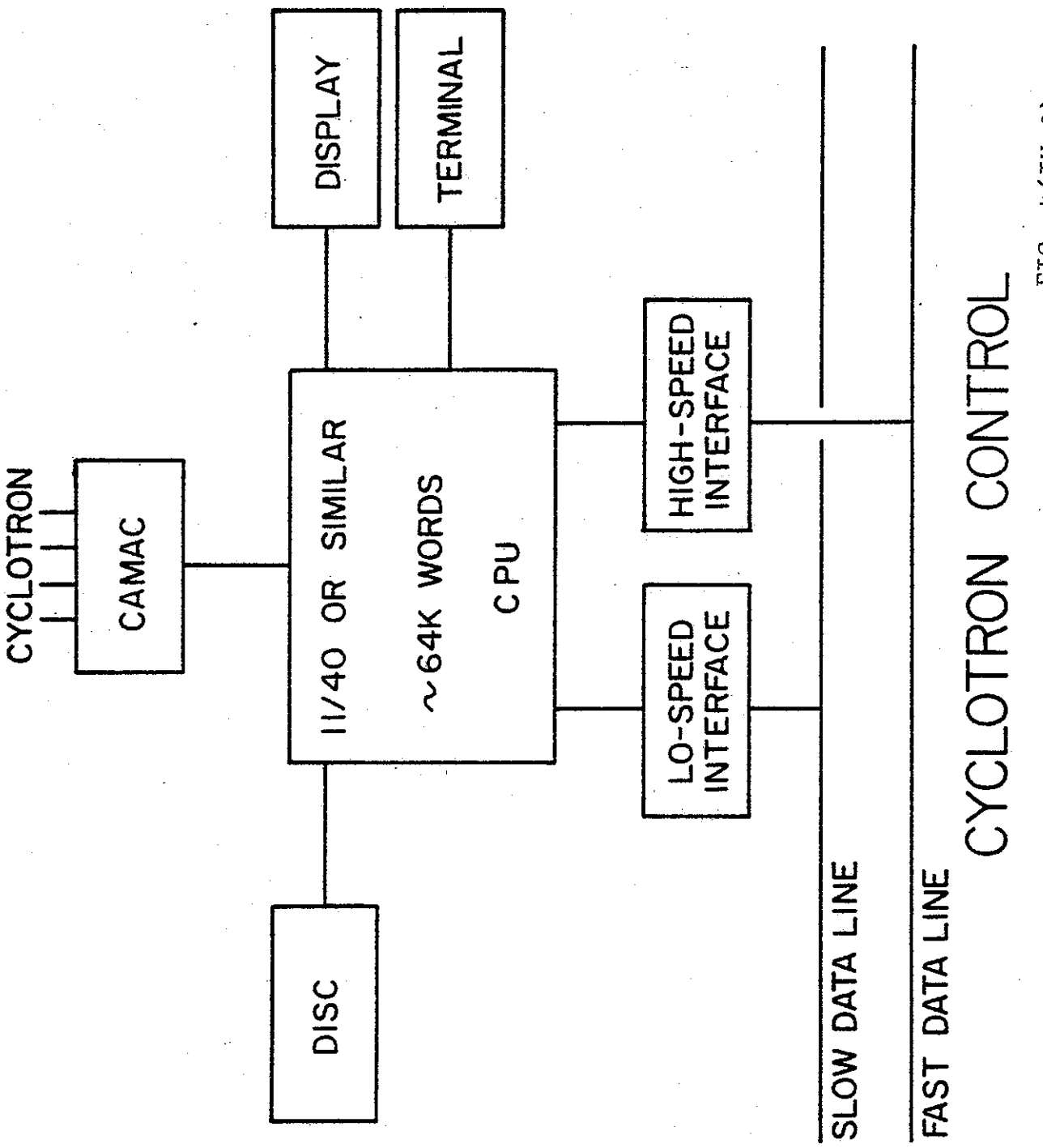
CYCLOTRON
CAMAC
11/40 OR SIMILAR
~64K WORDS
CPU
DISPLAY
TERMINAL
DISC
HIGH-SPEED INTERFACE
LO-SPEED INTERFACE
SLOW DATA LINE
FAST DATA LINE
CYCLOTRON CONTROL

FIG. 4(IV.3)

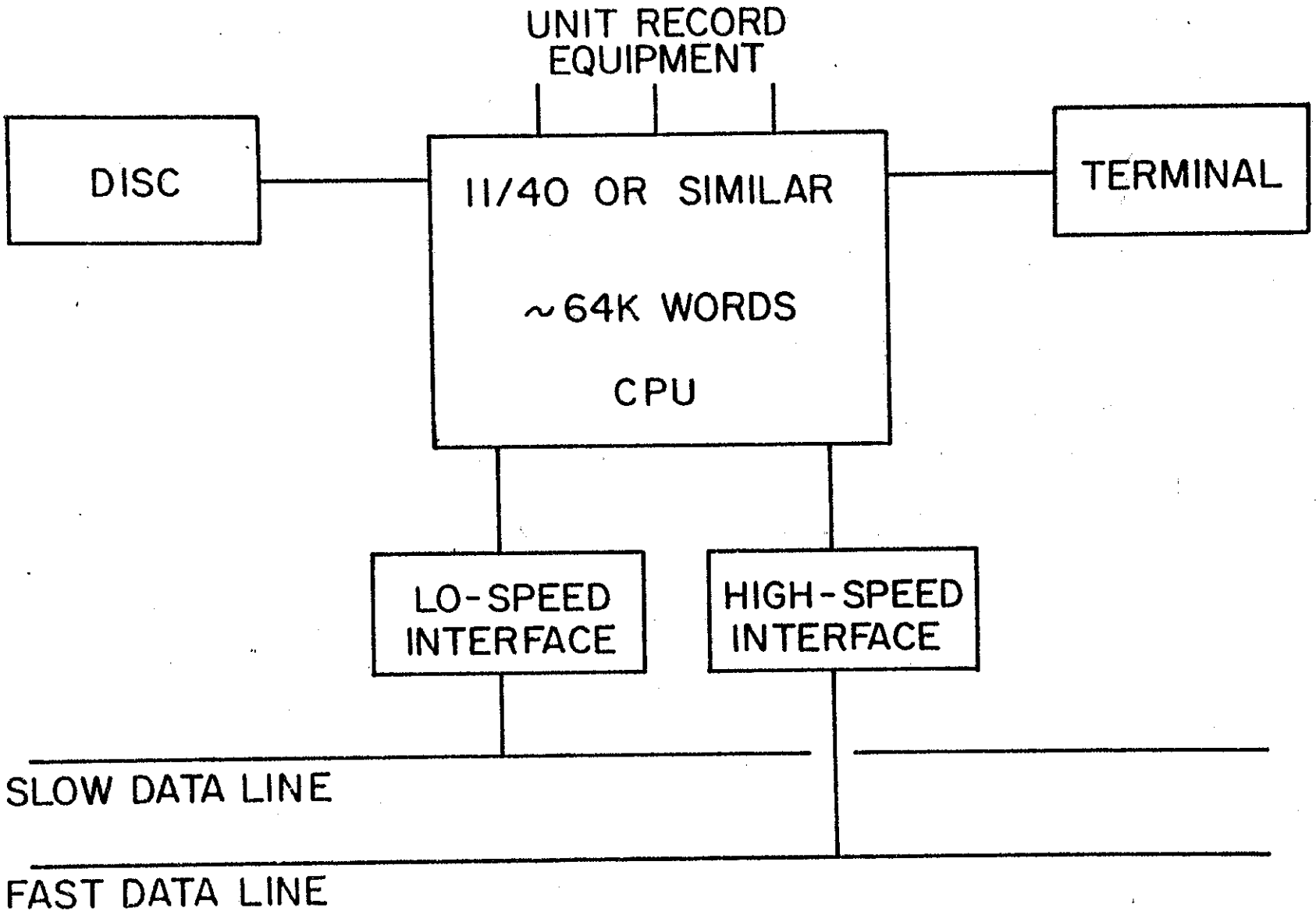

I/O PROCESSOR

FIG. 5(IV.3)

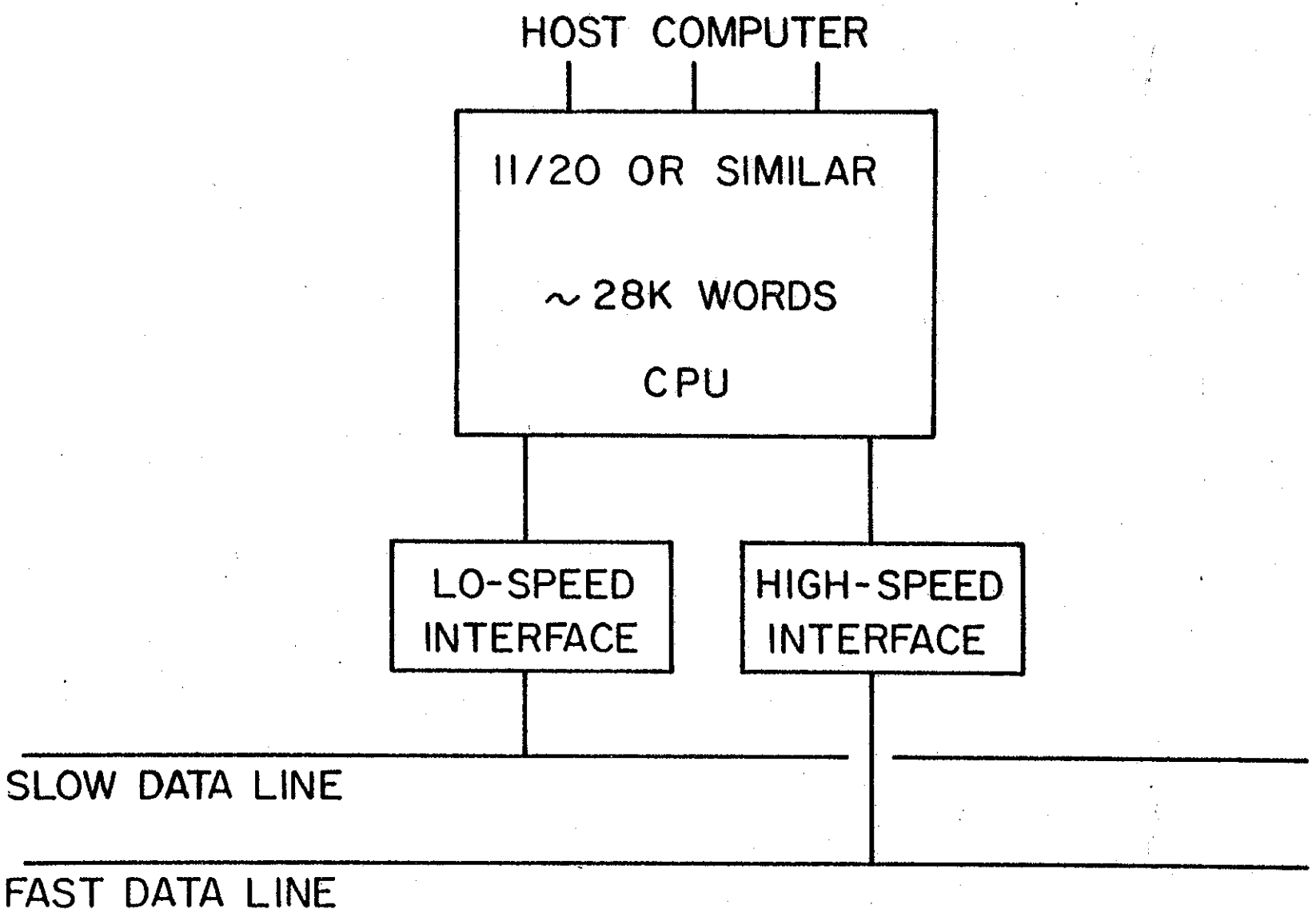

FRONT-END PROCESSOR

FIG. 6(IV.3)

IV.4. Analysis of reaction products with electric and magnetic fields

Electromagnetic devices which sort and analyze reaction products have traditionally played essential roles in the study of nuclear phenomena. In many laboratories magnetic spectrographs in various forms have been the facilities which made possible the acquisition of precise, reliable data in experiments that would have otherwise not been possible.

Heavy ion experiments pose special problems which can be greatly facilitated by the use of appropriately designed magnetic apparatus. Typically a great number of particles are produced with cross sections varying over many orders of magnitude, and it is often the very low yield products which are of the greatest interest. Furthermore, the kinematics of these reactions often cause the fragments of interest to be produced near the beam direction, and magnetic separation is then particularly valuable.

Armbruster in a recent article[1] has reviewed the problem of separating isotopes produced for on-line study. He describes the capabilities of four major European facilities: "Isolde II" (CERN '75), "Lohengrin" (Grenoble '74), "Joseph" (Julich '74), and "Ship" (Darmstadt '76). Consideration of these systems plus others currently being designed or proposed in the U.S.A. has led us to propose the following apparatus to aid most effectively in carrying out the scientific investigations discussed in Sec. III of this proposal: a) superconducting solenoids for large-solid-angle reaction-product collection and time-of-flight measurement, b) a K=150 recoil-mass spectrometer, c) a K=800

high resolution magnetic spectrograph, and d) continued use of the K=100 Enge split-pole broad range spectrograph. These items are described below. Other planned facilities not described in detail include particle- and-gamma-multiplicity detector arrays, He-jet transport system, and an electron solenoid spectrometer.

Reference

1. P. Armbruster, "International Conference on Nuclei Far from Stability", Corsica, May 1976 (in Press).

IV.4.1 Superconducting reaction-product and pion collector

In the study of high-energy heavy-ion collisions it is often necessary to detect with high efficiency the reaction products near a scattering angle of 0°. This calls for a collector with a large solid angle which is capable of adequate suppression of the unwanted beam particles. We have investigated the focusing properties of superconducting solenoids and have found them to be appropriate building blocks for such a system.

Figure 1 displays a possible geometry for a time-of-flight system consisting of two superconducting solenoids. This system is similar in many aspects to the quadrupole spectrometer currently in use at Florida State,[1] but it has the following distinctive features: a) it utilizes superconducting solenoids instead of quadrupoles, with each solenoid replacing a quadrupole doublet; b) since each solenoid is double focusing, the distance between them is adjustable and can be optimized to specific time-of-flight requirements; c) the acceptance aperture is circular and the solid angle can be very large; and d) the device can be used with an annular aperture centered at zero degrees if the reaction products of interest differ sufficiently in rigidity from the beam. When the time-of-flight system is used away from zero degrees, the annular aperture may still be useful if a narrow momentum band pass is desirable.

The first-order optical properties and other qualitative features of superconducting quadrupoles and solenoids are compared in a recent paper by Jaffey and Khoe,[2] and a very large solid angle system based on superconducting quadrupoles has been proposed recently by DeVries and Elmore.[3] The higher-order optical proper-

ties of superconducting solenoids and quadrupoles do not seem to be well documented however, so we are currently carrying out detailed ray tracing calculations to determine the limitations of such devices. The parameters of the solenoids illustrated in Fig. 1 are listed in Table 1. The pair of complete solenoid systems (coil, cryostats, power supplies, etc.) can be purchased as an operating system for about $160K. Purchase of component parts and then assembly will reduce this figure substantially.

The geometry indicated in Fig. 1 is intended to represent one of the many possible arrangements for the two solenoids. Solid angles for particles of various rigidities are indicated in Table 2. Our ray tracing calculations for the realistic solenoid field with the geometry of Fig. 1 show that particles of a given momentum from an object point on axis (beam spot diameter ≈1 mm) will focus through an aperture <10 mm in diameter at the image point.

The solid angles can be well over 100 msr for lower energy reaction products such as pions or particles from deep inelastic scattering (≃ 5 MeV per nucleon). The solenoid can simultaneously focus π^+ and π^- particles. An alternate geometry, which could provide additional beam rejection or momentum selection with slightly decreased solid angle, is one with an intermediate image between the solenoids. An aperture hole a few mm in diameter could be placed at the intermediate image position. Also a thin foil timing system could be placed at this location if desired.

Other tailored detector options include the assembly of large-solid-angle, low-dispersion spectrometers utilizing the solenoids and single wedge dipole magnets. The solenoids would

Table 1.(IV.4.1)--Parameters of superconducting solenoid for collecting reaction products.

Axial field strength	50 kg
Length	50 cm
Room temperature bore diameter	20 cm
Coil inside diameter	25 cm
Approximate He load	0.5 ℓ/hr
Approximate cost of 2 complete solenoid systems	$160K

Table 2.(IV.4.1)--Approximate focal lengths and solid angles of superconducting solenoid for selected reaction products.

Ion	q (charge state)	E/A (MeV per nucleon)	f(m) (focal length)	Ω^* (msr) (solid angle)
^{238}U	75	20	1.6	9
	73	10	0.85	33
^{40}Ca	20	200	6.4	0.6
	20	20	0.6	60
Pions		0-200 MeV		>100

*with annular aperture

also be useful as large-solid-angle particle detectors for particle-particle or particle-gamma coincidence experiments. The solid angles for collecting the higher rigidity particles can be increased significantly by using the standard beam line quadrupoles in place of the solenoids for these particles. (In the long focal length limit a comparable quadrupole doublet will have 1/4 the focal length of the solenoid.)

References

1. G.R. Morgan, et al., Nucl. Instr. and Methods 123(1975)439.
2. A.H. Jaffey and T. Khoe, Nucl. Instr. and Methods 121(1974) 413.
3. R.M. DeVries and D. Elmore, Bull. Am. Phys. Soc., to be published (1976).

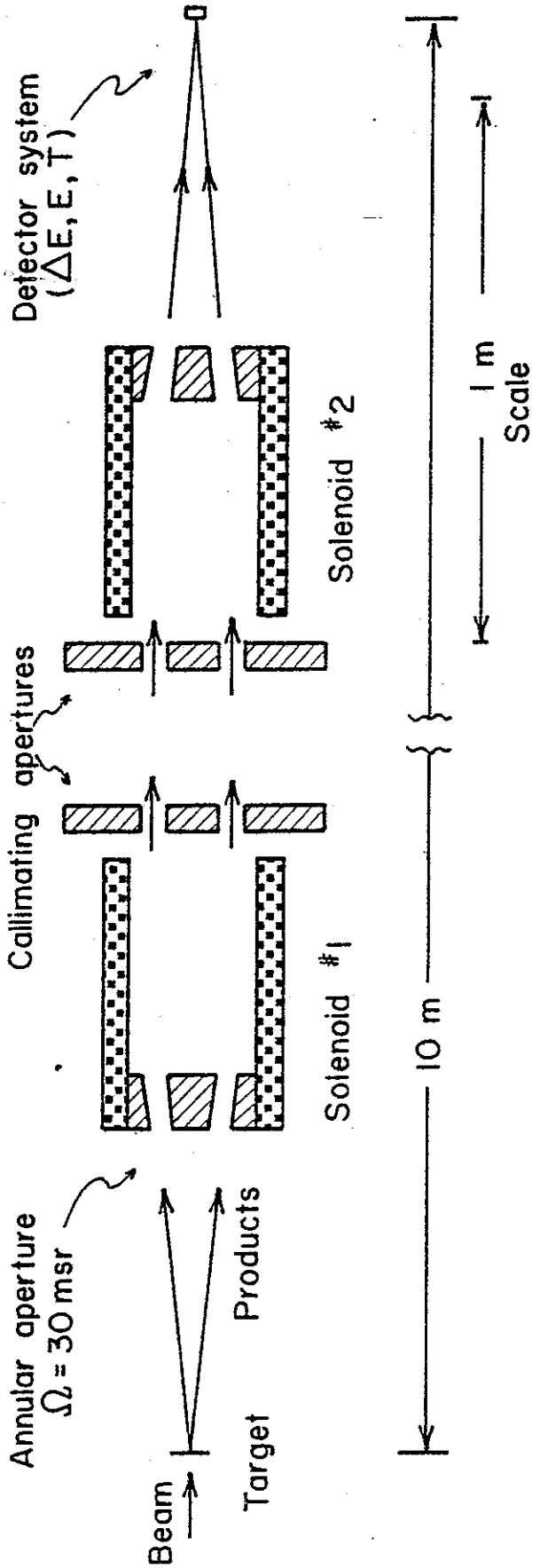

Fig. 1(IV.4.1).--Possible geometry for time-of-flight measurements with superconducting solenoid reaction product collector. This geometry is effective for rigidities as high as those for 10-MeV-per-nucleon 238U(K=106). The times-of-flight in this case would be >200 ns.

IV.4.2 Recoil-mass spectrometer

A device which disperses reaction products in mass, independent of their energy, would be a valuable experimental tool for use in conjunction with any heavy-ion accelerator. Two such instruments are now being designed, one by Harold Enge[1] of MIT for proposed use at the Oak Ridge heavy ion facility, and the other for the SuperHILAC accelerator. The components and tentative parameters of Enge's design are shown in Fig. 1. Both systems provide a velocity spectrum (independent of mass or charge state) at an intermediate cross-over point and then an m/q spectrum at the final focal plane. The proposal for MSU is for either a scaled up version of the Enge-Oak Ridge design or a modified version of the SuperHILAC device. In Table 1 are listed the relevant properties of the SuperHILAC heavy-ion spectrometer (in its mass spectrum operating mode) together with the proposed values for the MSU device.

The proposed MSU device would be designed assuming a small beam spot (<1 mm) and good position resolution for the detector (<0.3 mm). With constant resolving power (D/M_h), the mass resolution ($M/\Delta M$) is directly related to the size of the beam spot. With a mass resolution (FWHM) of 1000 it would be possible in favorable cases to measure masses directly to ~2 MeV precision at mass 100 with ~1000 counts. Attempts will be made to improve this specification further since accurate direct mass measurement capability is highly desirable. The charge-state ambiguity in these measurements would be eliminated by total energy measurements. Preliminary selection of particles with specific ranges of velocity can be accomplished by

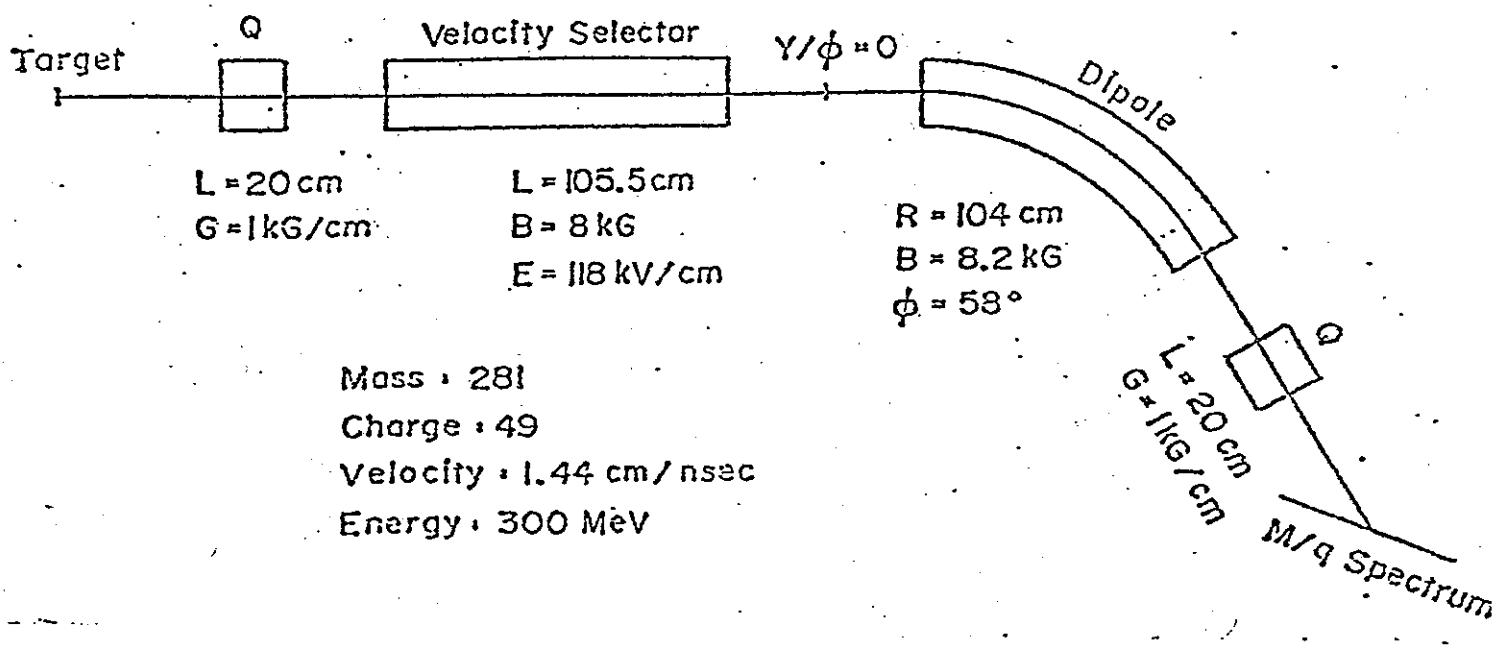

Fig. 1(IV.4.2).--Tentative layout and parameters of proposed MIT-ORNL recoil mass spectrometer.

appropriately placing slits at the position of the velocity spectrum (between the velocity selector and dipole magnet in Fig. 1).

The recoil-mass spectrometer would be used to study fusion products and evaporation residues which would typically have energies much lower than the beam. Hence a K value of 150, which corresponds roughly to 12 MeV per nucleon Uranium ions, seems adequate for the proposed device.

Reference

1. H.E. Enge, private communication.

Table 1.(IV.4.2)--Proposed properties of a recoil mass spectrometer

	SuperHILAC (Mode I)	MSU-CSC
Solid Angle	> 1 msr	1 msr
Energy acceptance	10%	6%
K value	∿ 110	150
	(∿8.5 MeV/amu)	(∿12 MeV/amu)
Dispersion (D)		
Mass	1 cm/%	0.3 cm/%
Velocity	1 cm/%	0.3 cm/%
Magnification (M_H)	1	0.3
Mass resolution (M/ΔM)	300	1,000
Angular range	-5 to +30°	-5° to 30°
Assumed beam spot width	3mm	< 1mm
Assumed detector resolution	∿ 1 mm	< 0.3 mm
Approximate cost	$500,000	$400,000

IV.4.3 A large, high-resolution magnetic spectrograph

Magnetic spectrographs have had their greatest impact in the study of nuclear structure via particle-transfer and elastic and inelastic scattering. The large solid angle, high resolving power, and kinematic correction capability are invaluable characteristics of such spectrographs. There is at present limited experience in the use of spectrographs for heavy ions and none for the energy expected for the CSC heavy-ion laboratory. However, the unique attributes of magnetic analysis, proven by the long history of successful deployment of such devices, strongly suggest that an appropriately scaled spectrograph will play a vital role in the research program of the CSC laboratory. Similar conclusions have been reached in the deliberations of other groups, examples being the spectrographs proposed at Lawrence Berkeley Laboratory for use at the SuperHILAC and Bevalac facilities,[1] and at Darmstadt for the GSI accelerator.

When magnetic spectrographs are used in an energy-loss mode of operation, the dispersion of the incident beam is matched to that of the outgoing particle of interest, thus obtaining spectra the resolution of which far exceeds that of the beam. Blosser et al.[2] have described the system currently used at the MSU Cyclotron Laboratory by which resolutions of $P/\Delta P=50,000$ have been obtained.[3] The clearest foreseeable use of a large magnetic spectrograph in the proposed CSC lab is in studies of relatively "light" heavy ions, i.e., $A\sim60$, where fully stripped ions are expected. Measurement of other parameters identifying the ions, i.e., time of flight, specific ionization, and total ion energy

would also be required. This information, when combined with knowledge of position along the focal plane (or orbit through the spectrograph), will lead to unambiguous specification of reaction product identities and parameters.

We expect to investigate a number of designs before arriving at a final decision for the CSC spectrograph configuration. For example, we plan to consider thoroughly the trade-offs between very high resolution vs. very large solid angle and between built-in aberration and kinematic corrections vs. ray tracing for accomplishing the same results. Table 1 compares some properties of the Jülich K=540 magnetic spectrograph and those for the proposed LBL SuperHILAC spectrograph. Also listed are properties which we currently think would best suit the new facility, although these may well change as we progress in our study of these devices.

There is no large angle beam dispersing magnet shown in the line leading to the spectrograph. We have not yet determined the required dispersion, which depends on both cyclotron beam and magnetic spectrograph design, but have allowed sufficient floor space for such a magnet, as can be seen from the size of vault 5.

References

1. Proposals from LBL for Bevalac and SuperHILAC.
2. H.G. Blosser, G.M. Crawley, R. de Forest, E. Kashy, and B.H. Wildenthal, Nucl. Instr. and Methods 91(1971)61.
3. J.A. Nolen, Jr. and P.S. Miller, Proc. 7th Int. Conf. on Cyclotrons and their Applications (Birkhäuser, Basel, 1975), p. 249-253.

Table 1.(IV.4.3)--Comparison of heavy ion spectrographs

Location:	Jülich	LBL SuperHILAC	MSU-CSC
Status	Under construction	Proposed	-
Configuration	QQDDQ	DQQD (Mode 2)	-
Solid angle (msr)	10	2	5
$\Delta E/E$ (%)	10	10	10
K	540.0	110.0	800
M_x	-0.85	1	0.3
Dispersion cm/%$\frac{\Delta P}{P}$	17	1	6.0
Resolving power (D/M)	20.0	1	20.0
Angular range	-20° → 160°	-10° → 160°	-20° → 160°
Approximate cost ($ x 10^6)	2.6	0.4	1.2

IV.4.4 K=100 split-pole magnetic spectrograph

The proposed experimental layout includes the Enge split-pole spectrograph now in use at the MSU Cyclotron Laboratory in its present location. This instrument will, hence, already be in place and ready for use when beams from the first cyclotron become available. The general properties of this spectrograph are well known (ref. 1). The MSU system is particularly characterized by a complex of instrumentation developed to optimize the basic capabilities of the magnet.

This spectrograph has been used extensively in measurements of nuclear masses and energy levels with precisions of from 0.2 to 10 keV (refs. 2,3). It has been notably valuable in searches for nuclei far from beta stability via low cross section multi-particle transfer reactions, a selection of which are shown in Table 1. The ability to measure the wide variety of cross sections seen in the table is due to the magnetic analyzing and filtering action of the spectrograph. Most previous work with the spectrograph has been high-resolution nuclear structure studies via the investigation of inelastic scattering and one or two particle transfer reactions. Figure 1 shows a high resolution spectrum measured recently and displays the power of the dispersion matching techniques with on-line optimization procedures.

The broad range aspect of this spectrograph will be especially useful in initial surveys of heavy-ion experiments. The 50-inch focal plane corresponds to an Emax/Emin ratio of 5/1.

Table 1.(IV.4.4)--Typical differential cross section for multi nucleon pickup with 25 MeV/amu ^{3}He ions. Note the wide range in the measurable yield made possible by a combination of magnetic analysis in the split-pole with time of flight, specific ionization, and total energy measurement. These values are to be compared to the 10^3 to 10^4 μb/sr typical cross section for inelastic scattering, one or two particle transfer reactions, or compound nucleus reactions.

ΔA	Reaction	ΔN	ΔP	ΔT_Z	$\sim d\sigma/d\Omega$ μb/sr
3	(p,He^4)	2	1	1/2	50
	(^{3}He,^{6}Li)	1	2	-1/2	50
	(^{3}He,^{6}Li)	3	0	3/2	1
4	(^{3}He,^{7}Be)	2	2	0	10
	(^{3}He,^{7}Li)	3	1	1	2
	(^{4}He,^{8}He)	4	0	2	0.01
5	(^{3}He,^{8}B)	2	3	-1/2	0.2
	(^{3}He,^{8}Li)	4	1	3/2	0.1
	(p,^{6}He)	4	1	3/2	0.1
	(^{3}He,^{8}He)	5	0	5/2	< 0.0002
6	(^{3}He,^{9}Li)	5	1	2	0.005

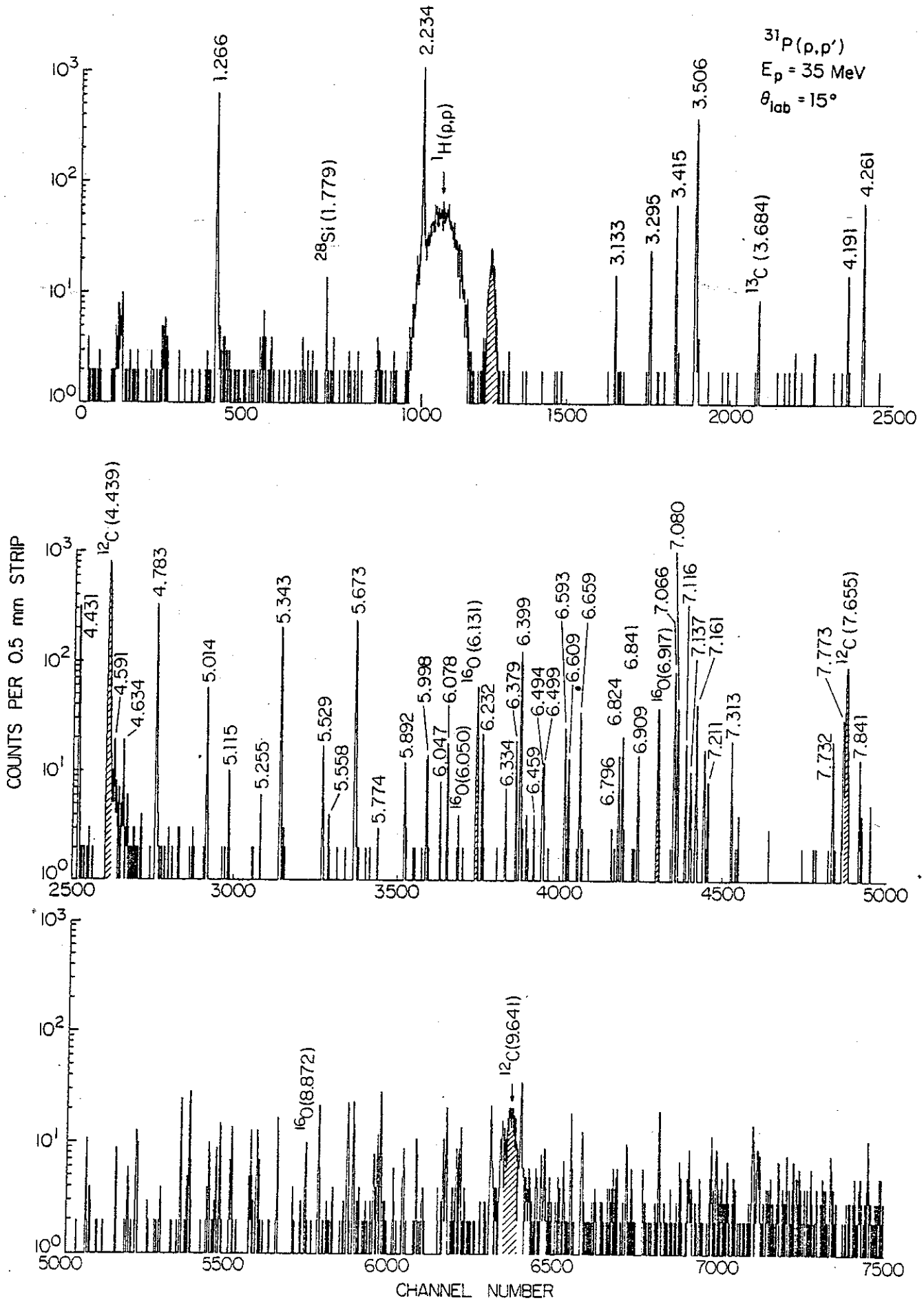

Fig. 1(IV.4.4) Spectrum of protons inelastically scattered by a ^{31}P target from a 35 MeV beam, showing 2.5 keV resolution.

For deuteron-like heavy ions, the spectrograph is capable of analyzing particles up to 25 MeV per nucleon, thus serving as an excellent tool for a number of studies. The more stringent vacuum requirements of heavy ion work will be met by installing additional pumping in the spectrograph camera box (currently unused additional pumping ports were provided in the initial construction).

References

1. J.E. Spencer and H.A. Enge, Nucl. Inst. and Meth. 49 (1967)181.
2. J.A. Nolen, Jr. and Sam M. Austin, Phys. Rev. C13(1976)1773.
3. E. Kashy, W. Benenson, D. Mueller, R.G.H. Robertson and D.R. Goosman, Phys. Rev. C11(1975)1959.

IV.5. Detectors, electronics, etc.

In the previous section, we have discussed magnetic devices suitable for heavy ion physics with the CSC. Such devices provide useful spatial displacements of the products of nuclear reactions. This section considers other types of equipment needed to perform experiments either without, or in conjunction with, the magnetic devices. It is not possible to have on hand equipment for all conceivable experiments, but there are basic building blocks which we feel should be available to users as part of the facility. These include position sensitive proportional counters, electron spectrometers, gamma detectors, scattering chambers, modular circuits, and a versatile computer system. Existing MSU equipment in these areas will be available, but it will not be adequate for meeting the needs of a large user-oriented facility.

The selection and design of experimental equipment is an aspect of laboratory planning in which users will be heavily involved. The subsections below are germinal ideas to be refined in discussions with users and will undoubtedly change substantially by the time firm planning for first experiments is necessary.

IV.5.1 Position-sensitive detectors

At long last, nuclear emulsions are effectively disappearing from nuclear physics experiments. This long sought goal has been reached through a veritable explosion in knowledge and technology of gas counters. The first generation multiwire proportional counters,

which were expensive and unreliable, have now been replaced by a whole series of new counters which one-by-one have eliminated the critical problems. Non-normal incidence on spectrograph focal planes was, for example, considered an undesirable spectrograph feature due to counter difficulties--the slanted trajectory thru counters, coupled with low ionization-density, severely limited resolution in many cases, and complicated expensive features were introduced in spectrograph designs to avoid this difficulty. The problem was however very simply solved by the slanted cathode delay-line counter,[1] a very reliable counter with intrinsic resolution approaching 0.2 mm at 45° incidence. Such counters are now readily constructed in lengths up to 0.5 meter while maintaining the high transparency necessary for the multiple-component detection systems required to accomplish definitive particle identification. The slanted-cathode counter was designed for protons and deuterons but will nevertheless be very useful in spectrographs designed for heavy ions. Freedom from the requirement of normal incidence makes design of such a spectrograph with large solid angle and low aberrations much easier and less costly. Table 1 for example compares calculated line width factors for 35 MeV protons and 32 and 160 MeV ^{16}O ions. The table shows that most of the line width for the protons and for the high energy oxygen ions is due to the energy-loss straggling which is not compensated for in the present design. Effects not included in the table are largely ones which are expected to be worse for protons than heavy ions; since the proton performance is experimentally established, good

Table 1.(IV.5.1)--Calculated line widths (mm FWHM).

Source	P 35 MeV	^{16}O 32 MeV	^{16}O 160 MeV
Window Scattering,[a]	0.05	0.43	0.08
Gas Scattering,[b]	0.04	0.30	0.06
Ionization Fluctuations	0.13	~0	<0.13
Noise	~0.05	-	-
Total	0.15	0.52	0.16
Best observed Minus Beam	0.22	-	-
Residual	0.16	-	-

[a] 6 μm thick mylar

[b] propane at 1/3 atmosphere

heavy ion performance in the energy range above 10 MeV per nucleon is clearly indicated.

The slanted cathode detector is an excellent choice for magnet systems with low aberrations, and some aberration correcting can perhaps be included by using time of flight measurements to infer the path length through the spectrograph. If aberrations are severe, a ray tracing approach is likely to be more effective. The idea of living with the aberrations of the spectrograph and correcting by means of ray tracing is very attractive from the standpoint of spectrograph cost and simplicity. A detector which shows considerable promise in this application is a modification of the hybrid chamber[2] in use for electrons at the MIT Bates Laboratory. A schematic of the proposed detector is shown in Fig. 1. The basic idea is to measure the drift time of the ionization electrons to the active wires. A knowledge of these drift times can be used to reconstruct both the angle and position of the particle trajectory. At least three signals are needed to reconstruct the event. In the proposed version of the Bates detector, every fifth wire will be connected together therefore giving five signals, and the position is accurately determined relative to each set of five wires. (To determine the position fully, the guard wires are connected to a tapped delay line and the relative time of arrival of the induced signal at each end gives coarse position. This setup is well suited to a CAMAC multistop time digitizer with relatively simple additional electronics.) Using a realistic estimate of the resolution of each individual cell one can estimate FWHM resolutions of 140 μm and 1° for position and angle

a)

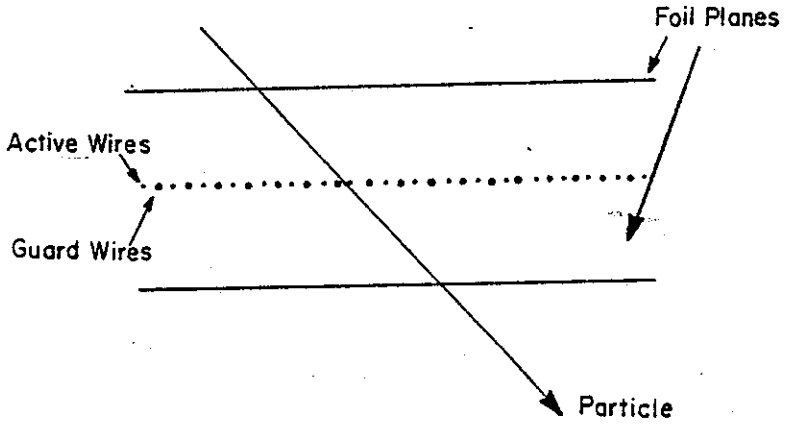

b)

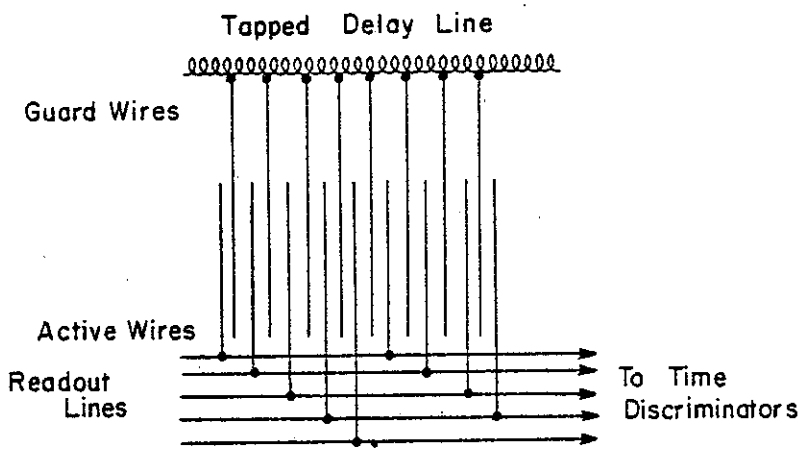

Fig. 1(IV.5).--Schematic of a proposed hybrid position sensitive proportional counter. The plan view is shown in a) and b) illustrates the readout scheme.

assuming 45° incidence angle. The multiple scattering contributions will dominate for heavy ions and will therefore be approximately the same as given in Table 1. To test these concepts we are now constructing a counter of this type for our present Enge spectrograph.

References

1. R.G. Markham and R.G.H. Robertson, Nucl. Instr. and Meth. 129(1975)131.

2. M.V. Hunes, W. Bertozzi, P. Dunn, J. Heisenberg, F. Rad, C.P. Sargent, T. Sasanuma, W. Torchinetz and C. Williamson, BAPS Vol. 21(1976)631.

IV.5.2 Other gas counters

A major detector development in recent years has been the reintroduction of gas counters for particle detection, particularly for detection of heavy ions. Besides providing the convenience of variable stopping-power (via the pressure), gas counters are now known to be capable of giving good time signals, good energy-loss resolution, and even spatial discrimination. Examples include the <200 psec time resolution obtained with parallel-foil avalanche detectors[1] at GSI and the high Z discrimination obtained at Berkeley with gas, silicon, and intrinsic germanium detectors.[2]

A recent experiment[3] at MSU has utilized an ultra-thin ΔE-E counter telescope[4] with position sensitivity in two dimensions. This detector will prove useful for situations in which a large solid angle is required for the detection of relatively short range particles. Examples include the detection of fission fragments, fusion products, target recoils and particle decays. A copy of this detector was used at BNL[5] to identify fusion products formed by the bombardment of ^{27}Al by 100 MeV ^{16}O ions. The position information was used in this case for compensation of kinematic effects, thus permitting very large solid angles and good energy resolution. Another likely use of such a counter in the CSC facility is at the focus of the solenoid spectrometer where position information will help with kinematic and time-of-flight corrections.

References

1. H. Stelzer, Nucl. Instr. and Meth. 133(1976)409.

2. H.H. Gutbrod, private communication.

3. R.G. Markham, S.M. Austin and M.A.M. Shahabuddin, Nucl. Phys. A509(1976)170.

4. R.G. Markham, S.M. Austin and H. Laumer, Nucl. Instr. and Meth. 129(1976)141.

5. G. Young, E.B. Blum, E.R. Cosman, A.J. Lazzarini, M.A. Newhausen, S.G. Steadman and N. Tsoupas, BAPS vol. 21(1976)607.

IV.5.3 Scattering chambers and other specialized equipment

Present MSU facilities include a variety of scattering chambers, most of which will be useful in the new laboratory (generally with upgrading of pumping systems and seals). The largest of these chambers is a 40" diameter computer-controlled scattering chamber with a high-precision movable table and an independent movable arm. A number of additional chambers will clearly be needed for the CSC laboratory, probably including: 1) a time-of-flight chamber for heavy ions with long tubes having high-vacuum and variable angle capability, 2) some form of multiplicity array consisting of many plastic scintillators, preferably transportable from one beam line to another to measure neutron yields in conjunction with experiments which could benefit from the knowledge of how many neutrons accompanied the events being studied, 3) a gamma-ray multiplicity array using many NaI detectors and Ge(Li) detectors, 4) an electron spectrometer of the solenoid plus intrinsic germanium type, 5) a large NaI or external pair spectrometer for high energy γ-rays, 6) a cryogenic helium jet apparatus and, 7) a high-performance cryopumped gas target which can be put into operation at selected experimental stations. The budget allocation for scattering chambers is adjusted to include all these items.

IV.5.4 Electronics

Since the CSC will be a national user facility, the requirements for electronics and related equipment will be extensive. Our plan is to provide standard, permanent electronic configurations for major experimental set ups in order to enhance the effectiveness of visiting scientists. In general users will then have complete instrumentation packages from detector to computer which they can depend on to exist in the same form on successive runs of a given experiment. This implies at least eight permanent setups of NIM modules, bins, cables, and preamps. In addition, a library of NIM modules should be provided for non-standard experiments and temporary additions to standard setups. It would be desirable but costly to provide, in addition, a complete computer plus CAMAC module system for each experimental configuration; we believe the easy flexibility of these systems will permit their being shared by various experiments without major modifications, except in software. (In general there will always be at least two complete computer plus CAMAC systems available, one for data taking and one for setup for the following run.)

Besides the NIM modules which will be either permanently mounted or in a pool ready for use, a great deal of other equipment will be required, such as power supplies, oscilloscopes, signal generators, frequency meters, and diagnostic instruments. Equipment of this nature will be needed on the experimental floor and also in the electronics shop, which will have capability in both maintenance and design. The budget allocation for electronics is tailored to meet all these needs.

Addendum to Secs. IV.4 and IV.5

Since the writing of the CSC proposal in 1976, several laboratory staff members have gained additional heavy ion experience during leaves or as outside users at major world heavy ion facilities. Additional valuable experience has been gained with the heavy ion beams which have come into use on our present 50 MeV cyclotron. The major experimental facilities contemplated in the CSC proposal have recently been reviewed with particular attention given to possible changes which might be considered as a result of the further evolution of the field, or reflecting changes in our own ideas from experience gained in the intervening months. We conclude from this review that the three major experimental facilities originally proposed remain very appropriate, namely a) superconducting solenoids or quadrupoles for large solid-angle reaction product collection and time of flight measurements; b) a K ≃ 150 recoil-mass spectrometer; and c) a K = 800 high resolution spectrograph.

We are currently considering the implications of recent observations of very narrow heavy ion line widths from the present cyclotron. Our 77 MeV ^{12}C beam has been focused to a line width of 1/8 mm (≃ 8 keV) in the focal plane of the split-pole spectrograph. This was with multiturn extraction (no phase slits) and an ion source slit more than 10 times the width we normally use for high resolution. The achievement of such narrow incoherent spot size definitely will affect the final design parameters of the proposed spectrograph. A preliminary report on these experiments is attached.

Focal plane detector capability is also a major consideration in spectrograph design and cost. The construction of the modified "Bates" detector system described in the proposal is now nearly complete and will soon be tested with our present light and heavy ion beams. We hope to achieve 0.1 to 0.3 mm resolution (FWHM) with this detector.

A new cryogenic He-jet transport system, appropriate for a wide variety of experiments with the present as well as the future cyclotrons, is now in the early stages of operation. Beta-delayed alpha spectra, associated with the transport of ^{20}Na through the system, have been observed. In addition, a new 4 m time-of-flight apparatus similar to the Heidelberg-GSI systems is currently being planned. This is a general purpose apparatus valuable for reaction mechanism studies with both the present and future cyclotrons.

Preliminary Report: Beam Quality Evaluation of Accelerator-Spectrograph System

An optical system has been developed[1] which allows direct viewing of line widths in the focal plane of a magnetic spectrograph, and thus greatly facilitates the tuning of the accelerator and beam transport system which is required to obtain optimum dispersion matching and focusing. To use this system, the spectrograph is set at a scattering angle of 0 degrees, and the optical system is used to view the direct beam image in the focal plane, first without the target and then with the target in place. The accelerator and beam transport controls are adjusted to give minimum line width. In actual use this system is extremely rapid and effective. The attached figure shows the image of a 77 MeV ^{12}C beam in the focal plane of the split-pole spectrograph. The line width is about 1/8 mm corresponding to an energy resolution of 9 keV FWHM, and was obtained with a beam energy spread of over 100 keV, indicating the effectiveness of the dispersion matching procedure. The line greatly broadens when a target is inserted, but the intriguing possibility of a new field of high resolution heavy ion experiments is indicated if target straggling can be sufficiently reduced.

A number of experiments with high energy heavy-ion beams depend on achieving high resolution. (One example is heavy ion elastic scattering as discussed in Sec. III of the CSC proposal.) The target effects which usually dominate the resolution obtained in heavy ion experiments are a combination of multiple scattering, energy loss straggling and thickness non-uniformities. These

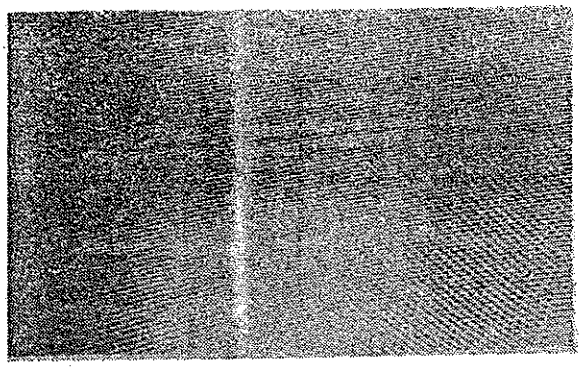

FIGURE 1.--Image of a 77 MeV ^{12}C beam in the focal plane of the split-pole spectrograph. The horizontal spacing between the two vertical wires is 2 mm. The line width of the beam image is about 1/8 mm or 9 keV.

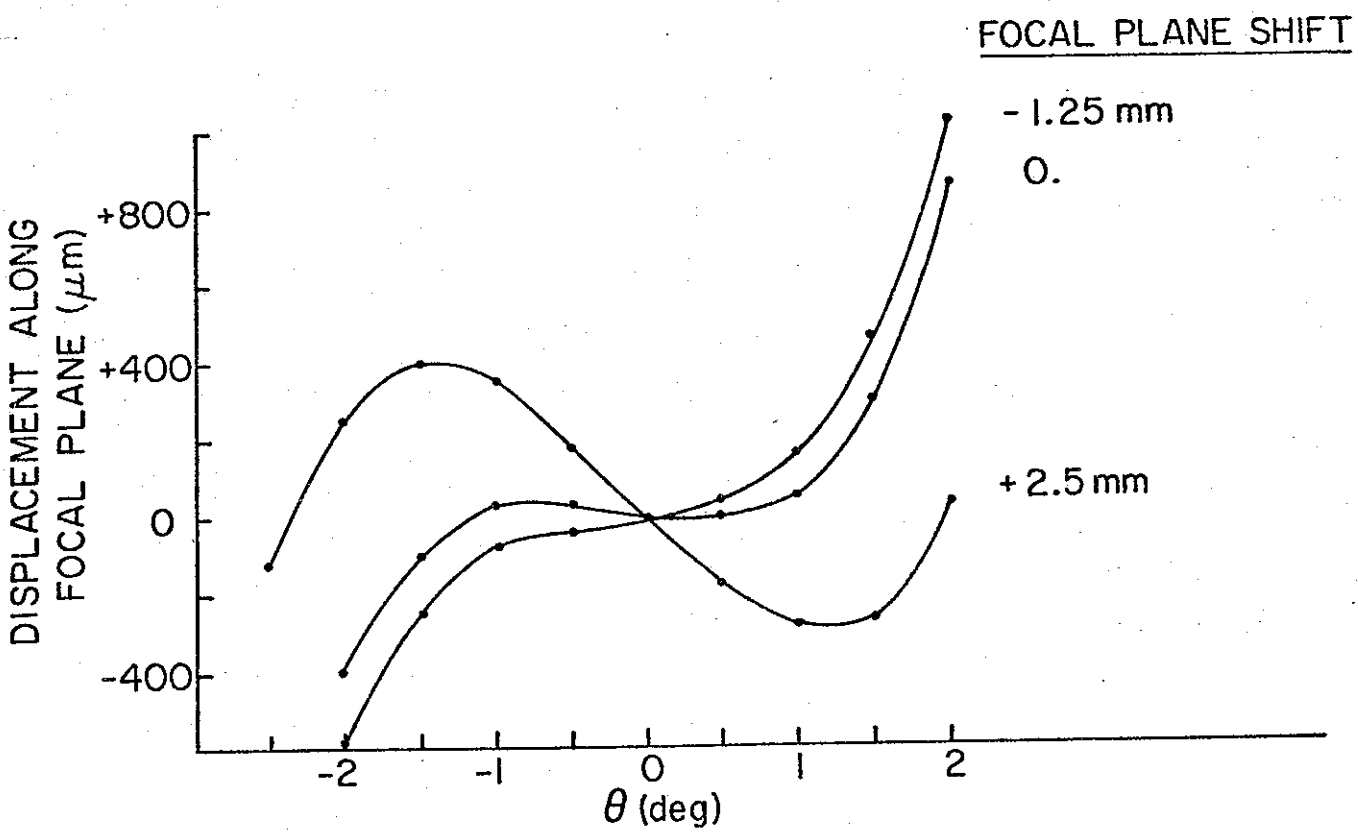

FIGURE 2.--Data for determination of the horizontal aberration coefficients x/θ^2 and x/θ^3. These data also determine precisely the zero-order focal plane position.

problems were discussed by Erskine at the Target Making Conference in 1975.[2] The energy spread from these target effects will immediately be much smaller at the higher energies available from the CSC; the absolute energy loss and straggling effects for a given target thickness are both lower. The high intensity from the CSC will also permit the use of ultrathin targets to further reduce target effects. In addition the excellent intrinsic beam quality will encourage other developments such as windowless gas targets which would eliminate target uniformity problems. Significant advances in the high resolution aspect of heavy-ion science then seem clearly possible.

The focal plane optical system in conjunction with a movable slit for measuring angular divergence also gives a rapid measure of beam emittance with the confusing effects of coherent energy spread and dispersion eliminated. Using this system, the overall quality of heavy ion beams from the 50 MeV cyclotron was found to be surprisingly high: the measured radial emittance is 4 mm-milliradions for 77 MeV $^{12}C^{4+}$, again implying the possibility of significant high resolution work if target effects can be adequately controlled.

The focal plane optical system is also valuable in studying misalignments and aberrations in beam line components, these effects being quickly observable as asymmetric or distorted images. Spectrograph aberrations are also quantitatively measurable as indicated in the lower part of the attached figure. This technique will obviously be of great value in setting up a high quality spectrograph system on the new cyclotron.

---

[1] E. Kashy, P.S. Miller and J.A. Nolen, Jr., submitted to Washington APS meeting (1978

[2] J.R. Erskine, Fourth Annual International Conference of the Nuclear Target Development Society, Argonne, Illinois (1975) p. 141.

V. Construction Costs, Operating Costs and Schedule

Table 1 is a summary of estimated construction costs for the proposed CSC facility. Table 2 gives a detailed breakdown of major items from Table 1. As indicated in the notes in Table 1, costs are in every case estimated on the basis of 1976 dollars. The budgets also assume that operating support for the laboratory will continue through the construction period with increases as outlined in a later paragraph and that accelerator personnel supported by this budget will be available for work on design and construction of the facility. Tables 1 and 2 are largely self-explanatory, but a few comments are perhaps useful.

First of all we note that the cost to complete the 500 MeV cyclotron is now estimated to be $740,000, which is sizeably lower than our estimate of two years ago. A number of factors contribute to this change, including 1) simplifications in the design such as the change from four sectors to three, elimination of supertubes, etc.; 2) the design now exists in much greater detail than it did two years ago--the present estimate is keyed to actual requirements to a greater degree and is therefore significantly more accurate, and 3) several components previously included have been incorporated in the prototype magnet using contingency funds from that budget--such items include conductor for the complete set of trim coils, all magnetic extraction elements, most of the cyclotron vacuum tank, and a control system computer (PDP11-15).

TABLE 1

BUDGET SUMMARY--COUPLED SUPERCONDUCTING CYCLOTRON FACILITY

	NSF	MSU
Complete 500 MeV Cyclotron	$ 740,000	
800 MeV Cyclotron	2,700,000	
West Building Addition		$300,000
East Building Addition (including fixed shielding)	3,370,000	
Moveable Shielding	630,000	
Beam Transport System	650,000	
Central Cryogenic System	845,000	
Beam Lines, Slits, Beam Plugs, Viewers	300,000	
Digital Data Processing Systems	1,200,000	
Nuclear Electronics	450,000	
Recoil-Mass Spectrometer	500,000	
800 MeV Spectrograph	1,200,000	
Superconducting Reaction Product Collector	160,000	
Scattering Chambers	250,000	
General Apparatus including Upgrading	200,000	
PROJECT TOTAL	$13,195,000	$300,000

Notes:

1. All costs are in 1976 dollars. (Supplemental funding will be requested to cover inflation factors based on applicable federal cost indices at the time of construction.)

2. Contingency for all items is included in the item and varies from 5%-30% depending on the nature of the item and its design status.

3. It is assumed that the operations budget of the Cyclotron Laboratory will increase as outlined in Table 3 and that accelerator personnel from this budget will be available to work on design and construction of the facility. Salary support for this group is not included in the above $13,195,000. As Table 3 indicates, expenditures from the operations budget for support of staff working on design and construction are estimated to total $4,500,000 for the five year construction period.

TABLE 2 . Cost estimate Details

Completion of 500 MeV Cyclotron:

Complete trim coils	80,000
RF system (mechanical)	130,000
RF system (electrical)	118,000
Electrostatic Deflectors & Power supplies	45,000
Ion source including automated insertion system & vacuum lock	85,000
Vacuum system (does not include existing main vacuum tank and Helium liquifier)	55,000
Control system and instrumentation	100,000
Probes and diagnostic devices	30,000
	643,000
Contingency 15%	97,000
	$ 740,000

800 MeV Cyclotron:

Magnet core cast steel 530,000 lb @ $0.80/lb	425,000
Pole Tips	55,000
Main coil conductor 132,000 k amp-ft @ $1.10	145,000
Main coil bobbin	80,000
Main coil winding	100,000
Main coil cryostat	45,000
Miscellaneous mechanical items	150,000
RF system mechanical	250,000
RF system electrical	250,000
Foil holder, magazine, airlock	60,000
Trim coils	125,000
Trim coil power supplies	90,000
Vacuum system	75,000
Helium liquifier/refrigerator (included elsewhere)	0
Deflectors and power supplies	80,000
Control system and instrumentation	145,000
	2,075,000
Contingency 30%	625,000
	2,700,000

TABLE 2 (continued, Page 2)

Building Addition*	
34,000 sq. ft. (new construction)	
6,000 sq. ft. (remodeling)	
A. PROFESSIONAL SERVICES	
1. Architectural and Engineering	190,000
2. Site Survey and Soil Investigation	10,000
B. CONSTRUCTION	
1. Structure (general, mechanical, electrical, fixed equipment)	
West High Bay Area 3100 sq. ft. @$60	186,000
Special Floor	75,000
East High Bay Area 11000 sq. ft. @$50	550,000
Special Floor	275,000
Shielding Walls	250,000
Office Area 20,000 sq. ft. @$65	1,300,000
Remodeling 6,000 sq. ft. @$35	210,000
Subtotal	3,046,000
Contingency 5%	154,000
*2. Services (off site utilities)	300,000
3. Site (Landscaping)	10,000
C. SUPERVISION & TESTING	60,000
D. FURNISHINGS AND EQUIPMENT	100,000
E. OTHER COSTS	
1.	
2.	
F. TOTAL PROJECT COST	3,670,000

*Estimate by MSU University Architect's Office.

TABLE 2 (continued, Page 3)

Shielding:	
Moveable walls	
Dry stacked 4"x8"x16" concrete blocks	116,000
Roof beams (prestressed concrete)	240,000
Beam dumps (cast steel)	70,000
Radiation monitoring system	65,000
Hydraulic door system	140,000
	$631,000
Beam Transport System:	
Superconducting dipoles including leads and dewar	
9 each 4" aperature x 17" long @ 15,000	135,000
7 each 6" aperature x 17" long @ 20,000	140,000
Quadrupole singlets including leads & dewar	
36 each 4" aperature @ 7,500	270,000
Power Supply	
D.C. source 20 volts @ 2,000 amps	16,000
60 each 50 amp Series regulators @ 1,500	90,000
	$651,000
Multi-purpose Refrigeration System:	
200 liter/hour liquifier refrigerator with compressors	700,000
Storage and Gas Handling	85,000
Cryogenic distribution lines 600 feet @ $100/ft	60,000
	$845,000

TABLE 2 (continued, page 4)

DIGITAL DATA PROCESSING SYSTEM

Mass Storage System--one required		
Multi-port access controller (4 ports)	90,000	
Storage media devices (8 units)	160,000	
1 @	250,000	250,000
Computation Systems--two required		
CPU hardware 128 K words	75,000	
IOP for peripherals	30,000	
Peripherals (disk pack, tape)	160,000	
Front-end & interface	50,000	
2 @	315,000	630,000
Data Acquisition System--three required		
CPU with 64 K words	28,000	
Terminal device	2,000	
CAMAC interface	8,000	
System device (disc)	10,000	
Removable media device (tape, disc)	9,000	
Display	10,000	
Low and High speed interface	3,000	
3 @	70,000	210,000
I/O System--one required		
CPU with 64 K words	28,000	
Terminal device	12,000	
System device (disc)	10,000	
Low and High speed interface	5,000	
Line printer	25,000	
Card reader	10,000	
Plotter	20,000	
1 @	110,000	110,000
		$1,200,000

The cost estimate for the 800 MeV cyclotron is largely a scaling of the 500 MeV costs. For the various magnet items this is based on actual procurement experience with the 500 MeV magnet. The 800 MeV cyclotron costs do not include a helium liquifier since cryogenic and superconducting techniques will be widely used in the new laboratory, and a large centralized liquifier is more economical.

The cost of the central liquifier/refrigerator is based on a commercial estimate. This liquifier would have adequate capacity to handle the 800 MeV cyclotron, the complete superconducting beam transport system, a possible superconducting spectrograph, and cryopumping in the accelerator and transport system.

Cost estimates for the superconducting magnet elements in the beam transport system are based on estimates from the Argonne National Laboratory proposal for a Superconducting Stretcher Ring for the ZGS accelerator.[1] We have increased the Argonne cost figures by 50% to allow for escalation in the two years since the SSR estimate and also to provide a comfortable contingency.

The cost estimates for shielding assume construction techniques as in our present laboratory, namely fixed poured-in-place walls at points where the shielding is part of the building structure (with costs for these walls included in the building budget) and movable dry-stacked concrete block walls at other points with stacking by a student labor force. Overhead shielding will consist of pre-stressed concrete beams of the type customarily used in highway bridges except without hollow cores. Costs for

these items are based on commercial estimates with a 30% contingency.

The computer cost estimate is based on commercial procurement of standard units such as CPU's, memory banks, input-output devices etc., and local development of systems programming and interfacing. Other items of experimental equipment are estimated more qualitatively based on general experience at other laboratories and judgments as to the degree to which major units of experimental equipment should be incorporated in an initial construction budget. Such judgments are substantially arbitrary. We hope the amounts included are approximately in the center of the spectrum.

The central question in reviewing our cost estimate is whether the estimate is basically accurate. Cost overruns have been frequent in major scientific projects, and some cynics automatically multiply any quoted estimate by π. The difficulty with this procedure is that there are in fact numerous examples of accurate estimates; the automatic factor of π discriminates against these well-founded estimates by lumping all estimates into the grossly low category. How can the funding agency and reviewers best assess the accuracy of the cost estimates given here? One major source of relevant evidence is an assessment of the past record of the group. Have our estimates been right before? Are the present estimates in qualitative agreement with our previous cost experience on similar items? To

provide information on these points we will review cost experience in the construction of present East Lansing facilities.

The most recent major construction project in the laboratory is the superconducting magnet. This project is not complete at this time but the costs are nevertheless clear since essentially all items are either received or on order at fixed price. The project is comfortably within its budget even though the technical scope of the project has been expanded to include several items not originally anticipated for reasons of construction convenience. The contingency item for the project is also largely uncommitted at this time. The cost experience on the superconducting magnet project is our key reference point in estimating other project costs; this reference point is both very recent and extremely relevant.

Another point of judgment is a comparison of the estimated cost for the proposed new facility with the actual cost of the existing laboratory and its equipment. Prior to the superconducting magnet, equipment grants to the Cyclotron Laboratory (from the National Science Foundation) totaled $2,526,000 over the life of the laboratory. These grants provided funds for all major present equipment including the cyclotron, the computer, the high resolution spectrograph, the beam transport system, the movable shielding, etc. In addition the existing building was constructed by the University at a cost of $1,400,000, giving a total present facility cost of approximately $4,000,000. The new laboratory is in most respects comparable to the old, i.e.,

the building addition is approximately the same as the original building, the two new cyclotrons are about the same physical size and therefore about the same cost as the present cyclotron, etc. Taking account of inflation in the intervening years and of added increments of special equipment in the new laboratory, the estimated cost of $13 million for the proposed additional facilities scales reasonably in comparison with the existing facility.

It is important and relevant to note that our cost estimates are based on continuing a "small laboratory" operating style following procedures evolved at the laboratory over many years. We feel this operating style is completely appropriate for producing sophisticated, reliable equipment of the types proposed here and is at the same time exceptionally cost effective. One of the key elements of this operating style is our pattern of internally handling most design work and most developmental fabrication. Commercial procurement is then mainly reserved for items which are standard products, thus avoiding support of design or development work by commercial concerns which in our experience is both costly and inefficient. (This does not necessarily imply that personnel in commercial concerns are less competent; the biggest efficiency loss is due to lack of knowledge of details of the actual application of the equipment therefore cutting off innovative thinking on design efficiencies.) As illustrative of this construction philosophy: 1) we would procure beam line components from local machine shops based on mechanical tolerances rather than from accelerator concerns based on vacuum requirements, 2) we would procure a standard

electronic module from the manufacturer, but for a special module we would buy components and internally fabricate, 3) magnets would be purchased based on mechanical and materials requirements rather than on magnetic field requirements, 4) when an invention is needed, the scientist, designer, machinist etc. would work together with a minimum of drawings, building trial devices and evolving ideas--formal drawings would only be made for the final device... This small laboratory style of operation is clearly highly efficient. There is also undoubtedly a maximum project size to which it is applicable, hinging probably on whether technical details of the project are at a level where they can be contained within the minds of one or a few persons. We are confident that the facility proposed here can in fact be constructed within the framework of our traditional operating procedures; this confidence hinges on the fact that the proposed new project is not greatly different in scale from assignments the group has previously handled and that the increased size which does exist is balanced by the added experience of the group.

The anticipated construction schedule for the facility is shown in Table 3 together with anticipated increases in operating support, and operating staff. The construction schedule is based on moving forward vigorously with the project beginning in fiscal year 1978, with major construction funding extending over a three-year period. It is also assumed that funding to complete the 500 MeV cyclotron will be provided in fiscal year 77 either as a first step toward the facility proposed here or as an independent accelerator development

Table 3.--Schedule for construction and funding of the CSC facility.

CALENDER YEAR			1976	1977	1978	1979	1980	1981
			1 2 3 4	1 2 3 4	1 2 3 4	1 2 3 4	1 2 3 4	1 2 3 4
CAPITAL		FIRST CYCLOTRON R.F. ETC.	(MAGNET UNDER CONSTRUCTION)	START	FIRST OPER. ←	EXPERIMENTS WITH 1ST CYCLOTRON →		BEGIN FULL EXPERIMENTAL PROGRAM
		FIRST BUILDING ADDITION		START	START COMP.			
		SECOND BUILDING ADDITION			START	COMP.		
		SECOND CYCLOTRON			START		FIRST OPER.	
		AUX. EQUIPMENT				START		
		NSF CONSTRUCTION $	(1000 K MAGNET)	740 K	4,500 K	4,500 K	2,500 K	910 K
OPERATIONS	STAFF	ACCELERATOR DEVEL. + CONST.	6			24		5
		MAINTENANCE & OPERATION	6			10		25
		COMPUTER	4			6		8
		CLER. - SHOP	10			20		18
	FACULTY		13			15		15
	NSF OPERATING BUDGET	DEVEL. + CONST.	200K	600 K	1000 K	1200 K	1200K	500 K
		MAIN. + OPER.	200 K	200K	250K	500K	500 K	1200 K
		MSU NUC. PHY. PROG.	700 K	700 K	750K	800 K	800 K	800 K
		TOTAL	1,100 K	1,500 K	2,000K	2,500 K	2,500 K	2,500 K

program for fully verifying and establishing the promising capabilities of the superconducting cyclotron.

To appropriately staff the proposed facility, the operating staff of the laboratory should approximately double from its present level of 26 to a final level of 56 with a slight intermediate peak at 60. This growth would be spread smoothly over the years 1977 and 1978. From 1979 to 1981 the assignments of the staff would change as the emphasis of the laboratory shifts from development and construction to operations. We would expect most of this change to be accomplished by transfer of assignments of construction personnel. (The knowledge accumulated in helping with construction would certainly be useful in solving operating problems.) The final staff of 56 is one which should adequately provide the appropriate high level of staff assistance needed for outside users to function efficiently. (In particular, we plan to shift away from our present run-it-yourself operating mode and would provide operators and maintenance personnel on all shifts.)

The operating costs in Table 3 are estimated on the assumption that the operating grant would continue as now to cover acclerator development, laboratory operations and support for the MSU experimental nuclear physics program. The indicated operating staff additions would be entirely funded from the operating grant increments. These increases together with increases for expendable materials, user equipment etc. give a total increase of $1.4 million over the present budget. For reference the present budget approximately divides $200,000 for accelerator development, $200,000 for cyclotron operations and $700,000 as research support for the eleven

experimental faculty and their postdoctorals and graduate students. The estimated operating budgets in Table III assume that this research support for the MSU nuclear physics group would stay approximately constant in 1976 dollars. The estimated operating costs also assume that present Michigan State University support for the operating staff will continue at its present level in accord with one of the commitments made by the University in the covering letter accompanying this proposal.

Summarizing we believe our cost estimates are sound and will provide adequately for constructing and operating a forefront nuclear science facility in East Lansing.

Reference

1. Superconducting Stretcher Ring for the zero gradient synchrotron, Argonne National Lab., May 1974.

Addendum to V

Developments in the 18 months since the CSC proposal was submitted support the conclusion that the cost estimate given therein is generally accurate. The prototype superconducting magnet for example was comfortably completed within its budget (also the contingency funds contained in the budget were not required to complete the original program, and were reprogrammed to permit a moderate expansion of project scope). The cost of the west building extension is also in accurate agreement with budget estimates, and the ongoing construction of the 500 MeV cyclotron gives no indication of cost over-run. The updating of our cost estimates in this addendum then consists of deducting those items included in the funded Phase I project, namely the items to complete the 500 MeV cyclotron and portions of the moveable shielding, beam transport system, etc. Finally total project costs are restated in 1978 dollars, using an escalation factor of 13% for the two years combined. These changes are then summarized in the "Table 1 addendum". We note that the cost of the 800 MeV cyclotron is 22.5% of the estimated total, the east building addition is 28%, shielding and beam transport systems are 17.5%, and the experimental facilities, data processing, etc. are 32% of the estimated total budget.

The revised schedule for the project is shown in the "Table 3 addendum." As the table indicates, initial beam tests of the 500 MeV cyclotron are expected in the summer of 1979 with gradual phasing to full time nuclear use in early 1980. Funding for the 800 MeV cyclotron and for the east building addition are assumed to be available at the beginning of 1980, and distributed

TABLE 1--Addendum

BUDGET SUMMARY--COUPLED SUPERCONDUCTING CYCLOTRON FACILITY

	NSF
800 MeV Cyclotron	2,700,000
East Building Addition (including fixed shielding)	3,370,000
Moveable Shielding	480,000
Beam Transport System	530,000
Central Cryogenic System	830,000
Beam Lines, Slits, Beam Plugs, Viewers	240,000
Digital Data Processing Systems	1,200,000
Nuclear Electronics	340,000
Recoil-Mass Spectrometer	500,000
800 MeV Spectrograph	1,200,000
Superconducting Reaction Product Collector	160,000
Scattering Chambers	250,000
General Apparatus including Upgrading	160,000
PROJECT TOTAL 1976 DOLLARS	$11,960,000
PROJECT TOTAL 1978 DOLLARS	$13,514,800

Notes:

1. Item costs are in 1976 dollars. Total is shown in 1976 dollars and also in 1978 dollars. (Supplemental funding will be requested to cover inflation factors based on applicable federal cost indices at the time of construction.)

2. Contingency for all items is included in the item and varies from 5%-30% depending on the nature of the item and its design status.

3. It is assumed that the operations budget of the Cyclotron Laboratory will increase as outlined in Table 3 and that accelerator personnel from this budget will be available to work on design and construction of the facility. Salary support for this group is not included in the above budget. As Table 3 indicates, expenditures from the operations budget for support of staff working on engineering and development for the Phase II project are estimated to total $5,400,000 for the four year construction period.

approximately uniformly over a three and one half year period. With this funding schedule, the experimental program on the full coupled cyclotron system would begin in early 1984.

This proposal is not a request for operating support, but it nevertheless assumes that operating support will be provided both in the construction years and in following utilization years. Costs associated with design and development of the accelerator system and ancillary facilities are included in the operating budget in accord with previous budget patterns used for our laboratory. (With this system, construction costs represent the cost of building a second identical copy of the acclerator system without further design and development.) As indicated in footnote 3 of the Table 1 addendum, total design and development costs associated with the Phase II project are $5,400,000, and correspond to 40% of construction costs. This proportion is higher than one might have in a more traditional accelerator and reflects two basic aspects of the project namely 1) construction costs are low because the superconducting cyclotron achieves major savings in hardware, basically by making the cyclotron much smaller and 2) the overall complexity of the cyclotron is if anything somewhat greater than that of a room temperature system, and design and development costs are then approximately the same as for a room temperature accelerator and hence fractionally are a much larger part of total project costs.

Operating costs in the Table 3 addendum (other than for Phase II engineering and development) are unrelated to the Phase II project but are nevertheless included for completeness. The figures have been increased

TABLE 3--Addendum. All costs are in 1978 dollars.

CALENDER YEAR			1978	1979	1980	1981	1982	1983	1984
			1 2 3 4	1 2 3 4	1 2 3 4	1 2 3 4	1 2 3 4	1 2 3 4	1 2 3 4
CAPITAL	PHASE I (500MeV CYCLOTRON)			FIRST OPER.	← EXPERIMENTS WITH 1ST CYCLOTRON →				BEGIN FULL EXPERIMENTAL PROGRAM
	FIRST BUILDING ADDITION		FINISH						
	PHASE II BUILDING ADDITION			START ARCHITECT	START CONST.				
	800 MeV CYCLOTRON		← DESIGN STUDIES →		START CONST.			FIRST OPER.	
	AUX. EQUIPMENT				DESIGN STUDIES	START CONST.			
	NSF CONSTRUCTION 1978 DOLLARS		(400K) (500 K) PHASE I		4,000 K	4,000 K	4,000 K	1,515 K	
						PHASE II			
OPERATIONS	STAFF	ACCELERATOR DEVEL.+ CONST.	15		24		24		6
		MAINTENANCE & OPERATION	6		12		12		30
		COMPUTER	4		6		6		10
		CLER. -SHOP	14		20		24		18
	FACULTY		14		15		16		17
	NSF OPERATING BUDGET 1978 DOLLARS	ENG. & DEVEL. I	550 K	900 K	100 K	100 K	100 K	100 K	300 K
		ENG. & DEVEL. II	50 K	250 K	1,200 K	1,400 K	1,400 K	1,400 K	
		MAIN. & OPER.	220 K	250 K	500 K	500 K	500 K	700 K	2,000 K
		MSU NUC. PHY. PROG.	780 K	900 K	1,000 K	1,000 K	1,000 K	1,000 K	1,200 K
		TOTAL	1,600 K	2,300 K	2,800 K	3,000 K	3,000 K	3,200 K	3,500 K

relative to the comparable figures in the original proposal by a larger factor than simply the 13% inflation correction, reflecting our feeling that the experimental program of the 500 MeV cyclotron will be of sufficient importance to warrant a higher support level than we had previously contemplated. The actual level of this support is of course an open question which will ultimately be fixed in the process of submission of operating proposals and review of these proposals. The operating figures in Table 3 are then presented for information and reflect our current feeling as to levels which we would request in future operating proposals.